

**Joint Meeting of the Austrian Neuroscience Association
(13th ANA Meeting) and the Austrian Pharmacological
Society (19th Scientific Symposium of APHAR)**

Vienna, 16–19 September 2013

**Joint Meeting of the Austrian
Pharmacological Society and the
Austrian Neuroscience Association**

**19th Scientific Symposium of
APHAR and 13th ANA Meeting**

**APHAR / ANA
2013**



www.aphar.at



**16–19 September 2013
V I E N N A**

[www.austrian-
neuroscience.at](http://www.austrian-neuroscience.at)

**Centre of Physiology and Pharmacology
of the Medical University of Vienna**

MEETING ABSTRACTS

Intrinsic Activity is an online, open-access publication medium published by the Austrian Pharmacological Society (APHAR). The Journal welcomes contributions in the fields of Pharmacology, Pharmacotherapy and other fields in biomedicine.

Contributions may be of type meeting abstracts, research articles, position papers, commentaries or similar. For submission instructions and all other information regarding publication in the journal visit: www.IntrinsicActivity.org

Correspondence

Intrinsic Activity

c/o Institute for Experimental and Clinical Pharmacology
Medical University of Graz
Universitätsplatz 4
8010 Graz, Austria
Tel.: +43 (316) 380-4305
Fax: +43 (316) 380-9645
E-mail: info@intrinsicactivity.org

Website: www.IntrinsicActivity.org
ISSN: 2309-8503

Austrian Pharmacological Society

c/o Institute of Pharmacology
Centre for Physiology and Pharmacology
Medical University of Vienna
Währinger Straße 13a
1090 Wien, Austria
E-mail: office@aphar.at

Copyright, open access and permission to use

Articles are published under a Creative Commons license (Creative Commons, attribution, non-commercial), that allows reuse subject only to the use being non-commercial and the article being fully attributed.

The Publisher and Austrian Pharmacological Society retain the license that allows publishing of the articles in *Intrinsic Activity*, any derivative product or any other *Intrinsic Activity* product (present or future) and allows sub-licensing such rights and exploit all subsidiary rights.

Authors retain the license to use their articles for their own non-commercial purposes, specifically:

- Posting a pdf of their own article on their own personal or institutional website for which no charge for access is made.
- Making a reasonable number of copies for personal or non-commercial professional use. This includes the contributors' own teaching activities.
- Republishing part or all of the article in a book or publication edited by the author (except for multiple publications in the same book or publication).
- Using individual figures or tables in other publications published by a third party. Extracts of text other than individual phrases or sentences may also be used provided that these are identified as quotations along with giving the appropriate reference to the original publication.
- Using the article in a course pack or compilation (whether paper or electronic) in the author's institution. This does not apply if a commercial charge is made for the compilation or course.

Third parties (other than the Publisher, Austrian Pharmacological Society, or authors) may download, print or store articles published in the journal for their private or professional, non-commercial use. The use of articles published in the journal, or any artwork contained therein, for educational, non-commercial purposes is granted provided that the appropriate reference to the journal and original article is given.

Any commercial use of articles published in *Intrinsic Activity* requires the permission of the Publisher.

Disclaimer

The Publisher, the Austrian Pharmacological Society and Editor(s) cannot be held responsible for errors or any consequences arising from the use of information contained in this journal. The views and opinions expressed do not necessarily reflect those of the Publisher, Austrian Pharmacological Society or Editor(s). Neither does the publication of advertisements constitute any endorsement by the Publisher, Austrian Pharmacological Society or Editor(s) of the products advertised.

Joint Meeting of the Austrian Neuroscience Association (13th ANA Meeting) and the Austrian Pharmacological Society (19th Scientific Symposium of APHAR)

Vienna, Austria, 16–19 September 2013

MEETING ABSTRACTS

(available online at <http://www.intrinsicactivity.org/2013/1/S1>)

Meeting sections:

Austrian Neuroscience Association (ANA) (A1.1–A1.52)	1
Special session SFB and DK (ANA and APHAR) (A2.1–A2.11)	22
Austrian Pharmacological Society (APHAR) (A3.1–A3.24)	27
APHAR Section of Clinical Pharmacology (A4.1–A4.7)	37
Author index	40

Austrian Neuroscience Association (ANA)

A1.1

The efficacy of NGF-secreting primary monocytes as therapeutic delivery vehicles in a cognitively impaired cholesterol rat model

Lindsay A. Hohsfield¹, Stephan Geley², Markus Reindl³ and Christian Humpel^{1,*}

¹Laboratory of Psychiatry and Experimental Alzheimer's Research, Department of Psychiatry and Psychotherapy, Innsbruck Medical University, Austria; ²Biocenter, Division of Molecular Pathophysiology, Innsbruck Medical University, Austria; ³Clinical Department of Neurology, Innsbruck Medical University, Austria

*E-mail: christian.humpel@i-med.ac.at

Intrinsic Activity, 2013; 1(Suppl. 1):A1.1

Background: Nerve growth factor (NGF) serves an important role in the maintenance and survival of cholinergic neurons in the basal forebrain and proves the most potent neuroprotective molecule against cholinergic neurodegeneration, a typical hallmark of Alzheimer's disease (AD). However, delivery of this factor to the brain remains difficult. The aim of the present study was (1) to test different transfer methods to generate NGF-secreting monocytes and (2) to evaluate the effects of intravenously (i.v.) applied primary monocytes alone or NGF-secreting monocytes in a cholesterol-induced cognitively impaired Brown Norway rat model.

Methods: Here, we assessed several different transfer methods (electroporation, nucleofection, viral transfer, Bioporter protein loading) in order to generate NGF-secreting monocytes. Monocytes alone or NGF-secreting monocytes were delivered *in vivo* via the dorsal penis vein in cholesterol-fed Brown Norway rats. Cognitive performance, including spatial learning and memory, was evaluated by an 8-arm maze. Neuroprotection was assessed by quantifying choline acetyltransferase (ChAT) neuron survival in the nucleus basalis of Meynert as well as measuring cortical NGF and acetylcholine (ACh) levels. Neuroinflammation was analysed by measuring cytokine and chemokine levels (MCP-1, MIP-2, TNF- α , IL-1 β) in brain lysates and by immunohistochemical evaluation of microglia staining in cortical regions.

Results: In this study, we demonstrate that lentiviral vectors and Bioporter protein delivery can successfully transduce primary rat monocytes and produce effective NGF secretion. Furthermore, our

results indicate that NGF is bioactive and that Bioporter-loaded monocytes do not exhibit functional disruptions (i.e. differentiation and phagocytosis potential). Following two months of monocyte i.v. treatment, animals treated with monocytes alone displayed significantly enhanced ACh, slightly enhanced ChAT neuron survival, and significantly reduced microglia activation. These findings, however, did not translate into a marked effect on cognitive performance. Animals which received NGF-loaded monocyte injections demonstrated significantly better cognitive performance compared to monocytes alone and significantly elevated ChAT neuron survival. However, these animals did show significantly elevated staining for microglia activation. Most importantly, we demonstrate that repeated i.v. injection of primary monocytes does not result in elevated release of proinflammatory cytokines and chemokines in the brain.

Discussion: Taken together, our data suggests that i.v. infusion of monocytes could serve as a potent cell-based therapy for neurodegenerative diseases. However, further studies are needed in order to evaluate the efficacy of these cells in counteracting cognitive impairments and disease pathogenesis in transgenic AD mice. This work has been published in [1,2,3].

Acknowledgements: This study was supported by the Austrian Science Fund (P24541-B24).

References

1. Hohsfield LA, Geley S, Reindl M, Humpel C: **The generation of NGF-secreting primary rat monocytes: a comparison of different transfer methods.** *J Immunol Methods*, 2013; 391(1–2):112–124.
2. Hohsfield LA, Ehrlich D, Humpel C: **Cholesterol diet counteracts repeated anesthesia/infusion-induced cognitive deficits in male Brown Norway rats.** *Neurobiol Learn Mem*, 2013; 106C:154–162.
3. Hohsfield LA, Ehrlich D, Humpel C: **Intravenous infusion of NGF-secreting monocytes supports the survival of cholinergic neurons in the nucleus basalis of Meynert in hypercholesterolemia Brown Norway rats.** *J Neurosci Res*, in press.

Edited by: Thomas Griesbacher (Austrian Pharmacological Society APHAR, and Institute of Experimental and Clinical Pharmacology, Medical University of Graz, Austria; thomas.griesbacher@medunigraz.at)

A1.2

Effect of sodium nitrite intoxication on the cerebellar morphology in mature and aged rats

Stella Dimitrova, Emilia Petrova*, Lilia Georgieva, Mashenka Dimitrova and Dimitar Kadiysky

Department of Experimental Morphology, Institute of Experimental Morphology, Pathology and Anthropology with Museum, Bulgarian Academy of Sciences, Sofia, Bulgaria

*E-mail: emiliapetrova@abv.bg

Intrinsic Activity, 2013; 1(Suppl. 1):A1.2

Abstract withdrawn before publication

A1.3

Activation of kappa opioid receptors reduces seizure activity in a mouse model of temporal lobe epilepsy

Luca Zangrandi and Christoph Schwarzer*

Department of Pharmacology, Innsbruck Medical University, Austria

*E-mail: schwarzer.christoph@i-med.ac.at

Intrinsic Activity, 2013; 1(Suppl. 1):A1.3

Background: Neuropsychiatric disorders are one of the main challenges of medicine with epilepsies representing some of the most frequent. Temporal lobe epilepsy (TLE) is the most common type of epilepsies and is often accompanied by marked neuronal degeneration. It was shown that the deletion of prodynorphin in mice and low expression in humans is associated with increased epilepsy vulnerability. Dynorphin targets opioid receptors and in particular the kappa opioid receptor (KOP). KOP receptors are located in strategically ideal places to control hippocampal excitability also in chronic TLE. The aim of this study was to investigate the potential of KOP receptor agonists as antiepileptic drugs and compare it to new generation of anti-epileptic drugs (AEDs) in a mouse model of drug-resistant TLE.

Methods: Fifteen C57BL/6N male mice were injected unilaterally with saline ($n = 5$) or kainic acid (KA; 1 nmol in 50 nl saline; $n = 10$) into dorsal hippocampus. While saline-injected animals did not show any signs of EEG or histopathological alterations, KA caused acute and delayed behavioral, pathological and EEG effects. Four-channel EEG traces were recorded from ipsi- and contralateral hippocampi and motorcortices applying depth and surface electrodes from freely moving mice, respectively. The KOP receptor-specific agonist U-50488H, saline, or one of the new AEDs oxcarbazepine, lamotrigine and levetiracetam were applied i.p. at different doses. Number and duration of EEG seizures were automatically evaluated (Sciworks software) for 45 min preceding and following the injections.

Results: Spike trains, sharp waves and paroxysmal discharges in the ipsilateral hippocampus were observed starting from about 14 days after KA injection. Prolonged EEG seizures occurred frequently after about 4 weeks. Such paroxysmal discharges were accompanied by behavioural arrest and stereotypic behaviour like head nodding. Application of KOP receptor agonists decreased EEG abnormalities caused by KA up to 2 hours in a dose-dependent manner, whereas the AEDs didn't show any significant effect. Animals treated with U-50488H were awake during the time of recordings, unlike those treated with diazepam.

Discussion: Our data demonstrate an anticonvulsant action of KOP receptor agonists in the chronic phase of epilepsy, comparable to the effect of 2.5 mg/kg diazepam.

Acknowledgements: This work was supported by the Austrian Science Fund FWF grant W1206-BO5.

A1.4

Galanin-receptor-3-deficient male mice exhibit anxiety-like phenotype

Susanne Brunner¹, Aitak Farzi², Felix Locker¹, Sabine Ebner¹, Barbara Holub¹, Andreas Lang¹, Johannes Mayr¹, Roland Lang³, Peter Holzer² and Barbara Kofler^{1,*}

¹Laura Bassi Centre of Expertise – THERAPEP, Research Program for Receptor Biochemistry and Tumor Metabolism, Department of Pediatrics, Paracelsus Medical University, Salzburg, Austria;

²Research Unit Translational Neurogastroenterology, Institute of Experimental and Clinical Pharmacology, Medical University of Graz, Austria; ³Department of Dermatology, Paracelsus Medical University, Salzburg, Austria

*E-mail: b.kofler@salk.at

Intrinsic Activity, 2013; 1(Suppl. 1):A1.4

Background: The neuropeptide galanin (GAL) has a wide distribution in the central and peripheral nervous system and is a modulator of various physiological and pathological processes. The GAL receptors, GAL₁, GAL₂, and GAL₃, are all G protein-coupled receptors. They show substantial differences in functional coupling and subsequent signaling activities contributing to the diversity of physiological effects of GAL. A role for GAL as modulator of mood and anxiety was suggested as GAL and its receptors are highly expressed in limbic brain structures of rodents. Injections of GAL into the ventricular system of the brain induce anxiolytic-like effects in Vogel's punished drinking test. Furthermore, increased anxiety-like behavior in the elevated plus maze (EPM) was reported for GAL₁- and GAL₂-receptor-deficient mice. However, up to date there is sparse literature implicating GAL₃ receptors in behavioral functions. Therefore, we measured behavior of GAL₃-receptor-deficient mice (GalR3-KO), to elucidate whether the GAL₃ receptor is involved in mediating behavior-associated actions of GAL.

Methods: Disruption of the GAL₃ receptor locus was achieved by homologous recombination with targeting both coding exons, and mice were maintained on a C57BL/6 background.

Results: The GalR3-KO mouse line exhibits normal breeding and physical development. Hematology and amino acid profile from serum and whole brain of male GalR3-KO mice were not different from wild-type (WT) littermates. In contrast to WT littermates male GalR3-KO mice exhibited an anxiety-like phenotype in the EPM, open field (OF) and light-dark (L/D) test. In the EPM, GalR3-KO mice spent significantly less time on the open arms and, conversely, significantly more time on the closed arms. In the OF test, time spent in the central area and number of visits to this area were significantly reduced in GAL₃-receptor-deficient mice, whereas the number of fecal boli shed was significantly enhanced compared to WT animals. GalR3-KO mice spent significantly less time in the light compartment of the L/D test and also displayed significantly decreased locomotion in the light compartment. Furthermore, GalR3-KO mice were less socially affiliated to a stranger mouse than WT animals in the social interaction test.

Discussion: Our data suggest an involvement of the GAL₃ receptor on GAL-mediated effects on mood, anxiety and behaviour, making it a possible target for new treatment strategies of mood disorders. Additionally, similar anxiety-related results for GAL₁ and GAL₂ receptors hint at a possible heterodimerization of GAL receptors in the context of mediating anxiety and related behaviors.

A1.5

Expression and function of the skeletal muscle calcium channel splice variant Ca_v1.1ΔE29

Nasreen Sultana¹, Gerald J. Obermair¹, Ariane Benedetti¹, Petronel Tuluc² and Bernhard E. Flucher^{1,*}

¹Department of Physiology, Innsbruck Medical University, Austria;

²Department of Pharmacology, University of Innsbruck, Austria

*E-mail: bernhard.e.flucher@i-med.ac.at

Intrinsic Activity, 2013; 1(Suppl. 1):A1.5

Background: The Ca_v1.1 voltage-gated calcium channel is the voltage sensor in skeletal muscle excitation–contraction coupling. Its primary role is to activate gating of the calcium release channel (type 1 ryanodine receptor) in the sarcoplasmic reticulum. Recently, our lab discovered a Ca_v1.1 splice variant with increased voltage sensitivity and current amplitude. The splice variant lacking exon 29 (Ca_v1.1ΔE29) is expressed at low levels in adult muscle, but it is the dominant isoform in embryonic muscle. A recent study showed the presence of Ca_v1.1ΔE29 in patients with muscle weakness and the requirement of the Ca_v1.1 channel in neuromuscular junction development.

Methods: In order to reveal the role of Ca_v1.1ΔE29 in developing muscle and its possible involvement in muscle disease we generated a mouse model where we specifically knocked out exon 29. Quantitative real-time PCR analysis of specific muscle types at different developmental stages was performed to analyze the expression levels of both splice variants (Ca_v1.1 and Ca_v1.1ΔE29). Phenotypic characterization to analyze muscle strength and motor activity was done using home-cage activity, rotarod and treadmill. In order to study the development and patterning of neuromuscular junctions (NMJs) we stained diaphragms isolated from mouse embryos (E14) with α-bungarotoxin conjugated with Alexa 488.

Results: Quantitative real-time PCR analysis of specific muscle types at different developmental stages indicate the possible requirement of Ca_v1.1ΔE29 in prenatal development of muscle as postnatal development was associated with a rapid decrease of Ca_v1.1ΔE29 paralleled by a strong increase of Ca_v1.1. In contrast to a published report showing upregulation of Ca_v1.1ΔE29 in patients with muscle weakness, exclusive expression of Ca_v1.1ΔE29 in exon 29 knockout mice did not result in significant muscle weakness or altered motor activity examined with a battery of behavioral tests. Although published data also suggest the requirement of Ca_v1.1 in neuromuscular junction development, preliminary results indicate that lack of the long Ca_v1.1 isoform does not result in aberrations of acetylcholine receptor prepatterning in embryonic mouse diaphragm.

Discussion: So far our experiments did not reveal effects of the exclusive expression of the embryonic Ca_v1.1ΔE29 on the normal development and function of the mature muscle. Ongoing experiments on single muscle fibers are expected to expose potential effects of increased calcium influx on excitation–contraction coupling. Further analysis of older and damaged muscle will indicate an involvement of Ca_v1.1ΔE29 in disease or reveal potential compensatory mechanisms in the knockout mice.

Acknowledgements: FWF P23479, W1101.

A1.6

Asymmetry in the song of crickets: preferences of females and proximate mechanism of discrimination

Heiner Römer and Stefan Hirtenlehner*

Institute of Zoology, Karl-Franzens University of Graz, Austria

*E-mail: stefan.hirtenlehner@uni-graz.at

Intrinsic Activity, 2013; 1(Suppl. 1):A1.6

Background: Subtle random deviations from perfect symmetry in bilateral traits are suggested to signal reduced phenotypic and genetic quality of a sender, but only little is known about the related receiver mechanisms for discriminating symmetrical from asymmetrical traits. We investigated these mechanisms in behavioural and neurophysiological experiments in the

Mediterranean field cricket, *Gryllus bimaculatus*. A downward frequency modulation at the end of each syllable in the calling song has been suggested to indicate morphological asymmetry in sound radiating structures between left and right forewings.

Methods: Phonotaxis of female crickets was quantified on a trackball system in two-choice situations. Under identical stimulus paradigms, the discharge of the pair of AN1 neurons was recorded, known for its importance in female phonotaxis.

Results: Even under ideal laboratory conditions on a trackball system, female crickets only discriminated between songs of symmetrical and asymmetrical males in two-choice experiments at carrier frequencies of 4.4 kHz and large modulation depth of 600 and 800 Hz. Under these conditions they preferred the pure tone calling songs over the modulated (asymmetrical) alternative, whereas no preference was observed at carrier frequencies of 4.9 and 5.2 kHz. These preferences correlate well with responses of a pair of identified auditory interneurons (AN1). The interneuron is tuned to an average frequency of 4.9 kHz, and the roll-off towards lower and higher frequencies determines the magnitude of responses to pure tone and frequency-modulated calling songs. The difference in response magnitude between the two neurons appears to drive the decision of females towards the song alternatives.

Discussion: It is unlikely that song differences based on asymmetry in the morphology of song-producing structures play an essential role under natural conditions.

Acknowledgements: The research was funded by the Austrian Science Fund (FWF): P20882-B09.

A1.7

Levels of α5-containing nicotinic receptors in animal models of neuropathic pain

Bogdan Ianosi¹, Dimitris Xanthos², Johannes Beiersdorf¹, Ariane Thrun¹, Sigismund Huck¹ and Petra Scholze^{1,*}

¹Department of Pathobiology of the Nervous System, Center for Brain Research, Medical University of Vienna, Austria; ²Department of Neurophysiology, Center for Brain Research, Medical University of Vienna, Austria

*E-mail: petra.scholze@meduniwien.ac.at

Intrinsic Activity, 2013; 1(Suppl. 1):A1.7

Background: Neuronal nicotinic acetylcholine receptors (nAChR) are pentameric ligand-gated cation channels made up by nine α and three β subunits that can assemble into a multitude of different homo- or hetero-pentameric receptors. Both the pharmacological and biochemical properties of a given receptor are greatly affected by the subunit composition receptors are being made of. One of the subunits that have recently attracted particular attention is α5. This is a special subunit, since it cannot participate in the formation of a binding site, but requires at least one other α and one other β subunit to form a functional receptor. α3β4 and α4β2 receptors have, however, changed properties if they contain the α5 subunit as well. According to a recent report, deletion of the α5 subunit abolished the inhibitory effects of higher nicotine doses on brain reward systems. Likewise, recent publications suggest that α5-containing nicotinic receptors in the spinal cord might be up-regulated in a rat model of neuropathic pain. In the current study, we examined the levels of α5-containing nicotinic receptors in different brain regions and in the spinal cord of mice, subjected to an animal model of neuropathic pain.

Methods: A partial sciatic nerve ligation (PSNL) or a chronic constriction injury (CCI) was performed in wild-type mice in order to induce neuropathic pain. Animals were sacrificed at the peak of pain symptoms (5 days post PSNL or 10 days post CCI). We collected tissue from the ipsi- and contralateral spinal cord either at the lumbar region L3–L6 (the myelomere corresponding to the sciatic

nerve) or at the thoracic region. Furthermore, we dissected thalamus, hippocampus, habenula, interpeduncular nucleus and striatum, all of which are brain regions that have been shown to be involved in pain processing. In order to analyze the levels of $\alpha 5$ -containing receptors we performed immunoprecipitation of nAChRs labeled with the nicotinic agonist [^3H]epibatidine, using our recently generated, highly specific polyclonal antibodies.

Results: We could not detect any significant changes in $\alpha 5$ levels neither in the spinal cord (comparing the injured ipsilateral to the contralateral side), nor in any other brain region tested (comparing receptor levels in PSNL or CCI mice with those in sham-operated animals).

Discussion: In the tested regions, neither the expression of $\alpha 5$ nAChR nor the total number of nAChRs seems to be modified by acute pain.

Acknowledgements: Grant support: Austrian Science Fund FWF (project P19325-B09). We thank Mrs. Karin Schwarz and Mrs. Gabriele Koth for excellent technical assistance.

A1.8

$\alpha 5$ -containing nicotinic receptors in animal models of neuropathic pain and response to nicotine

Johannes Beiersdorf¹, Dimitris Xanthos², Ariane Thrun¹, Sigismund Huck¹ and Petra Scholze^{1*}

¹Department of Pathobiology of the Nervous System, Center for Brain Research, Medical University of Vienna, Austria; ²Department of Neurophysiology, Center for Brain Research, Medical University of Vienna, Austria

*E-mail: petra.scholze@meduniwien.ac.at

Intrinsic Activity, 2013; **1**(Suppl. 1):A1.8

Background: Nicotinic acetylcholine receptors (nAChR) are pentameric ligand-gated cation channels made up by nine α and three β subunits that can assemble into a multitude of different homo- or hetero-pentameric receptors. The subunit composition crucially influences the pharmacological and biochemical properties of a given receptor. nAChR are of obvious clinical interest: in the central nervous system they have been connected, among others, with learning and memory, neurodegeneration, development, addiction and pain. The nAChR subtypes mediating pain mechanisms are largely unknown. Recent data suggest, that the incorporation of the accessory subunit $\alpha 5$ into the receptor pentamer might change pain-related behavior and might also influence the sensitivity to the analgetic action of nicotine. In the current study, we examined the role of $\alpha 5$ -containing nicotinic receptors in mouse animal models of neuropathic pain and in the analgesic response to nicotine.

Methods: A chronic constriction injury was performed in $\alpha 5^{-/-}$ mice and in wild-type mice, in order to induce neuropathic pain symptoms. Animals were followed with nociceptive tests over a timecourse and the thermal analgesic response to acute subcutaneous nicotine was assessed.

Results: In the nociception time course, $\alpha 5^{-/-}$ mice showed no significantly different behavior as compared to wild-type mice after the nerve injury. Thermal analgesia to nicotine at different time points after a nerve injury was similar in $\alpha 5^{-/-}$ animals as compared to wild-type mice.

Discussion: Our results suggest that the $\alpha 5$ nicotinic receptor subunit does not play a major role in mouse animal models of neuropathic pain or in the thermal analgesic response to nicotine.

Acknowledgements: Grant support: Austrian Science Fund FWF (project P19325-B09). We thank Mrs. Karin Schwarz and Mrs. Gabriele Koth for excellent technical assistance.

A1.9

Mouse cerebellum: physiological and morphological development of the Purkinje neurons

Bruno Benedetti* and Bernhard E. Flucher

Department of Physiology and Medical Physics, Innsbruck Medical University, Austria

*E-mail: bruno.benedetti@i-med.ac.at

Intrinsic Activity, 2013; **1**(Suppl. 1):A1.9

Background: The mouse cerebellum is immature at birth. Most of its structure develops within the first postnatal weeks while pups learn to walk. During this period the shape and innervations of the Purkinje neurons undergo most dramatic changes. While a correct maturation leads to healthy motor behavior, developmental dysfunctions often lead to ataxia. Here we describe the physiological (and morphological) development of Purkinje neurons in this critical period.

Methods: With patch clamp experiments in acute cerebellar slices we quantified the spontaneous excitatory (ePSC) and inhibitory (iPSC) post synaptic currents received by Purkinje neurons. Furthermore, we correlated this physiological characterization with a measurement of the dendrite arborization at different postnatal days (P).

Results: The ePSC and iPSC frequency increased between P7 and P20. Moreover, upon blockade of GABAergic receptors the ePSC frequency increased twofold between P9 and P20. Thus, from the second postnatal week the neurotransmitter GABA has an inhibitory control over the excitatory synapses. Such inhibitory control was absent at an earlier age (P7), in agreement with the predicted intracellular chloride concentration during the first postnatal week. At youngest age (P7), PSCs with fast kinetics prevailed. Later (P9–P20), a second population of iPSC and ePSCs with slower kinetics appeared.

Discussion: PSC frequencies and kinetics correlate with the size and complexity of the dendritic arborization which increased with age. We suggest that the peri-somatic synapses mediate fast events and distal synapses mediate slower events due to distance-dependent filtering by the dendritic arborization of the Purkinje neurons. We hypothesize that distal synapses and slow-kinetics events would be selectively affected by a reduced arborization in ataxic mice. This novel insight on the cerebellar development will be used as baseline for similar analysis in a mouse model of ataxia.

Acknowledgements: This project is funded by SFB F44 (Cell signaling in chronic CNS disorders), by Innsbruck Medical University and by FWF P23479.

A1.10

Phosphomimetic mutation S605D affects the C-terminal sensitivity of mouse glycine transporter GlyT1b to calpain cleavage

Andrea Miháliková, Martina Baliová and František Jurský*
Laboratory of Neurobiology, Institute of Molecular Biology, Slovak Academy of Sciences, Bratislava, Slovak Republic

*E-mail: frantisek.jursky@savba.sk

Intrinsic Activity, 2013; **1**(Suppl. 1):A1.10

Background: Both N-terminal and C-terminal cytosolic regions of glycine transporter 1 (GlyT1) contain calpain cleavage sites. While the role of the N-terminal part of the transporter is not clear, the C-terminus contains regulatory elements crucial for its cellular trafficking. Recombinant GlyT1 C-terminus (GlyT1C) contains at least four calpain cleavage sites but it is unclear whether all these sites are cleaved *in vivo* [1,2]. Our recent experiments indicate that GlyT1C might be protected against calpain cleavage via phosphorylation.

Methods: We performed bioinformatic search for potentially phosphorylated residues in the GlyT1C protein sequence. The effects of phosphorylation on calpain cleavage were investigated *in vitro* and in mouse N2a cells via introduction of phosphomimetic mutations.

Results: We performed bioinformatic search where we identified several potentially phosphorylated threonine and serine residues. Serine 605 in mouse GlyT1b is highly conserved between species and has a high probability of being phosphorylated. In the recombinant protein where this residue was replaced by phosphomimetic mutation S605D the cleavage of GlyT1C at the previously detected calpain cleavage site T602/T603 [2] was blocked. Interestingly, no other cleavage sites were affected, which indicates that the general 3D structure of GlyT1C is not modified extensively by this mutation. In addition, the neutral mutation S605A did not block cleavage at this site. To investigate this effect *in situ* we prepared GlyT1 constructs containing S605D or S605A mutations and transfected these DNA constructs into N2a cells. After treatment with calpain, in the case of phosphomimetic S605D mutation, immunoreactivity was preserved indicating that phosphorylation may protect the transporter against cleavage. Wild-type protein preserved moderate immunoreactivity, indicating its partial phosphorylation, while the S605A mutant lost immunoreactivity almost completely.

Discussion: Our results suggest that phosphorylation of GlyT1 at serine 605 might prevent the calpain cleavage of the transporter C-terminus at the T602/T603 site.

Acknowledgements: This work was supported by the Slovak grant agency VEGA, grants 2/0084/13 and 2/0086/13.

References

1. Baliova M, Jursky F: **Calpain sensitive regions in the N-terminal cytoplasmic domains of glycine transporters GlyT1A and GlyT1B.** *Neurochem Res*, 2005; 30(9):1093–1100.
2. Baliova M, Jursky F: **Calcium dependent modification of distal C-terminal sequences of glycine transporter GlyT1.** *Neurochem Int*, 2010; 57(3):254–261.

A1.11

Changes in the expression of histone deacetylase (HDAC) 1–11 mRNAs in the hippocampus of a mouse model of temporal lobe epilepsy

Rohan Jagirdar, Meinrad Drexel, Ramon O. Tasan and Günther Sperk*

Department of Pharmacology, Medical University of Innsbruck, Austria

*E-mail: guenther.sperk@i-med.ac.at

Intrinsic Activity, 2013; 1(Suppl. 1):A1.11

Background: Gene expression can be regulated epigenetically by DNA methylation and post-translational histone modification. Histone modifications involve deacetylation of histone proteins contributing to transcriptional silencing of gene expression. Deacetylation of histone proteins is carried out by the histone deacetylase (HDAC) family of enzymes, which is classified in four different classes comprising 11 HDAC isoforms. We now investigated changes in the expression of HDAC mRNAs in an animal model of temporal lobe epilepsy (TLE).

Methods: C57BL/6N mice were injected unilaterally with kainic acid (KA; 0.35 nmol / 70 nl) into the dorsal hippocampus (CA1). EEGs were continuously recorded subdurally of the ipsilateral hemisphere for 4 weeks. After an initial status epilepticus (lasting for 3 days) the animals exhibit about 2 severe spontaneous seizures per day. In the injected hippocampus losses in CA1 and CA3 pyramidal cells are observed after 24 hours and granule cell dispersion after 14 days.

Expression levels of HDAC1–11 mRNAs were investigated by *in situ* hybridization 4, 12, 24, 48 hours and 14 days after KA injection.

Results: In the dentate gyrus, mRNA expression of HDAC1, 2, 7 and 11 was significantly decreased 4 hours after KA both ipsilaterally and contralaterally to the injection, recovering after 48 hours. In contrast, HDAC5 mRNA levels were significantly increased 4 and 12 hours after KA injection, remaining increased in the injected hippocampus at later time points. There was also a pronounced increase in HDAC9 mRNA expression 2 and 14 days after KA restricted to the injected hippocampus. For HDAC3 we observed a transient increase in mRNA levels after 24 to 48 hours (contralaterally) and a decrease of HDAC4 mRNA expression after 24 hours (ipsi- and contralaterally).

Discussion: Our data show distinctly different and specific expression patterns for the different HDAC mRNAs indicating rather specific changes in the expression of numerous genes after KA-induced seizures. The early bilateral decreases in HDAC1, 2, 7 and 11 mRNAs may relate to the initial status epilepticus. They may induce fast expression of various genes described earlier and could be compensated by the subsequent overexpression of HDACs 2 and 3. The increase in HDAC5 mRNA expression was restricted to the injected hippocampus and its time course coincided with occurring neurodegeneration. The increase in HDAC9 mRNA, markedly increasing after 14 days at the injection site, may be associated with the granule cell dispersion developing at this time.

Acknowledgements: Supported by the Austrian Science Fund (Project I664 to G.S.).

A1.12

Effects of lysine mutants of fibroblast growth factor receptor 1 on axon growth

Barbara Hausott, Alexandra Förste, Stefan Mangger and Lars Klimaschewski*

Division of Neuroanatomy, Innsbruck Medical University, Austria

*E-mail: lars.klimaschewski@i-med.ac.at

Intrinsic Activity, 2013; 1(Suppl. 1):A1.12

Background: Fibroblast growth factors (FGFs) and their cognate receptors (FGFR1–4) promote axon growth during development and regeneration of the nervous system. The Ras/ERK and the PI3K/Akt pathway represent two major FGF signaling pathways for axon growth. Ligand-induced FGFR activation is followed by endocytosis and degradation in lysosomes, which leads to the termination of FGF signaling. Alternatively, receptors may be recycled back to the cell surface resulting in prolonged signaling. Among the four types of FGFRs, FGFR1, FGFR2 and FGFR3 are mainly sorted to lysosomes for degradation, whereas FGFR4 is predominantly recycled back to the plasma membrane. FGFR1 contains 29 lysine residues in its intracellular domain, which represent possible ubiquitination sites. By contrast, the intracellular part of FGFR4 harbours only 16 lysine residues. In adult sensory neurons, FGFR1 is expressed at much higher levels than FGFR4. We previously reported that overexpression of FGFR1 promotes FGF2-induced elongative axon growth. This effect is further enhanced by the protease inhibitor leupeptin, which inhibits degradation of FGFR1 and promotes receptor recycling.

Methods: Adult sensory neurons were transfected with FGFR1 mutants with reduced numbers of lysines and analyzed for axon growth as well as for ERK activation.

Results: In the present study, we analyzed the effects of FGFR1 mutants with reduced numbers of lysines on axon growth of adult sensory neurons *in vitro*. The FGFR1 lysine mutant FGFR1-15R contains 14 lysine residues. Accordingly, FGFR1-15R is preferentially recycled back to the plasma membrane similar to FGFR4. This lysine mutant FGFR1-15R with enhanced recycling

capabilities strongly promoted elongative axon growth of adult sensory neurons without additional branching. ERK signaling of adult sensory neurons was not enhanced by mutant FGFR1-15R compared to the wild-type FGFR1. Furthermore, the ERK inhibitor PD98059 revealed no inhibitory effect on elongative axon growth induced by mutant FGFR1-15R. In comparison, the lysine mutant FGFR1-26Ra with three lysine residues and reduced signaling activity as well as the signalling-inactive lysine mutant FGFR1-29R without lysine residues had no effect on axon growth.

Discussion: Together, our results strongly imply that lysine mutant FGFR1-15R with 14 lysine residues promotes axon elongation, but not axonal branching, of adult sensory neurons *in vitro*. This effect seems not to be mediated by the ERK pathway, which is commonly involved in elongative axon growth. Thus, alternative signaling pathways induced by FGFR1-15R need to be explored.

A1.13

A supercritical density of fast Na⁺ channels ensures rapid propagation of action potentials in GABAergic interneuron axons

Hua Hu and Peter Jonas*

Institute of Science and Technology (IST) Austria, Klosterneuburg, Austria

*E-mail: peter.jonas@ist.ac.at

Intrinsic Activity, 2013; 1(Suppl. 1):A1.13

Background: Fast-spiking, parvalbumin-expressing GABAergic interneurons/basket cells (BCs) play a key role in fast feedforward and feedback inhibition, network oscillations in the gamma frequency range, and information processing in cortical circuits. For these functions, the fast and reliable propagation of action potentials (APs) from the soma to the presynaptic terminals of these interneurons is critically important. It is generally thought that fast AP propagation in axons is achieved by either large axon diameter or myelination. However, the functional properties of interneuron axons have remained elusive.

Methods: Here, we examined interneuron axons directly by confocally targeted subcellular patch clamp recording.

Results: Simultaneous axonal and somatic recordings revealed that APs were initiated at a constant site, ~20 μm from the soma, and were propagated to distal axonal sites with high reliability and speed. Subcellular mapping revealed a unique Na⁺ channel distribution in the BC axon, with a stepwise increase of conductance density from the soma to the proximal axon, followed by a further gradual increase in the distal axon. Both active cable modeling and experiments in which a fraction of Na⁺ channels was blocked indicated that a low axonal Na⁺ channel density is sufficient to ensure reliability, but a high density is required to support a high velocity of AP propagation.

Discussion: Thus, it is concluded that BC axons express Na⁺ channels at a supercritical density value to ensure rapid AP propagation.

A1.14

Searching for active forms of sanguinarine inhibiting the glycine transporter GlyT1

František Jurský*, Martina Baliová and Andrea Miháliková
Laboratory of Neurobiology, Institute of Molecular Biology, Slovak Academy of Sciences, Bratislava, Slovak Republic

*E-mail: frantisek.jursky@savba.sk

Intrinsic Activity, 2013; 1(Suppl. 1):A1.14

Background: Sanguinarine is a natural alkaloid highly abundant in vesicles of certain plants, which are part of traditional medicinal extracts. This alkaloid has many biological targets and their

identification might help to decipher its pleiotropic action. We recently identified glycine transporter GlyT1 as a new target of sanguinarine [1]. Here, we compared the inhibitory potency of known forms of sanguinarine on GlyT1.

Methods: The effect of sanguinarine on GlyT1-mediated uptake was compared in limiting conditions where the individual forms of sanguinarine were preferentially present in the uptake assay.

Results: To investigate the role of individual forms of sanguinarine in inhibition of GlyT1 we transfected human GlyT1 into HEK293T cells and measured the uptake of glycine in conditions of low or high pH, when mainly sanguinarine base or pseudobase is present, as previously described [1]. In these conditions sanguinarine pseudobase appears to be the active substance. To obtain a third sanguinarine form we used described method [2] to transform sanguinarine to dihydrosanguinarine using borohydride. Results showed that such a reduction eliminated the inhibitory activity of sanguinarine. Since dihydrosanguinarine represents the first step of sanguinarine metabolic elimination, this alkaloid will be active in GlyT1 inhibition *in vivo* only for a limited period of time. However, because of the irreversibility of inhibition, it is difficult to predict the time course of the effect of sanguinarine on GlyT1 *in vivo*.

Discussion: Sanguinarine pseudobase is the likely active form of the alkaloid inhibiting GlyT1. The duration of its action *in vivo* is, however, likely limited by the metabolic transformation of sanguinarine to inactive dihydrosanguinarine.

Acknowledgements: This work was supported by the Slovak grant agency VEGA, grants 2/0084/13 and 2/0086/13.

References

- Jursky F, Baliova M, Mihalikova A: **Molecular basis for differential glycine transporters sensitivity to sanguinarine.** *Toxicol Lett*, 2012; 212(3):262–267.
- Vicar J, Soural M, Hlavac J: **Separace kvartérních benzo[c]fenathridinových alkaloidů z *Macleaya cordata* [Separation of quaternary benzo[c]phenanthridine alkaloids from *Macleaya cordata*].** *Chem Listy*, 2010; 104:51–53.

A1.15

Cell-type- and synapse-specific STORM superresolution imaging of the endocannabinoid system: a new approach to combine physiology, anatomy and quantitative molecular imaging at the nanoscale

Barna Dudok¹, László Barna¹, Szilárd I. Szabó¹, Eszter Szabadits¹, Balázs Pintér¹, Stephen G. Woodhams¹, Christopher M.

Henstridge¹, Gyula Y. Balla¹, Rita Nyilas¹, Csaba Varga², Sang-Hun Lee², Máté Matolcsi³, Judit Cervenak⁴, Imre Kacs Kovics⁴, Masahiko Watanabe⁵, Miriam Melis⁶, Marco Pistis⁶, Ivan Soltesz² and István Katona^{1,*}

¹*Institute of Experimental Medicine, Hungarian Academy of Sciences, Budapest, Hungary;* ²*Department of Anatomy and Neurobiology, University of California, Irvine, CA, USA;* ³*Alfréd Rényi Institute of Mathematics, Hungarian Academy of Sciences, Budapest, Hungary;* ⁴*ImmunoGenes Kft, Budakeszi, Hungary;* ⁵*Department of Anatomy, Hokkaido University School of Medicine, Sapporo, Japan;* ⁶*Department of Biomedical Sciences, University of Cagliari, Città Universitaria di Monserrato, Italy*

*E-mail: katona@koki.hu

Intrinsic Activity, 2013; 1(Suppl. 1):A1.15

Background: Correlative investigations on morphological and physiological parameters, together with their underlying molecular dynamics, have been difficult to perform in the brain. To circumvent this limitation, we present a rapid and versatile approach, which enables the correlation of physiological and morphological data with nanoscale molecular imaging in a cell-type- and synapse-specific manner.

Methods: *In vitro* patch clamp or *in vivo* juxtacellular electrophysiological recordings and anatomical reconstructions in combination with STORM (stochastic optical reconstruction microscopy) superresolution microscopy was achieved within a week and with high yield (50–100 axon terminals per cell).

Results: The experiments established new organizational principles of CB₁ cannabinoid receptor subaxonal distribution on distinct types of hippocampal GABAergic boutons at the nanoscale level. Moreover, we uncovered that a distinct subsynaptic architecture results in an increased perisynaptic CB₁ receptor population on hippocampal basket cells compared to dendritic cells. Finally, the power of this approach was further demonstrated by uncovering robust CB₁ down-regulation upon Δ^9 -THC administration, which has important implications for the amnesic effects of this psychoactive cannabis compound.

Discussion: These findings demonstrate that cell-type-specific STORM superresolution imaging is a very efficient experimental approach and suggest that cell-type-specific quantitative differences of CB₁ receptor distribution in a dedicated perisynaptic nanodomain on boutons may underlie the different efficacy of cannabinoid-mediated regulation of neurotransmitter release in a synapse-specific manner.

Acknowledgements: The studies were supported by the European Research Council. The authors are also grateful for the Nikon Microscopy Center at the Institute of Experimental Medicine, Hungarian Academy of Sciences, and Nikon Austria GmbH and Auro-Science Consulting Ltd for their support with STORM super-resolution microscopy.

A1.16

The role of the NPY Y₂ receptor in GABAergic neurotransmission within the extended amygdala

James Wood*, Dilip Verma, Günther Sperk and Ramon O. Tasan
Department of Pharmacology, Innsbruck Medical University, Austria

*E-mail: james.wood@i-med.ac.at

Intrinsic Activity, 2013; **1**(Suppl. 1):A1.16

Background: The extended amygdala, comprising primarily the central nuclei of the amygdala and the bed nucleus of the stria terminalis (BNST), is a key component of the brain's survival circuitry and thereby plays a central role in the pathogenesis of anxiety disorders. Neuropeptide Y (NPY) is an evolutionarily conserved, widely expressed neuropeptide that provides a prominent NPY innervation within the extended amygdala. Previous studies have shown that modulating NPY signalling throughout the amygdala influences affective behaviours. Thus, NPY signalling is a potential therapeutic target in the treatment of anxiety disorders. The primary aim of the present study was to characterise how the NPY Y₂ receptor modulates GABAergic neurotransmission within the extended amygdala.

Methods: Whole-cell patch clamp recordings were performed in the medial and lateral central amygdala (CeM and CeL) and BNST in the presence and absence of the NPY Y₂ receptor agonist, PYY_{3–36}. Loss-of-function experiments were performed by selectively deleting the Y₂ receptor gene (NPY2R) in the central amygdala using transgenic mice (floxed NPY2R) and local stereotactic microinjections of AAV-CRE.

Results: Bath application of PYY_{3–36} (50 nM) did not alter GABAergic neurotransmission in the CeL or CeM. However, consistent with previous studies, PYY_{3–36} reduced the frequency, but not amplitude or kinetics, of spontaneous inhibitory postsynaptic currents (sIPSCs) in the BNST. Paired-pulse recordings demonstrated that PYY_{3–36} increased the paired-pulse ratio indicating a reduction in presynaptic release probability in the BNST. Deletion of the Y₂ receptor gene in the central amygdala did

not alter GABAergic neurotransmission in the BNST in the presence or absence of PYY_{3–36}.

Discussion: Our data indicate that activation of the Y₂ receptor does not alter GABAergic neurotransmission in the CeL or CeM. However, we show that Y₂ receptor activation reduces inhibition of the BNST by a presynaptic mechanism and that the central amygdala is not the exclusive Y₂-receptor-expressing projection to the BNST.

Acknowledgements: Supported by FWF (P25851, P22830) and MUI Start (ST20130420001).

A1.17

Electrical and morphological properties of neurites investigated by a novel microelectrode–microfluidic device

Johann K. Mika¹, Heinz D. Wanzenböck^{1,*}, Karin Schwarz², Petra Scholze² and Emmerich Bertagnolli¹

¹*Institute for Solid State Electronics, Vienna University of Technology, Austria;* ²*Center for Brain Research, Medical University of Vienna, Austria*

*E-mail: heinz.wanzenboeck@tuwien.ac.at

Intrinsic Activity, 2013; **1**(Suppl. 1):A1.17

Background: The understanding of the electrical and morphological properties of nerve cells *in vitro* plays an important role in electrophysiology. While the number of cells to record from is limited using the patch clamp technique, microelectrode arrays offer the possibility to record a growing cell population with many electrodes simultaneously. In order to investigate the influence of drugs on the electrical activity of growing neurites we developed a test setup that separates the neurites from the whole culture and arrange microelectrodes near them. We will show a combined approach of a microfluidic device aligned on top of a multielectrode array. This setup enables the electrical recording of growing neurites, through a microchannel, and optical investigation of the whole growing cell population.

Methods: We present a novel device that combines a neurite separation part with two culture chambers connected via 30 custom-designed microchannels. The microchannels (diameter < 10 μ m) act as physical barriers for neuronal somata allowing only neurites to enter. A multielectrode array is precisely aligned within the microchannels so that each microchannel is equipped with two gold microelectrodes. In total 60 electrodes are available for simultaneously recording of neuronal signals. Cells are loaded into the rectangular-shaped culture chambers using one of four cylindrical receptacles located at the end of the chambers. Fabrication in a cleanroom environment involves optical lithography, sputtering, chemical vapour deposition, reactive ion etching and sputtering.

Results: A proof of concept was demonstrated with the growth of sympathetic neurons from the superior cervical ganglion of P5 wild-type mice responding to different levels of nerve growth factor (NGF). Seeded nerve cells were confined in their growing compartment but extended neurites passed the microchannels. Ten days post seeding, neuronal activity was recorded and analyzed using MATLAB. The transparent microelectronic platform also enabled optical monitoring of the cells. Even the isolated neurites grown into the microchannel could be imaged by confocal laser microscopy. Optical investigations were accomplished by immunocytochemistry. Using this novel device we investigated the influence of different NGF concentrations on the electrical activity.

Discussion: The combination of microelectrode array and microfluidic device allows the simultaneous monitoring of electrical and morphological properties of nerve cells in culture. The presented device will provide a versatile platform for future

metabolical and pharmaceutical studies where neurites and somata need to be treated independently of each other.

A1.18

The K_v7 channel openers retigabine and flupirtine exert anti-seizure activity independently of K_v7 channels

Elham Assadpour, Stefan Boehm and Helmut Kubista*

Department of Neurophysiology and Neuropharmacology, Centre of Physiology and Pharmacology, Medical University of Vienna, Austria

*E-mail: helmut.kubista@meduniwien.ac.at

Intrinsic Activity, 2013; 1(Suppl. 1):A1.18

Background: Retigabine and flupirtine are marketed as openers of K_v7 channels and are used to treat epilepsies and pain syndromes, respectively. Here, the mechanisms underlying their anti-seizure activity were investigated.

Methods: Patch clamp recordings were performed in primary cultures of hippocampal neurons from neonatal rats to investigate the effects of retigabine and flupirtine on seizure-like activity (SLA). SLA was evoked by various pharmacological means. Normal electrical activity and SLA were quantified by measuring the area under the curves of the membrane potential recordings.

Results: The area under the curves of discharge activity in primary hippocampal neurons was enhanced four- to twelve-fold by XE 991 (block of K_v7 channels), removal of Mg²⁺ (removal of the physiological block of NMDA receptors), and bicuculline (block of GABA_A receptors), respectively, reflecting the induction of SLA. Retigabine and flupirtine reduced SLA triggered by low Mg²⁺ in a concentration-dependent and reversible manner with half-maximal effects at 3–8 μM. Both agents also reduced SLA triggered by either XE 991 or bicuculline to the same extent.

Discussion: Since the two K_v7 channel openers reduced SLA even when K_v7 channels are unable to open (i.e. in the presence of XE 991), they must be acting via an additional, independent mechanism of action.

Acknowledgements: Supported by the Austrian Science Fund FWF (P19710). It is acknowledged that Mag.^a Ulla Schandl performed a few electrophysiological recordings in the early stages of this study.

A1.19

An Nav1.4 mutant with defective inactivation is extraordinarily sensitive to lidocaine

Vaibhavkumar S. Gawali¹, Péter Lukács¹, René Cervenka¹, Xaver Koenig¹, Lena Rubi¹, Karlheinz Hilber¹, Eugen Timin² and Hannes Todt^{1,*}

¹*Department of Neurophysiology and Neuropharmacology, Medical University of Vienna, Austria;* ²*Department of Pharmacology and Toxicology, University of Vienna, Austria*

*E-mail: hannes.todt@meduniwien.ac.at

Intrinsic Activity, 2013; 1(Suppl. 1):A1.19

Background: Local anaesthetics (LA) exert their action by use-dependent block of voltage-gated Na⁺ channels. This use-dependent block results from prolongation of the time course of recovery of channel availability after the action potential. Prolongation of the time course of recovery may result from slow drug dissociation from fast-inactivated states or from stabilization of native slow-inactivated states. We sought to determine the effect of application of the LA lidocaine on recovery from fast and slow inactivation in a number of mutant Nav1.4 channels with perturbations in inactivation gating.

Methods: We investigated rNav1.4 channels in which the native amino acids at positions 1579–1586 were exchanged by cysteines.

These positions are located in the pore-lining transmembrane S6 segment of domain IV and are important determinants of inactivation gating and LA block. Whole-cell patch clamp measurements were done on tsA201 cells transiently transfected with plasmids coding the rNav1.4 α subunit and its mutants, the sodium channel β1 subunit and GFP. We examined the time course of recovery from fast and slow inactivation produced by 50 ms and by 10 s conditioning pulses to –20 mV, respectively.

Results: Lidocaine (500 μM) significantly slowed recovery from fast inactivation in wild-type channels and in all tested constructs except F1579C, which has previously been identified as major binding site for LA. F1584C did not express sufficient current to be examined. On the other hand, lidocaine had almost no effect on recovery from slow inactivation in any of the tested constructs except M1585C. This mutant was special in that it significantly slowed the time course of recovery from fast inactivation (1.66 ± 0.48 ms vs. 0.87 ± 0.07 ms, *n* = 3 and 8; *p* = 0.02) and dramatically increased the fraction of fast recovery following 10 s conditioning pulses (27 ± 0.05% vs. 5 ± 0.09%, *n* = 3 and 7, *p* = 0.009) when compared to wild-type.

Discussion: The gating perturbations produced by the mutation M1585C most probably result from a stabilization of the fast-inactivated state relative to slow-inactivated and closed states. The fact that lidocaine dramatically increases slow recovery in this construct despite the substantial reduction in occupancy of slow inactivation argues against binding of lidocaine to slow-inactivated states. In conclusion, lidocaine slows recovery from inactivation mainly by slow dissociation from fast-inactivated states, rather than stabilization of slow inactivation.

Acknowledgements: This study was funded by the Austrian Science Fund FWF (grants P210006-B11 and W1232-B11).

A1.20

On the implication of L-type calcium-channel-dependent conductances in hippocampal discharge activity

Manuel Rieß and Helmut Kubista*

Department of Neurophysiology and Neuropharmacology, Medical University of Vienna, Austria

*E-mail: helmut.kubista@meduniwien.ac.at

Intrinsic Activity, 2013; 1(Suppl. 1):A1.20

Background: Ca²⁺-dependent conductances have been suggested to play a crucial role in the regulation of neuronal discharge activity: For example, the non-specific cation channel (CAN)-mediated ion current (ICAN) has been implicated by its excitatory virtue in burst firing, whereas a Ca²⁺-dependent K⁺ channel (K_{Ca})-mediated current (I_{K(Ca)}) has—by its inhibitory virtue—been strongly linked also to regular firing patterns. In a previous study employing current-injection-induced depolarizations [1] we found that primary hippocampal neurons can be distinguished with respect to their preferential L-type calcium channel (LTCC)-coupling to CAN or K_{Ca} channels: in the presence of the action potential blocker tetrodotoxin and the LTCC agonist Bay K8644 these conductances gave rise to either after-depolarizations (ADPs) or after-hyperpolarizations (AHPs) as the injection of current was switched off. Hence we aimed in this study to test the above-mentioned functional links by determination of the preferential LTCC-coupling together with registration of the predominant pattern of discharge activity in the presence of the LTCC agonist.

Methods: Current-clamp experiments were performed in the minimally invasive perforated patch mode. Discharge activity was quantified by determination of the area under the curve in recordings of the membrane potential. LTCC-coupling was tested as described in [1].

Results: Both burst firing and regular firing was observed in neurons showing ADPs, but also in those showing AHPs. However, the area under the curve of burst firing was significantly larger in neurons with excitatory coupling than in those showing the inhibitory coupling mode.

Discussion: Our data support the view that LTCC-mediated activation of ICAN enables particularly long-lasting depolarization waves (long bursts). However, burst firing does not require a predominant LTCC–CAN coupling, because we observed it also in neurons which displayed LTCC–K_{Ca} channel coupling. This also shows that the latter coupling does not force neuronal electrical activity into a tonic firing mode, but may solely restrict bursts to rather short durations. Conversely, LTCC–CAN coupling does not necessarily lead to burst firing. Hence our data suggest that LTCC-induced ICAN and I_{K(Ca)} have no decisive, but only a modulatory role in hippocampal firing patterns.

Reference

1. Geier P, Lagler M, Boehm S, Kubista H: **Dynamic interplay of excitatory and inhibitory coupling modes of neuronal L-type calcium channels.** *Am J Physiol Cell Physiol*, 2011; 300(4):C937–C949.

A1.21

Experiences during cardiac arrest: myth or reality?

Michael L. Berger^{1,*}, Fritz Sterz², Sam Parnia³ and Roland Beisteiner⁴

¹Center for Brain Research, Medical University of Vienna, Austria;

²Department of Emergency Medicine, Medical University of Vienna, Austria; ³Resuscitation Research, Stony Brook University, Stony Brook, NY, USA; ⁴Department of Neurology, Medical University of Vienna, Austria

*E-mail: michael.berger@meduniwien.ac.at

Intrinsic Activity, 2013; 1(Suppl. 1):A1.21

Background: Anecdotal accounts of patients claiming auditory or visual perceptions during resuscitation (partly from an elevated point of view) are quite popular; however, unequivocal documentation of such phenomena is missing. Given functional brain data on disintegration of body and space coordinates with dysfunction of the right temporoparietal junction [1], a systematic investigation on possible perceptions during resuscitation appeared warranted.

Methods: Within the frame of the AWARE study (AWAREness during REsuscitation, S. Parnia, New York), a multicenter prospective study comprising 25 hospitals in the US, UK and Austria, we developed an extended setup including questionnaires and computer stimuli and performed standardized interviews with cardiac arrest patients after cardiopulmonary resuscitation. Above several emergency beds at the participating hospitals, A4-sized images were installed facing the ceiling, invisible from below and changed in a double-blind fashion monthly. At the Department of Emergency Medicine (Medical University of Vienna), these images were presented by a computer screen and changed at random intervals. Here, we present first data of the Vienna part (EK Nr.: 609/2007) of this ongoing study.

Results: Between September 2010 and 2013, 28 resuscitated cardiac arrest patients were deemed appropriate for this study. One of them turned out as cognitively incapable of completing the questionnaire, with two others we lost contact after hospital discharge, and three patients refused the interview. The remaining 22 patients (6 females) ranged from 39 to 83 years of age (mean 54.8). Most of them were interviewed still in hospital 1–21 days (mean 7.3) after resuscitation, 6 patients only after discharge 38–109 days after resuscitation. None of these 22 patients reported any recollections from their time period of unconsciousness.

Discussion: While an earlier study on 344 resuscitated cardiac arrest patients returned a figure of 18% with recollections from the time of unconsciousness [2], the frequency of recollections in our small cohort was lower. However, our number of patients is still too small to draw definite conclusions. The completed AWARE study comprises 152 interviews; their evaluation will be presented at the annual meeting of the American Heart Association in November 2013.

References

1. Blanke O, Landis T, Spinelli L, Seeck M: **Out-of-body experience and autoscapy of neurological origin.** *Brain*, 2004; 127(2):243–258.
2. van Lommel P, van Wees R, Meyers V, Elfferich I: **Near-death experience in survivors of cardiac arrest: a prospective study in the Netherlands.** *Lancet*, 2001; 358(9298):2039–2045. Erratum in: *Lancet*, 2002; 359(9313):1254.

A1.22

Functional characterization of a novel kinase loop phosphoserine during MuSK signal transduction

Bahar Z. Camurdanoglu¹, Christina Hrovat¹, Matthias Tomschik¹, Mathias Madalinski², Gerhard Dürnberger², Karl Mechtler² and Ruth Herbst^{1,*}

¹Center for Brain Research, Medical University of Vienna, Austria;

²Protein Chemistry Facility, IMP/IMBA Research Institute of Molecular Pathology, Vienna, Austria

*E-mail: ruth.herbst@meduniwien.ac.at

Intrinsic Activity, 2013; 1(Suppl. 1):A1.22

Background: Muscle-specific kinase (MuSK) is the main organizer of the neuromuscular synapse. MuSK plays an essential role in formation and maintenance of the neuromuscular synapse during embryonic and postnatal development. MuSK becomes autophosphorylated and initiates its kinase activity in response to agrin, a heparan sulfate proteoglycan released by motor neurons. Activated MuSK phosphorylates downstream targets to induce a signaling cascade driving presynaptic differentiation as well as postsynaptic specialization characterized by the clustering of acetylcholine receptors (AChRs). Impaired MuSK function results in acute neuromuscular deficiencies as shown during Myasthenia gravis or more severely to perinatal death in MuSK-deficient mice due to respiratory failure. Since MuSK kinase activity and downstream signaling is essential for synapse formation, we hypothesized that proteins which are phosphorylated during MuSK signaling represent crucial regulatory factors involved in AChR clustering and neuromuscular synapse development. The main aim of our project is to identify and investigate the phosphoproteomic map during MuSK signaling. Ongoing experiments have focused on elucidating the role of a newly identified phosphoserine site in MuSK.

Methods: A proteomic strategy has been designed for global and quantitative analysis of phosphopeptides during MuSK signaling using mass spectrometry (MS). Analysis of MS revealed a novel phosphoserine site in the MuSK kinase domain. The identified serine was mutated and MuSK mutant constructs were assayed for signaling activity in terms of MuSK activation and downstream events like AChR phosphorylation and clustering.

Results: Analysis of MS identified ~16.000 unique peptides relevant to cytoskeletal rearrangement, protein stability, signaling pathways and nuclear actions. We further identified a novel phosphoserine site in the MuSK kinase domain, which is phosphorylated late during MuSK activation. Preliminary results show that this phosphosite alters the activation mode of MuSK.

Discussion: We propose two possible roles for the novel phosphoserine site: (i) its phosphorylation regulates the extent and

duration of MuSK activation and/or (ii) as binding site for an interaction partner it modulates MuSK downstream signaling.

Acknowledgements: This project is funded by the Austrian Science Fund FWF (grant P24685).

A1.23

Targeting of Smad7 for the modulation of neurogenesis and cognition in the aged mouse

Lara Bieler¹, Julia Marschallinger¹, Pia Zaunmair¹, Ingo Kleiter², Ludwig Aigner¹ and Sébastien Couillard-Després^{1,3,*}

¹Institute of Molecular Regenerative Medicine, Spinal Cord Injury and Tissue Regeneration Center Salzburg (SCI-TReCS), Paracelsus Medical University, Salzburg, Austria; ²Zentrum für Klinische Forschung I, Neuroimmunologisches Labor, Ruhr-Universität Bochum, Germany; ³Institute of Experimental Neuroregeneration, Spinal Cord Injury and Tissue Regeneration Center Salzburg (SCI-TReCS), Paracelsus Medical University, Salzburg, Austria

*E-mail: s.couillard-despres@pmu.ac.at

Intrinsic Activity, 2013; 1(Suppl. 1):A1.23

Abstract withdrawn before publication

A1.24

miRNA expression in learned safety

Marianne Ronovsky, Giorgia Savalli and Daniela D. Pollak*
Department of Neurophysiology and Neuropharmacology, Center for Physiology and Pharmacology, Medical University of Vienna, Austria

*E-mail: daniela.pollak@meduniwien.ac.at

Intrinsic Activity, 2013; 1(Suppl. 1):A1.24

Background: The ability to identify and react properly to signals of safety that may predict absence of danger is critical for preventing chronic stress and anxiety. Learned safety encompasses learning processes, which lead to the identification of episodes of security and regulation of fear responses. Pathological forms of learned safety share features of severe psychopathologies including post-traumatic stress disorder and depression. One of the brain regions critically involved in learned safety is the amygdala, where specific gene expression changes resulting from safety learning have been observed in mice. The aim of the present study is to show how changes of gene expression in the amygdala during learned safety are orchestrated focusing on the role of microRNAs (miRNA).

Methods: In a first experiment, mice were trained for learned safety, and memory was tested 24 hours after the last training session. Expressional levels of 11 miRNAs previously implicated in the regulation of emotions were analyzed in amygdala tissue of learned-safety- and learned-fear-trained control mice by qRT-PCR. Furthermore, in a second experiment the expression of the same 11 miRNAs were analyzed in mice trained in a learned fear paradigm and compared to tone alone and shock alone controls. Finally, a bioinformatical scan was performed, to search for potential microRNA target genes.

Results: Amygdala expression of 5 miRNAs (miR-132, miR-212, miR-15b, miR-100, miR-92) has been found to differ significantly between animals trained for learned safety and for learned fear. In an additional experiment, no changes in the expressional level of these miRNAs were found between learned fear respective control groups. A bioinformatical scan revealed various potential target genes for the miRNAs with learned-safety-specific expression related to stress and depression.

Discussion: The selective modulation of expression of 5 specific miRNAs in the amygdala following learned safety suggests that these miRNAs may account for the regulation of various target

genes forming the molecular basis for the neural mechanisms underlying learned safety.

A1.25

Phosphorylation-mediated surface expression of voltage-gated K_v7 channels

Fatma A. Erdem¹, Xaver Koenig², Wei-Qiang Chen³, Gert Lubec³, Stefan Boehm² and Jae-Won Yang^{1,*}

¹Institute of Pharmacology, Center for Physiology and Pharmacology, Medical University of Vienna, Austria; ²Department of Neurophysiology and Neuropharmacology, Center for Physiology and Pharmacology, Medical University of Vienna, Austria;

³Department of Pediatrics, Medical University of Vienna, Austria

*E-mail: jae-won.yang@meduniwien.ac.at

Intrinsic Activity, 2013; 1(Suppl. 1):A1.25

Background: Voltage-gated K_v7 potassium channels K_v7.2, K_v7.3 and K_v7.5 are important regulators of neuronal excitability. K_v7.3 can form heterotetramers with either K_v7.2 or K_v7.5 via the assembly domain (A-domain) that consists of head, linker and tail regions at the C-terminus. This heteromeric assembly, especially of K_v7.2/K_v7.3, increases the channel current and surface expression. Phosphorylation has been implicated in K_v7 channel function but also in trafficking/surface expression of other K_v channels, such as K_v1.2 and K_v1.1. However, specific *in vivo* phosphorylation sites of K_v7 channels with the claimed properties have not been elucidated.

Methods: *In vivo* phosphorylation sites in K_v7.2 and K_v7.3 were identified by liquid chromatography–tandem mass spectrometry (LC-MS/MS) following in-gel digestion of immunopurified K_v7 channels from transiently transfected heterologous cells and rat brain. Based on their localization, 2 pairs of identified phosphorylated serine (pS) and/or threonine (pT) in K_v7.3 were replaced by site-directed mutagenesis to alanine (A) and aspartic acid (D) to mimic dephosphorylated and phosphorylated forms, respectively, to subsequently measure the current density by patch clamping on cells upon co-expression of wild-type (WT) or mutant K_v7.3 with WT K_v7.2.

Results: LC-MS/MS identified a major portion of phosphorylation at the C-terminal ends, with 12 sites for K_v7.2 and 7 sites for K_v7.3 from heterologous cells and rat brain. Among them, pS541/pT542 and pS558/pS561 in the A-domain of rat K_v7.3 were mutated to either AA or DD and co-expressed with K_v7.2 for electrophysiological studies. Patch clamp recordings showed a significant decrease of K_v7.2/K_v7.3 heteromeric channel current density with the non-phospho-mimic K_v7.3 SS558/561AA, while other mutants (ST541/542AA, ST541/542DD and SS558/561DD) were comparable to WT K_v7.3.

Discussion: The phosphorylation sites identified *in vivo* under physiological conditions indicate constitutively phosphorylated K_v7.2 and K_v7.3 in heterologous cells and rat brain. In addition, the non-phosphorylated form of pS558/pS561 in the A-domain of K_v7.3 shows a reduced current density, which does not change in its phospho-mimic analogue, suggesting that the phosphorylation status at S558 and S561 on K_v7.3 regulates the surface expression of K_v7.2/K_v7.3 channels.

Acknowledgements: We thank Mirja Kastein, Azmat Sohail, Florian Koban and Dr. Oliver Kudlacek for their technical support. This study is supported by the Austrian Science Fund FWF (grant P23670-B09).

A1.26

Comparative models of GABA_A receptors based on homologous pentameric ligand-gated ion channels co-crystallized with ligands

Roman V. Feldbauer, Roshan Puthenkalam and Margot Ernst*

Department of Biochemistry and Molecular Biology, Center for Brain Research, Medical University of Vienna, Austria

*E-mail: margot.ernst@meduniwien.ac.at

Intrinsic Activity, 2013; 1(Suppl. 1):A1.26

Background: GABA_A receptors are major mediators of inhibitory neurotransmission in the brain and belong to the superfamily of pentameric ligand-gated ion channels (pLGIC). They are targets of many clinically important drugs, like benzodiazepines and many general anesthetics. No experimental data on the protein structure exist; however, several X-ray crystal structures of bacterial and eukaryotic homologs are available. These include acetylcholine-binding proteins, bacterial pLGICs and a glutamate-gated chloride channel. Here, we create comparative models of GABA_A receptors based on two bacterial superfamily members, which were co-crystallized with different GABA_A receptor ligands.

Methods: Template structures were obtained from the protein data bank and analyzed for conserved elements with the PDBFold webserver. Initial amino acid sequence alignments of various GABA_A receptor chains ($\alpha 1$, $\beta 3$, $\gamma 2$) and four different bacterial and eukaryotic pLGICs were done with Clustal 2.1. They were modified using the secondary structure alignment from PDBFold. Comparative models were created with Modeller 9.12. In each template protein, residues binding their ligands were labeled by LigPlot⁺, and the corresponding amino acid residues in the homology models were examined.

Results: Models were built considering a total of ten template structures, and six ligand-bound crystal structures were analyzed. So far we can conclude that the binding motifs seen in the crystal structures contain highly conserved ones, and variable ones that may not be informative for GABA_A receptors. For example, the models based on a zopiclone-bound pLGIC indicate a possible binding mode of this ligand in the high-affinity benzodiazepine pocket. Other models that are based on a bromoform-bound pLGIC structure suggest a similar binding site of haloforms in the transmembrane domain of GABA_A receptors as in the template. Other binding sites found in the bacterial channels seem to have no correspondence in the mammalian receptors.

Discussion: Our comparative models indicate several possible binding pockets and provide candidate binding modes of ligands in GABA_A receptors. They can be used to analyze conserved and variable features of ligand recognition in pLGICs and will serve as basis for further computational and experimental studies. The long-term goal is structure-guided drug design.

Acknowledgements: Financial support by the graduate school program MolTag (Austrian Science Fund FWF, grant W1232) to R.P. is gratefully acknowledged.

A1.27

L-type voltage-gated calcium channels in epileptiform activity

Lena Rubi, Ulla Schandl, Michael Lagler, Petra Geier, Daniel Spies, Kuheli D. Gupta, Stefan Boehm and Helmut Kubista*

Department of Neurophysiology and Neuropharmacology, Medical University of Vienna, Austria

*E-mail: helmut.kubista@meduniwien.ac.at

Intrinsic Activity, 2013; 1(Suppl. 1):A1.27

Background: The role of L-type voltage-gated calcium channels (LTCCs) as regulators of neuronal excitability relies on the coupling of LTCC-mediated Ca²⁺ influx to Ca²⁺-dependent conductances. We have shown previously that in moderate depolarisations excitatory Ca²⁺-activated nonspecific cation channel activation prevails, which diminishes and gives way to the activation of hyperpolarising Ca²⁺-dependent potassium channels as the depolarization grows [1]. Thereby, LTCC-mediated Ca²⁺ influx is capable of both augmenting

brief discharge patterns (e.g. bursts of spike firing lasting less than 1 s) and restriction of longer-lasting discharge activity. These findings prompted us to test in a similar approach the effects of LTCC modulation on abnormal firing patterns, namely (long-lasting) seizure-like activity (SLA) and (brief) paroxysmal depolarization shifts (PDS).

Methods: We performed current-clamp experiments on primary hippocampal neurons. SLA was induced by pharmacological means (e.g. low-Mg²⁺ buffer). Induction of PDS was facilitated by caffeine. LTCC activity was modulated by Bay K 8644 (an LTCC agonist) and isradipine (an LTCC antagonist).

Results: Potentiation of LTCCs affected SLA activity in opposing manners, leading to enhancement involving plateau potentials on the one hand and reduction involving more pronounced after-hyperpolarisations on the other hand. In line with our previous finding that small current injection-induced depolarizations are always enhanced by LTCC activity, spontaneous depolarizing events increased upon application of Bay K8644, albeit to varying degrees. Eventually, in about 15% of the neurons, PDS were evoked. However, in caffeine treated neurons, PDS were readily induced in about 60% of the neurons after addition of BayK 8644. Importantly, exerting oxidative stress onto these neurons also led to the formation of PDS in an entirely LTCC-dependent manner.

Discussion: Our data demonstrate that the bimodal effects of LTCC activation on excitability described previously [1] can be extended to epileptiform discharges. Hence, therapeutic reduction of LTCC activity may have little beneficial or even adverse effects on epileptic seizures. However, our data identify enhanced activity of LTCCs as one precipitating cause of PDS. Because evidence is continuously accumulating that PDS represent important elements in epileptogenesis, LTCC inhibitors may prove useful in anti-epileptogenic therapy.

Acknowledgements: This work was supported by a grant of the Austrian Science Fund (FWF) to H.K. (project P19710).

Reference

1. Geier P, Lagler M, Boehm S, Kubista H: **Dynamic interplay of excitatory and inhibitory coupling modes of neuronal L-type calcium channels.** *Am J Physiol Cell Physiol*, 2011; 300(4):C937–C949.

A1.28

Allergic lung inflammation enhances proliferation and modulates microglial activity in the hippocampal dentate gyrus

Barbara Klein^{1,2}, Richard Weiss³, Sébastien Couillard-Després^{1,2}, Josef Thalhammer³ and Ludwig Aigner^{1,2,*}

¹Institute of Molecular Regenerative Medicine, Paracelsus Medical University Salzburg; ²Spinal Cord Injury and Tissue Regeneration Center Salzburg (SCI-TReCS), Paracelsus Medical University Salzburg; ³Division of Allergy and Immunology, Department of Molecular Biology, University of Salzburg

*E-mail: ludwig.aigner@pmu.ac.at

Intrinsic Activity, 2013; 1(Suppl. 1):A1.28

Background: Allergies are affecting a substantial part of the world-wide population and are typically characterized by chronic inflammatory reactions. Since there is increasing evidence that the immune system modulates the functions of the central nervous system (CNS), we asked the question if an acute allergic reaction influences the CNS. For allergy induction in C57BL/6 mice we used a clinically relevant allergen derived from Timothy-grass pollen (Phl p 5).

Methods: Female C57BL/6 mice (aged 10–12 weeks) were divided into 2 groups: age-matched control and allergy ($n = 10$). All experimental procedures were approved by the local authorities. The allergy group was immunized intraperitoneally (i.p.) with 1 μ g

Phl p 5 plus 100 µl of the adjuvant aluminium hydroxide in PBS at weeks 0, 2, and 6. This group was challenged 4 days before the perfusion with 3 doses of 5 µg Phl p 5 in 40 µl PBS intranasally on 3 consecutive days. Blood samples were taken at week 6 (before the 3rd boost) to determine levels of Phl p 5-specific IgG1 and IgG2a (with ELISA), and of IgE (using a rat basophil leukemia cell release assay). For the detection of proliferating cells, a solution of 10 mg/ml bromodeoxyuridine (BrdU) in 0.9% NaCl (w/v) was injected i.p. in a dose of 50 mg/kg body weight on 5 consecutive days during week 7. At week 11, mice were perfused and their brains processed for immunohistochemical analyses. Statistical significance was evaluated using independent-samples *t*-tests.

Results: The measurements of allergen-specific IgG1, IgG2 and IgE antibody titers confirmed a successful sensitization procedure. In comparison to the control group, the allergy group had a higher number of BrdU-positive cells in the granular layer and subgranular zone of the hippocampal dentate gyrus. In the same region, cell proliferation was also increased (assessed by proliferating cell nuclear antigen, PCNA). Moreover, microglial activity in the hippocampal dentate gyrus was altered, since there were fewer cells positive for ionized calcium-binding adaptor molecule-1 (IBA1), and their cell soma was smaller in comparison to the control group.

Discussion: An acute allergic reaction seems to have an effect on cell proliferation in the hippocampal dentate gyrus and to modulate microglial activation. However, it still needs to be determined which cell types are proliferating.

Acknowledgements: This project was supported in part by European Union's Seventh Framework Programme (FP7/2007-2013) under grant agreement no. HEALTH-F2-2011-278850 (INMIND).

A1.29

Biomedical research areas in human neurodegeneration

Gábor G. Kovács*

Institute of Neurology, Medical University of Vienna, Austria

*E-mail: gabor.kovacs@meduniwien.ac.at

Intrinsic Activity, 2013; 1(Suppl. 1):A1.29

Background: Neurodegenerative diseases are characterised by progressive loss of neurons and deposition of abnormal conformers of proteins. There have been only few observations on the full spectrum of proteinopathies in the ageing human brain; furthermore, novel disease phenotypes, disease spreading, selective vulnerability, evaluation of gene products during disease process are also topics which are studied.

Methods: Studies were performed in different levels using immunohistochemistry, genetic analysis, immunoblotting, morphometry, and mathematical analysis.

Results: During a community-based study we performed comprehensive mapping of neurodegeneration-related proteins in the brains of 233 individuals (age at death 77–87). We found that non-Alzheimer's/disease type neurodegenerative pathologies and their combinations have been underestimated but are frequent in reality. We described novel phenotypes of neurodegenerative diseases that affect the glia predominantly. Our mathematical analysis of patterns of tau pathology in 24 subregions of the hippocampus revealed that tau pathology may progress through hippocampal circuitries; however, in a subset of patients the pattern suggests possible local phosphorylation of neuronal tau as a response to a pathogenetic event. Evaluation of products of genes associated with healthy brain ageing revealed complex patterns of the expression of sirtuins in relation to tissue damage.

Discussion: Our observation on the wide spectrum of pathologies in the elderly brain should be considered in diagnostic evaluation of biomarkers, and for better clinical stratification of patients.

Understanding patterns of pathology might serve as rationale to develop selective neurotransmitter- or receptor-based therapies. Evaluation of protective gene products in the brain emphasises that these have complex interactions, which need to be taken into account when searching for therapies.

Acknowledgements: Supported by the Project EU FP7-HEALTH-2011-DEVELAGE no. 278486.

A1.30

Ca_v1.2 and Ca_v1.3 L-type calcium channels are expressed within the neurogenic regions and have functional impact on adult neurogenesis

Julia Marschallinger^{1,2,*}, Alexander Waclawiczek^{1,2}, Peter Rotheneichner^{1,2}, Claudia Schmuckermair³, Nicolas Singewald³, Sébastien Couillard-Després^{1,2} and Ludwig Aigner^{1,2}

¹*Institute of Molecular Regenerative Medicine, Paracelsus Medical University, Salzburg, Austria;* ²*Spinal Cord Injury and Tissue Regeneration Center Salzburg (SCI-TReCS), Salzburg, Paracelsus Medical University, Salzburg, Austria;* ³*Department of Pharmacology and Toxicology, Institute of Pharmacy and CMBI, Leopold-Franzens University of Innsbruck, Austria*

*E-mail: j.marschallinger@pmu.ac.at

Intrinsic Activity, 2013; 1(Suppl. 1):A1.30

Background: L-type voltage-gated Ca²⁺ channels (LTCCs) are widely expressed within the CNS and play an important modulatory role in brain function. Aberrant activity of brain LTCCs is very likely involved in various CNS pathologies (e.g. epilepsy, Parkinson's, Alzheimer's disease), and modulation of LTCCs is discussed as a therapeutic approach for treatment of these disorders. However, LTCCs, and more specifically the channel subtypes Ca_v1.2 and Ca_v1.3, are additionally expressed within the neurogenic regions of the adult CNS (dentate gyrus, subventricular zone), and modification of these Ca²⁺ channels may have profound impact on adult neurogenesis. Hence, this study aimed to elucidate the involvement of LTCCs in adult neurogenesis. Expression patterns of Ca_v1.2 and Ca_v1.3 within the neurogenic regions were examined, and the impact of Ca_v1.3 inhibition on adult neurogenesis was analysed in Ca_v1.3^{-/-} mice.

Methods: Presence and distribution of Ca_v1.2 and Ca_v1.3 within the dentate gyrus and subventricular zone were assessed immunohistologically in adult C57BL/6 mice. Due to the absence of reliable Ca_v1.3 antibodies, the Ca_v1.3-EGFP^{switch+} mouse model was used to detect Ca_v1.3 expression. To address the impact of Ca_v1.3 inhibition on adult neurogenesis, the neurogenic regions of adult (2 months) Ca_v1.3^{-/-} C57BL/6 mice were analysed histologically for different neurogenesis parameters (cell proliferation, differentiation, survival).

Results: Co-labelling analyses with cell-type-specific markers revealed Ca_v1.2 expression predominately in mature granular neurons in the dentate gyrus, while neural stem cells and neuronal progenitor cells were only rarely stained for Ca_v1.2. Ca_v1.3 expression was observed in neural stem cells and in mature neurons, but was nearly absent in the proliferating neuronal progenitor population. Further, astrocytes showed weak Ca_v1.3 expression. Concerning the effects of Ca_v1.3 knockout on adult neurogenesis, histological analyses revealed increased dentate gyrus cell proliferation, reduced survival of newly generated cells, and a significantly reduced number of neural stem cells in adult Ca_v1.3^{-/-} mice compared to wild-type controls. In addition to these effects on neurogenesis, Ca_v1.3^{-/-} mice exhibited a reduced surface area of GFAP⁺ astrocytes in the hippocampus compared to wild-type controls.

Discussion: The present work demonstrates abundant expression of Ca_v1.2 and Ca_v1.3 within the neurogenic niches in the adult

mouse brain. These results, together with the observed alterations of adult neurogenesis in *Ca_v1.3^{-/-}* mice, strongly suggest an involvement of LTCCs in adult neurogenic processes. Thus, modulation of *Ca_v1.2* and *Ca_v1.3* activities may have a crucial impact on neurogenic responses, which should be considered for future therapeutic administration of LTCCs.

A1.31

Abcd2 expression prevents a severe metabolic phenotype in Abcd1-deficient mouse peritoneal macrophages

Zahid Muneer¹, Christoph Wiesinger¹, Till Voigtländer², Johannes Berger¹ and Sonja Forss-Petter^{1*}

¹Center for Brain Research, Medical University of Vienna, Austria;

²Institute of Neurology, Medical University of Vienna, Austria

*E-mail: sonja.forss-petter@meduniwien.ac.at

Intrinsic Activity, 2013; 1(Suppl. 1):A1.31

Background: The inherited neurodegenerative disorder X-linked adrenoleukodystrophy (X-ALD) is caused by mutations in the ATP-binding cassette transporter subfamily D1 gene (*ABCD1*) encoding a peroxisomal membrane transporter. X-ALD is biochemically characterized by the accumulation of very-long-chain fatty acids (VLCFA) in tissues of X-ALD patients and *Abcd1*-deficient mice due to a decreased rate of peroxisomal β -oxidation. *ABCD2*, another peroxisomal ABCD transporter and the closest homologue of *ABCD1*, has been shown to compensate for *ABCD1* deficiency when overexpressed. Macrophages and microglia play an important role in the disease progression. Here, we used mouse primary macrophages to study the compensatory role of *Abcd2* in *Abcd1* deficiency.

Methods: We used thioglycollate-elicited mouse peritoneal macrophages (MPM Φ) from male wild-type, *Abcd1*-, *Abcd2*- and *Abcd1/Abcd2* double-deficient C57BL/6J mice. Immunofluorescence with macrophage marker F4/80 and DAPI (nuclear staining) was used to determine the purity of the isolated MPM Φ . Quantitative RT-PCR was used to determine the *Abcd1*, *Abcd2*, *Elovl1* and *Hprt* mRNA levels. VLCFA levels were determined by tandem GC-MS analysis. The rates of peroxisomal (C26:0) and mitochondrial (C16:0) β -oxidation were determined by the β -oxidation activity assay.

Results: Endogenous *Abcd2* mRNA was expressed at about half the level of *Abcd1* mRNA in wild-type MPM Φ . There was a 2.5-fold accumulation of VLCFA (C26:0/C22:0) in *Abcd1*-deficient MPM Φ compared with wild-type. VLCFA levels in *Abcd2*-deficient MPM Φ were normal. However, VLCFA levels in *Abcd1/Abcd2* double-deficient MPM Φ were strongly increased compared with wild-type (13-fold) and *Abcd1*-deficient (5-fold) cells. The mRNA expression of *Elovl1*, which is responsible for elongation of VLCFA, did not differ among the four genotypes. β -Oxidation activity for C26:0 was significantly decreased (62% of wild-type) in *Abcd1*-deficient MPM Φ and this defect was more severe in *Abcd1/Abcd2* double-deficient MPM Φ (29% of wild-type levels).

Discussion: Our results show that moderate *Abcd2* expression in MPM Φ can prevent more extensive accumulation of VLCFA in *Abcd1*-deficient cells. The strong increase in VLCFA storage upon combined loss of *Abcd1* and *Abcd2* was due to an aggravated defect in the β -oxidation activity for C26:0. This study suggests that a level of *Abcd2* expression approaching that of *Abcd1* is sufficient to normalize the metabolic phenotype of macrophages in X-ALD.

Acknowledgements: This work was supported by the EU project "LEUKOTREAT" no. 241622; Z.M. was supported by a scholarship from the Higher Education Commission of Pakistan.

A1.32

Theta-gamma-modulated synaptic currents in hippocampal granule cells *in vivo* define a mechanism for network oscillations

Peter Jonas* and Alejandro Pernía-Andrade

Institute of Science and Technology (IST) Austria, Klosterneuburg, Austria

*E-mail: peter.jonas@ist.ac.at

Intrinsic Activity, 2013; 1(Suppl. 1):A1.32

Background: Theta-gamma network oscillations are thought to represent key reference signals for memory and spatial information processing in neuronal ensembles in the brain, but the underlying synaptic mechanisms remain unclear.

Methods: To address this question, we performed simultaneous whole-cell patch-clamp recordings from mature granule cells (GCs) and local field potential (LFP) recordings *in vivo* at the dentate gyrus of the hippocampal formation of anesthetized and awake rats.

Results: GCs *in vivo* fired action potentials at low frequency, consistent with sparse coding in the dentate gyrus. GCs were exposed to barrages of fast AMPA-receptor-mediated excitatory postsynaptic currents (EPSCs), primarily relayed from the entorhinal cortex, and inhibitory postsynaptic currents (IPSCs), presumably generated by local interneurons. EPSCs exhibited coherence with the LFP activity predominantly in the theta frequency band, whereas IPSCs showed coherence primarily in the gamma range. Action potentials in GCs were phase locked to network oscillations.

Discussion: Theta-gamma-modulated synaptic currents may provide a framework for sparse temporal coding of information in the dentate gyrus.

Acknowledgements: This study was supported by the Austrian Science Fund FWF (P24909-824) and the European Union (European Research Council Advanced grant to P.J.).

A1.33

Association between P300 amplitudes and ventral striatum BOLD response during gain and loss anticipation

Daniela M. Pfabigan^{1,*,#}, Eva-Maria Seidel^{1, #}, Ronald Sladky², Andreas Hahn³, Katharina Paul¹, Arvina Grahl¹, Martin Küblböck², Christoph Kraus³, Allan Hummer², Georg S. Kranz³, Christian Windischberger², Rupert Lanzenberger³ and Claus Lamm¹
(*contributed equally)

¹*Social, Cognitive and Affective Neuroscience Unit, Department of Basic Psychological Research and Research Methods, Faculty of Psychology, University of Vienna, Austria;* ²*Center for Medical Physics and Biomedical Engineering, Medical University of Vienna, Austria;* ³*Department of Psychiatry and Psychotherapy, Medical University of Vienna, Austria*

*E-mail: daniela.pfabigan@univie.ac.at

Intrinsic Activity, 2013; 1(Suppl. 1):A1.33

Background: The anticipation of favourable or unfavourable events is a key component in our daily life. However, the temporal dynamics of anticipation processes in relation to brain activation are still not fully understood.

Methods: A modified version of the monetary incentive delay (MID) task was administered during separate functional magnetic resonance imaging (fMRI) and electroencephalogram (EEG) sessions in the same 25 participants to assess anticipatory processes with a multi-modal set-up.

Results: During fMRI, gain and loss anticipation were both associated with heightened activation in ventral striatum and reward-related areas. EEG revealed largest P300 amplitudes for gain anticipation, whereas CNV amplitudes distinguished neutral from gain and loss anticipation. Importantly, P300, but not CNV

amplitudes, were related to neural activation in the ventral striatum for both gain and loss anticipation. Larger P300 amplitudes indicated higher ventral striatum blood-oxygen-level-dependent (BOLD) response.

Discussion: Early stimulus evaluation processes indexed with EEG seem to be positively related to sustained activation levels in parts of the ventral striatum which is usually associated with reward processing. The current results, however, point towards a more general mechanism processing salient stimuli during anticipation and transferring motivation into motor responses.

Acknowledgements: This study was supported by the research cluster MMI-CNS, funded by the University of Vienna and the Medical University of Vienna, Austria.

A1.34

Unexpected properties of δ -containing GABA_A receptors in response to ligands interacting with the $\alpha\beta$ - site

Joachim Ramerstorfer¹, Pantea Mirheydari¹, Zdravko Varagić¹, Laurin Wimmer², Marko Mihivilić², Werner Sieghart¹ and Margot Ernst^{1,*}

¹Department of Biochemistry and Molecular Biology, Center for Brain Research, Medical University Vienna, Austria; ²Institute of Applied Synthetic Chemistry, Vienna University of Technology, Austria

*E-mail: margot.ernst@meduniwien.ac.at
Intrinsic Activity, 2013; 1(Suppl. 1):A1.34

Background: GABA_A receptors are the major inhibitory neurotransmitter receptors in the central nervous system and are the targets of many clinically important drugs, which modulate GABA-induced chloride flux by interacting with separate and distinct allosteric binding sites. Recently, we described an allosteric modulation of these receptors occurring upon binding of pyrazoloquinolinones to a novel binding site at the extracellular $\alpha\beta$ - interface [1].

Methods: GABA_A receptors were expressed in *Xenopus laevis* oocytes, and the effects of newly synthesized pyrazoloquinolinones were investigated at different GABA_A receptor subtypes composed of $\alpha\beta$, $\alpha\beta\gamma$ and $\alpha\beta\delta$ receptors using the two-electrode voltage clamp method.

Results: The pyrazoloquinolinones enhanced GABA-induced currents at all receptors investigated, and the extent of modulation depended on the type of α and β subunits present within the receptors. One compound, which exhibited a comparable efficacy at receptors containing $\alpha1\beta3$ or $\alpha1\beta3\gamma2$ subunits, exhibited an unexpected dramatic increase in modulatory efficacy at $\alpha1\beta3\delta$ receptors. Steric hindrance experiments as well as inhibition by a functional $\alpha\beta$ - site antagonist indicated that the effects of this compound were mediated via the $\alpha\beta$ - interface at all receptors investigated. Other experiments indicated that the efficacy of the pyrazoloquinolinones for enhancing GABA-induced currents depended on the structure of the pyrazoloquinolinone as well as on the identity of each individual subunit present in these receptors.

Discussion: This newly identified modulator of GABA_A receptors can unmask extrasynaptic $\alpha1\beta3\delta$ receptors that are assumed to be functionally rather silent in the absence of modulatory agents such as neurosteroids [2]. In contrast to already published modulators of δ -containing GABA_A receptors, such as tracazolate or DS2, this new compound acts via a known binding site at the extracellular $\alpha\beta$ - interface, making it more suitable for a rational design of drugs exhibiting such an action profile. In addition, the existence of a functional antagonist at the $\alpha\beta$ - site can be used for terminating the effects of this compound in *in vivo* studies and for the identification of further compounds from different compound classes interacting with this binding site.

Acknowledgements: The study was supported by the graduate school program MolTag (Austrian Science Fund FWF, grant W1232).

References

1. Ramerstorfer J, Furtmüller R, Sarto-Jackson I, Varagic Z, Sieghart W, Ernst M: **The GABA_A receptor $\alpha\beta$ - interface: a novel target for subtype selective drugs.** *J Neurosci*, 2011; 31(3):870–877.
2. Zheleznova N, Sedelnikova A, Weiss DS: **$\alpha1\beta2\delta$, a silent GABA_A receptor: recruitment by tracazolate and neurosteroids.** *Br J Pharmacol*, 2008; 153(5):1062–1071.

A1.35

Sex-specific effects of plasmalogen deficiency on A β peptides and plaque load in the APP^{swe}/PS1^{dE9} transgenic mouse model for Alzheimer's disease

Markus Redl¹, Iduna Liou¹, Zeljka Topalović¹, Jan Bauer¹, Wilhelm W. Just², Johannes Berger¹ and Sonja Forss-Petter^{1,*}

¹Center for Brain Research, Medical University of Vienna, Austria;

²Heidelberg Center of Biochemistry, University of Heidelberg, Germany

*E-mail: sonja.forss-petter@meduniwien.ac.at
Intrinsic Activity, 2013; 1(Suppl. 1):A1.35

Background: Plasmalogen deficiency has been observed at early stages of Alzheimer's disease (AD). The biosynthesis of ether phospholipids, including plasmalogens, starts in peroxisomes by the enzyme dihydroxyacetone-phosphate acyltransferase (DHAPAT). Plasmalogens are major constituents of biological membranes including lipid rafts, implicated in the pathogenic cleavage of amyloid precursor protein (APP) that generates amyloidogenic A β peptides. Furthermore, plasmalogens are slightly reduced in transgenic mice carrying familial AD mutations in APP and presenilin 1 (PS1). Here, we studied the effects of complete plasmalogen deficiency, as well as of gender, on A β peptide and amyloid plaque formation in APP^{swe}/PS1^{dE9} transgenic mice with either *Dhapat* knockout (KO) or wild-type (WT) status.

Methods: Cohorts of sex- and age-matched double and single mutant littermates and wild-type controls were used for all experiments. Immunohistochemical staining of transgene-derived humanized A β deposited into amyloid plaques was quantified in paraformaldehyde-fixed brain sections. Western blots were used to determine the levels of human A β 40 and A β 42 and of APP^{swe} in mouse brain homogenates. The mRNA levels of APP^{swe} and mouse ApoE were quantified by real-time PCR.

Results: Quantitative immunohistochemical analyses, surprisingly, revealed a decreased A β plaque load in the neocortex of female APP^{swe}/PS1^{dE9}/*Dhapat* KO mice compared with females with normal plasmalogen status. In males, plaque deposition was not affected by *Dhapat* genotype. Biochemical analyses confirmed the histological findings and allowed discrimination between different A β species. A plasmalogen-associated reduction in A β 42 levels was observed in female, but not in male, APP^{swe}/PS1^{dE9}/*Dhapat* KO brains compared with APP^{swe}/PS1^{dE9}/*Dhapat* WT. When comparing gender effects in APP^{swe}/PS1^{dE9}/*Dhapat* WT mice, females produced substantially more A β peptides and amyloid plaques than males. By qRT-PCR and immunoblot analyses, APP^{swe} mRNA and protein levels were similar across genotypes. Thus, differences in expression of the APP^{swe} transgene were excluded as the cause of the sex bias in A β deposition. Finally, starting to address clearance of A β from the brain, we analyzed the endogenous mouse ApoE mRNA levels in the different genotypes; however, neither sex nor *Dhapat* status had any effect.

Discussion: In APP^{swe}/PS1^{dE9} mice, A β peptide levels and plaque load are clearly elevated in females. In ether-lipid deficiency, these sex-specific differences are abolished and females deposit

reduced amounts of A β , similar to the extent in males. Our findings indicate that plasmalogens, or another ether-lipid-derived metabolite, promote the amyloidogenic pathway in female mice. Possibly some endocrine factor modifies APP processing or A β clearance in a plasmalogen-dependent manner.

Acknowledgements: This work was supported by the Austrian Science Fund FWF (P248343-B24).

A1.36

The cell adhesion molecule neuroplastin-65 regulates synaptic localization of GABA_A receptors

Isabella Sarto-Jackson^{1,*}, Rodrigo Herrera-Molina², Karl-Heinz Smalla², Dirk Montag², Eckart Gundelfinger² and Werner Sieghart³
¹Konrad Lorenz Institute for Evolution and Cognition Research, Altenberg, Austria; ²Department of Neurochemistry and Molecular Biology, Leibniz Institute for Neurobiology, Magdeburg, Germany; ³Department of Biochemistry and Molecular Biology of the Nervous System, Center for Brain Research, Medical University of Vienna, Austria

*E-mail: isabella.sarto-jackson@kli.ac.at

Intrinsic Activity, 2013; **1**(Suppl. 1):A1.36

Background: GABA_A receptors are pentameric ligand-gated ion channels that mediate fast inhibitory transmission. Depending on their subunit composition, they exhibit distinct pharmacology and electrophysiology. In addition, receptor subtypes differ in their ability to interact with proteins anchoring receptors at synaptic sites. Neuroplastin-65, a cell adhesion molecule of the immunoglobulin superfamily, is involved in synaptic plasticity and can be regulated by synaptic activity. It mediates homophilic trans-interactions between opposing synaptic membranes and might, thus, contribute to structural integrity of synapses.

Methods: Neuroplastin-65 and GABA_A receptors were co-purified by co-immunoprecipitation from rat brain. Co-localization of neuroplastin-65 and individual GABA_A receptor subtypes was shown in brain sections as well as in hippocampal neurons in culture using immunofluorescence and confocal microscopy. The regulation of GABA_A receptor subtypes by neuroplastin-65 was demonstrated using RNAi studies and a newly generated neuroplastin-65 knockout mouse.

Results: Neuroplastin-65 interacts and specifically co-localizes with GABA_A receptors containing α 1 or α 2, but not α 3 subunits. Down-regulation of neuroplastin-65 by shRNA leads to a loss of synaptic α 2-subunit-containing GABA_A receptors. Characterization of a neuroplastin-65 knockout mouse confirms a significant decrease in the localization of GABA_A receptor α 2 subunits at inhibitory synapses. Receptor surface expression seems to critically depend on the p38 MAPK pathway and is mediated via neuroplastin-65.

Discussion: Neuroplastin-65 appears to be crucial for the matching fidelity of certain postsynaptic proteins with their presynaptic counterparts and to contribute to GABA_A receptor anchoring and/or confining at synaptic sites. The supramolecular structures of these trans-synaptic cell adhesion molecules can provide a platform for concentrating neurotransmitter receptors and associated proteins where information from the cell exterior is conveyed to intracellular signaling cascades that in turn can regulate receptor trafficking. Extracellular activation of neuroplastin-65 induces p38 MAPK that might regulate neurotransmitter receptor abundance or mobility at the cell surface and thus synaptic strength.

A1.37

Amygdala clock gene expression and its relation to depression-like behavior in mice

Giorgia Savalli*, Weifei Diao, Stefan Schulz, Kristina Todtova and Daniela D. Pollak

Department of Neurophysiology and Neuropharmacology, Medical University of Vienna, Austria

*E-mail: giorgia.savalli@meduniwien.ac.at

Intrinsic Activity, 2013; **1**(Suppl. 1):A1.37

Background: Several physiological and behavioral processes are known to exhibit 24-hour rhythmicity. Mood disorder patients show biological rhythm-related symptoms such as disturbances in the sleep/wake cycle, diurnal mood changes and alterations in the circadian pattern of body temperature. However, a causal relationship as well as the molecular mechanism involved have not yet been fully elucidated. In mammals, the suprachiasmatic nucleus (SCN) of the hypothalamus is the master neuronal circadian pacemaker, in which circadian rhythms are autonomously regulated by clock genes. Circadian rhythmicity of clock gene expression can also be found in various other brain regions, including the amygdala, a limbic area implicated in mood disorders. The aim of the present study was to investigate whether the expression of the canonical clock genes exhibit rhythmic expression in the amygdala and whether this potential rhythmicity might be altered in animal models of mood disorder.

Methods: Depression-like behavior was induced in C57BL/6N adult male mice based on a chronic mild stress (CMS) protocol consisting of daily exposure to one of three different stressors (exposure to rat, space restraint, and tail suspension) for 28 days. Mice showing a robust decrease in sucrose preference following CMS, an indicator of anhedonia in rodents, are defined as "responders" and were used as a model of depression. Brains of these anhedonic and of the control mice were collected at six equally spaced time points during a 24-hour interval and samples of the basolateral nucleus of the amygdala (BLA) were isolated using a micro-punch procedure.

Results: Quantitative RT-PCR from control mice revealed that the BLA exhibits rhythmic expression of *Bmal*, *clock*, *Cry2*, *CycloB*, *Id2*, *Per1*, *Per3*, *Reverb- α* , *ROR- β* , *ROR- γ* . Further analysis showed that the rhythmic expression of these genes, except *Bmal*, is abolished in the BLA of anhedonic mice.

Discussion: The present study for the first time analyzed circadian rhythmicity of all known core clock genes in the amygdala and identified a profound dysregulation of clock gene expression in an animal model of depression. Disturbed circadian oscillation of amygdala clock gene expression is proposed as potential molecular mechanisms involved in the pathophysiology of depression.

A1.38

Brain-derived neurotrophic factor genotype status impacts on hippocampal serotonin 5-HT_{1A} receptor binding

Christoph Kraus¹, Pia Baldinger¹, Andreas Hahn¹, Christina Rami-Mark², Wolfgang Wadsak², Markus Mitterhauser², Siegfried Kasper¹ and Rupert Lanzenberger^{1,*}

¹Department of Psychiatry and Psychotherapy, Division of Biological Psychiatry, Medical University of Vienna, Austria; ²Department of Biomedical Imaging and Image-guided Therapy, Division of Nuclear Medicine, Medical University of Vienna, Austria

*E-mail: rupert.lanzenberger@meduniwien.ac.at

Intrinsic Activity, 2013; **1**(Suppl. 1):A1.38

Background: Existing evidence indicates a tight interconnection between serotonin (5-HT) and brain derived neurotrophic factor (BDNF). A functional polymorphism in the promoter region of the BDNF gene (Val66Met), resulting in reduced extracellular BDNF levels in Met carriers, was previously demonstrated to impact on the 5-HT transporter but not the 5-HT_{1A} receptor in humans [1]. However, recent studies show that reduced BDNF levels affect especially hippocampal 5-HT_{1A} functionality [2,3]. The aim of this work was to closer investigate the impact of the Val66Met

polymorphism on subcortical 5-HT_{1A} binding in humans by positron emission tomography (PET).

Methods: Thirty-four healthy subjects from our existing PET database (19 female, 36.4 ± 10.4; 15 male, 37.7 ± 8.7) were matched according to sex, age and BDNF Val66Met genotype status. All subjects underwent PET using the 5-HT_{1A}-selective radiotracer [*carbonyl*-¹¹C]WAY-100635. DNA was extracted from peripheral blood monocyte cells obtained by 9 ml EDTA blood samples using the QIAamp DNA Mini Kit (QIAGEN®). Genotyping was performed for Val66Met (rs6265) using the MassARRAY platform (SEQUENOM®). PET data were spatially normalized to standard MNI space and 5-HT_{1A} receptor binding potential was calculated. A subcortical mask was designed for both hippocampi, amygdalae, insulae and anterior cingulate cortices. Differences in 5-HT_{1A} binding were assessed by ANOVA calculated in SPM8 incorporating sex and genotype status as factors, and age as nuisance variable. The statistical threshold was set to $p < 0.05$ corrected for multiple comparisons using family-wise error rate (FWE).

Results: A significant main effect was found in the left hippocampus ($p = 0.02$). We observed higher 5-HT_{1A} binding in Met allele carriers compared to Val homozygotes in the left ($p = 0.017$) and right ($p = 0.038$) hippocampus. No further region exhibited significant results. Although there was no significant sex × genotype interaction ($p = 0.08$), we detected significantly less 5-HT_{1A} binding in female Val homozygotes than in male in the left ($p = 0.03$) and right ($p = 0.032$) hippocampus. There was no difference between female and male Met carriers.

Discussion: These results demonstrate an impact of BDNF genotype status on hippocampal 5-HT_{1A} receptor binding underlining strong crosslinks between BDNF and the serotonergic system. Female Val carriers exhibited the least amount of hippocampal 5-HT_{1A} binding which is in line with previous evidence showing sex effects of the BDNF × 5-HT interaction. While our dataset points towards elevated hippocampal 5-HT_{1A} binding upon BDNF impairment, the molecular mechanisms of this interaction are assumingly complex and still unresolved.

Acknowledgements: This research was supported by grants of the Oesterreichische Nationalbank (Anniversary Fund, grants no. 11468, 12809) to R.L. and S.K., respectively, and an intramural grant of the Department of Psychiatry and Psychotherapy (Forschungskostenstelle); A.H. was recipient of a DOC fellowship of the Austrian Academy of Sciences (OeAW) at the Department of Psychiatry and Psychotherapy.

References

1. Henningsson S, Borg J, Lundberg J, Bah J, Lindström M, Ryding E, Jovanovic H, Saijo T, Inoue M, Rosén I, Träskman-Bendz L, Farde L, Eriksson E: **Genetic variation in brain-derived neurotrophic factor is associated with serotonin transporter but not serotonin-1A receptor availability in men.** *Biol Psychiatry*, 2009; 66(5):477–485.
2. Burke TF, Advani T, Adachi M, Monteggia LM, Hensler JG: **Sensitivity of hippocampal 5-HT_{1A} receptors to mild stress in BDNF-deficient mice.** *Int J Neuropsychopharmacol*, 2013; 16(3):631–645.
3. Wu YC, Hill RA, Klug M, van den Buuse M: **Sex-specific and region-specific changes in BDNF-TrkB signalling in the hippocampus of 5-HT_{1A} receptor and BDNF single and double mutant mice.** *Brain Res*, 2012; 1452:10–17.

A1.39

Serotonergic organization of the human brain: a multi-tracer positron emission tomography study of healthy subjects

Markus Savli¹, Yu-Shin Ding², Alexander Neumeister², Andreas Bauer³, Wolfgang Wadsak⁴, Markus Mitterhauser⁴, Siegfried Kasper¹ and Rupert Lanzenberger^{1,*}

¹Department of Psychiatry and Psychotherapy, Medical University of Vienna, Austria; ²Department of Radiology and Psychiatry, New York University School of Medicine, New York, NY, USA; ³Institute of Neuroscience and Medicine (INM-2), Research Centre Jülich, Germany; ⁴Department of Biomedical Imaging and Image-guided Therapy, Division of Nuclear Medicine, Medical University of Vienna, Austria

*E-mail: rupert.lanzenberger@meduniwien.ac.at

Intrinsic Activity, 2013; 1(Suppl. 1):A1.39

Background: The cerebral cortex has often been subdivided into numerous areas characterized by structural, functional and cytoarchitectonic features while protein-based organizations schemes are lacking [1]. In the current study we propose a new organizational model of the brain based on protein distributions of the serotonergic system including the major inhibitory (5-HT_{1A} and 5-HT_{1B}), the major excitatory (5-HT_{2A}) receptors and the transporter (SERT) of healthy subjects measured with positron emission tomography (PET) and dedicated radioligands.

Methods: Dynamic PET scans were performed in 95 healthy subjects (age 28.0 ± 6.9 years; 59% males) divided into 4 groups using the selective radioligands [*carbonyl*-¹¹C]WAY100635 for 5-HT_{1A}, [¹⁸F]altanserin for 5-HT_{2A}, [¹¹C]P943 for 5-HT_{1B} and [¹¹C]DASB for SERT. Similarities between receptor distribution patterns were analyzed by means of a hierarchical cluster analysis using Euclidean distances in combination with the Ward linkage method as implemented in R2.15.2. All values were Z-transformed across areas prior to analysis in order to establish equal weight between the protein bindings.

Results: Hierarchical cluster analysis of group average binding potential values revealed two main protein-distinct clusters (Fig. 1). The first exclusively comprised subcortical areas such as the raphe nuclei, thalamus, pallidum, caudate nucleus, putamen, midbrain and striatum, whereas in the second the remaining cortical areas were aggregated. The two main subclusters from the cortical areas partly

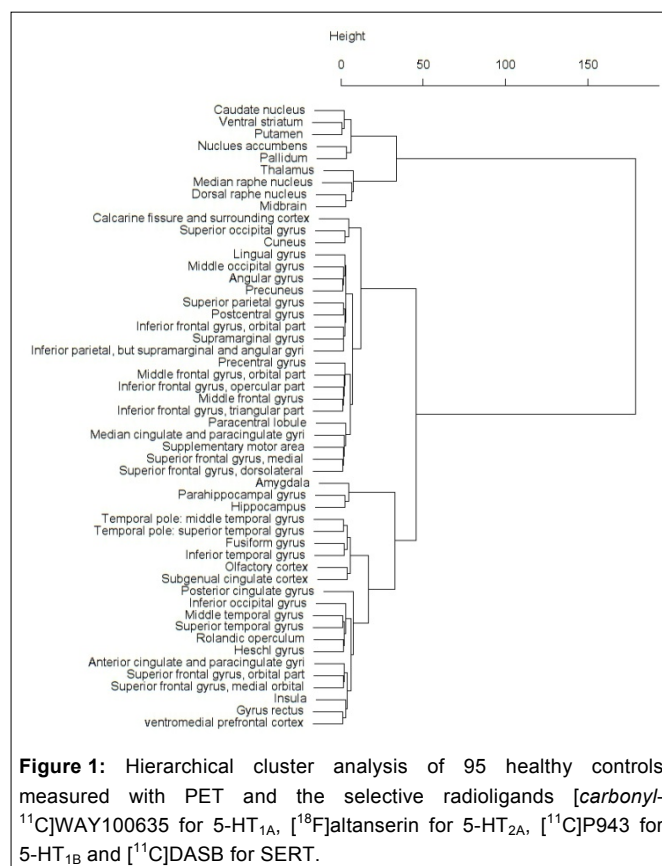


Figure 1: Hierarchical cluster analysis of 95 healthy controls measured with PET and the selective radioligands [*carbonyl*-¹¹C]WAY100635 for 5-HT_{1A}, [¹⁸F]altanserin for 5-HT_{2A}, [¹¹C]P943 for 5-HT_{1B} and [¹¹C]DASB for SERT.

follow lobular definitions. The first predominantly comprises frontal, parietal, occipital and cingulate regions of interest (ROIs), while no marked distinctions are found in further subclusters. The second mainly contains temporal ROIs, but also some frontal ROIs and the hippocampal-amygdala ROIs although with stronger Euclidean distance than cortical ROIs.

Discussion: Applying a data-driven approach we identified brain regions of similar features within the serotonergic system. Interestingly, spatially distant ROIs such as the subcortical areas were identified with close molecular similarity in contrast to cortical ROIs as given by the large Euclidean distance between these two clusters. The two clusters found were in accordance with the familiar classification of cortical and subcortical ROIs. In the lower clusters stringent lobular definition vanishes. This result reflects an explicit hierarchical organization of the serotonergic system and emphasizes functions and interactions of the binding proteins beyond topologies.

Acknowledgements: This research was partly supported by grants from the Austrian National Bank (OeNB 13214 to R.L. and OeNB 13675 to M.M.), the Austrian Science Fund FWF and by an unrestricted investigator-initiated research grant from H. Lundbeck A/S to S.K.

Reference

1. Savli M, Bauer A, Mitterhauser M, Ding YS, Hahn A, Kroll T, Neumeister A, Haeusler D, Ungersboeck J, Henry S, Isfahani SA, Rattay F, Wadsak W, Kasper S, Lanzenberger R: **Normative database of the serotonergic system in healthy subjects using multi-tracer PET.** *NeuroImage*, 2012; 63(1):447–459.

A1.40

Vision impairment in congenital stationary night blindness type 2 (CSNB2): insights from gain-of-function mutations in Cav1.4 L-type calcium channels

Klaus W. Schicker¹, Dagmar Knoflach¹, Vasily Kerov^{2,3}, Simone B. Sartori⁴, Gerald J. Obermair⁵, Claudia Schmuckermair⁴, Xiaoni Liu², Vithiyajali Sothilingam⁶, Marina García Garrido⁶, Markus Bongard⁷, Eduardo Fernández⁷, Sheila Baker³, Martin Glösmann⁸, Mathias Seeliger⁶, Amy Lee² and Alexandra Koschak^{1,*}

¹Department of Neurophysiology and Neuropharmacology, Centre for Physiology and Pharmacology, Medical University Vienna, Austria; ²Department of Molecular Physiology and Biophysics, and ³Department of Biochemistry, University of Iowa, Iowa City, IA, USA; ⁴Department of Pharmacology and Toxicology, Institute of Pharmacy and Centre for Molecular Biosciences Innsbruck, University of Innsbruck, Austria; ⁵Division of Physiology, Innsbruck Medical University, Austria; ⁶Division of Ocular Neurodegeneration, Institute for Ophthalmic Research, Centre for Ophthalmology, University of Tübingen, Germany; ⁷Department of Histology and Institute of Bioengineering, Universidad Miguel Hernández, Alicante, Spain; ⁸Vetcore, University of Veterinary Medicine, Vienna, Austria
*E-mail: alexandra.koschak@meduniwien.ac.at
Intrinsic Activity, 2013; 1(Suppl. 1):A1.40

Background: Mutations in *CACNA1F*, the gene coding for the L-type Ca²⁺ channel Cav1.4, are associated with X-linked congenital stationary night blindness type 2 (CSNB2). Despite the increasing knowledge about the functional behavior of mutated channels in heterologous systems, the pathophysiologic mechanisms that result in defective retinal synaptic transmission remain to be elucidated. Here, we study such functional effects using a gain-of-function mutation (I745T) previously reported in a New Zealand CSNB2 family [1].

Methods: Retinal network activity was assessed using extracellular multielectrode recordings from retinal ganglion cells in a whole mount preparation from wild-type (WT) and mutant (IT) animals. For

comparison with patient data, electroretinograms (ERG) were collected in WT and IT mice. Morphology of WT and IT retinas was studied using immunofluorescence microscopy.

Results: Only half of the retinal ganglion cells recorded in IT mouse retinas did react to light stimulation, while nearly all WT retinal ganglion cells did so. Furthermore a massive increase in the stimulus–response latency of ON cells in IT mouse retinas could be observed and the contrast sensitivity of mutant retinas was vastly reduced. ERG recordings in IT mice showed patterns nicely reflecting pathology seen in human CSNB2 cases. Morphologically, the retinal outer nuclear layer (ONL) in adult IT mutants was reduced in size, and cone outer segments appeared shorter. The organization of the outer plexiform layer (OPL) was disrupted, and synaptic structures of photoreceptors had a variable, partly immature, appearance.

Discussion: The IT mouse line as a specific model for the gain-of-function form of CSNB2 may help to further understand and possibly treat the synaptic dysfunction in CSNB.

Acknowledgements: This work was supported by the Austrian Science Fund FWF (P22528 to A.K.), SFB F44 (F4402 to A.K., F4406 to G.J.O.), P24079-B21 (to G.J.O.), the German Research Council DFG (Se837/6-2), the National Institutes of Health (DC009433 and HL87120 to A.L., DC010362 (Iowa Center for Molecular Auditory Neuroscience), EY020542 to S.A.B.) and the Medical University of Vienna.

Reference

1. Hope CI, Sharp DM, Hemara-Wahanui A, Sisingh JI, Landon P, Mitchell EA, Maw MA, Clover GM: **Clinical manifestations of a unique X-linked retinal disorder in a large New Zealand family with a novel mutation in *CACNA1F*, the gene responsible for CSNB2.** *Clin Experiment Ophthalmol*, 2005; 33(2):129–136.

A1.41

Alterations of tryptophan metabolism in serum and cerebrospinal fluid of patients after stroke

Brenda Semler-Sedlitzky^{1,2}, Berthold Kepplinger^{1,3#,4}, Jochen Reuss³ and Halina Baran^{1,2#,*}

¹Karl-Landsteiner-Institut für Neurochemie, Neuropharmacologie, Neurorehabilitation und Schmerztherapie, Mauer, Austria; ²Department für Biomedizinische Wissenschaften, Veterinärmedizinische Universität Wien, Austria; ³Neurologische Abteilung, Landesklinikum Amstetten, Austria; ⁴SeneCura Neurologisches Rehabilitationszentrum, Kittsee, Austria (#former institution)

*E-mail: halina.baran@neuro-lab.eu

Intrinsic Activity, 2013; 1(Suppl. 1):A1.41

Background: During the last decades alterations of tryptophan metabolites have been described in several neurological diseases as Alzheimer's, Parkinson's, Huntington's disease or epilepsy. In the present study we investigated alterations of tryptophan metabolites in the serum and cerebrospinal fluid of patients suffering from stroke and compared them with corresponding control subjects.

Methods: The content of tryptophan, L-kynurenine, kynurenic acid and anthranilic acid in serum and cerebrospinal fluid of stroke patients ($n = 54$) and in control subjects ($n = 26$) was determined by high performance liquid chromatography. Ratios between the metabolites were analysed. The results were evaluated regarding to sex and age. The statistical analysis was carried out by one-way ANOVA and Student's *t*-test. The study was performed according to the ethical regulations of the government of Lower Austria.

Results: Tryptophan levels were significantly increased in the serum and in cerebrospinal fluid in stroke patients comparing to controls. The increase of tryptophan was more pronounced in stroke

patients aged over 50 years. L-Kynurenine and anthranilic acid content was increased too, but this effect was not statistically significant. Interestingly, kynurenic acid levels were not altered in stroke patients.

Discussion: After stroke, the alterations of tryptophan metabolites were found not only in the central nervous systems but also in the periphery. This increased tryptophan levels indicate disruption of tryptophan metabolism likely due to pathological tissue conditions induced by stroke.

Acknowledgements: This study is supported by Life Science LS-10-37.

A1.42

Alterations of tryptophan metabolites in the serum of stroke patients after repetitive transcranial magnetic stimulation

Brenda Semler-Sedlitzky^{1,2}, Berthold Keplinger^{1,3#4,*}, Sabine Eigner³ and Halina Baran^{1,2#}

¹Karl-Landsteiner-Institut für Neurochemie, Neuropharmakologie, Neurorehabilitation und Schmerztherapie, Mauer, Austria;

²Department für Biomedizinische Wissenschaften, Veterinärmedizinische Universität Wien, Austria; ³Neurologische Abteilung, Landesklinikum Mauer, Austria; ⁴SeneCura Neurologisches Rehabilitationszentrum, Kittsee, Austria

([#]former institution)

*E-mail: berthold.keplinger@neuro-lab.eu

Intrinsic Activity, 2013; 1(Suppl. 1):A1.42

Background: Repetitive transcranial magnetic stimulation (rTMS) as a new non-invasive painless procedure has been tested for augmentation of motor performance and reduction of spasticity in patients suffering from stroke with spastic hemiparesis. The therapeutic effect with respect to a reduction of spasticity and/or an enhancement of motor performance was evaluated. In addition, changes of tryptophan metabolites in the serum before and after the 5th and 10th TMS application were investigated.

Methods: All patients (46) recruited for rTMS treatment underwent brain activity analysis (EEG). The content of tryptophan, L-kynurenine, kynurenic acid and anthranilic acid was determined using high performance liquid chromatography. For statistical analysis the one-way-ANOVA and Student's *t*-test were applied. The study was performed according to the ethical regulations of the government of Lower Austria.

Results: A reduction of spasticity and an enhancement of motor performance could be observed after rTMS. A significant increase of L-kynurenine and a moderate increase of anthranilic acid in the serum were found after rTMS. However, no alterations of tryptophan levels could be seen. After the 5th TMS the L-kynurenine / kynurenic acid ratio increased significantly, while the L-kynurenine / anthranilic acid ratio was significantly lowered. In seven of the rTMS-treated patients an increase of brain activities in the EEG was found. These patients were not further treated with rTMS.

Discussion: A reduction of spasticity and an enhancement of motor performance could be observed by stroke patients after rTMS treatment. Although L-kynurenine increased significantly, only anthranilic acid but not kynurenic acid was increased. It is questionable if the observed neurochemical alterations are relevant for the improvement of the clinical outcome. On the other hand it cannot be excluded that in some rTMS-treated patients alterations of tryptophan metabolism might contribute to enhanced brain activities, for example formation of quinolinic acid. Further studies need to clarify this observation.

A1.43

Early vs. late neural mechanisms during certain vs. uncertain pain anticipation: an EEG and fMRI experiment

Eva-Maria Seidel^{1#,*}, Daniela M. Pfabigan^{1#}, Andreas Hahn², Ronald Sladky^{3,4}, Arvina Grah¹, Katharina Paul¹, Christoph Kraus², Martin Küblböck^{3,4}, Georg S. Kranz², Allan Hummer^{3,4}, Rupert Lanzenberger², Christian Windischberger^{3,4} and Claus Lamm¹

¹Social, Cognitive and Affective Neuroscience Unit, Department of Basic Psychological Research and Research Methods, Faculty of Psychology, University of Vienna, Austria; ²Department of Psychiatry and Psychotherapy, Medical University of Vienna, Austria; ³MR Center of Excellence, Medical University of Vienna, Austria; ⁴Center for Medical Physics and Biomedical Engineering, Medical University of Vienna, Austria

([#]contributed equally)

*E-mail: eva-maria.seidel@univie.ac.at

Intrinsic Activity, 2013; 1(Suppl. 1):A1.43

Background: Anticipatory processes prepare the organism for upcoming experiences. The aim of this study was to investigate neural responses related to anticipation and processing of painful stimuli occurring with different levels of uncertainty.

Methods: Twenty-five participants (13 females) took part in an electroencephalography (EEG) and functional magnetic resonance imaging (fMRI) experiment. A visual cue announced the occurrence of an electrical painful or non-painful stimulus, delivered with certainty or uncertainty (50% chance), at some point during the following 15 seconds.

Results: During the first 2 s of the anticipation phase, a strong effect of uncertainty was reflected in a pronounced frontal stimulus-preceding negativity (SPN) and increased fMRI activation in higher visual processing areas. In the last 2 s before stimulus delivery, we observed stimulus-specific preparatory processes indicated by a centroparietal SPN and insular cortex activation that was most pronounced for the certain pain condition. Uncertain anticipation was associated with prefrontal control processes. During actual stimulation, the results revealed that unexpected painful stimuli produced the strongest activation in the affective pain processing network and a more pronounced offset P2.

Discussion: Our results indicate that during early anticipation uncertainty is strongly associated with affective neural mechanisms and seems to be a more salient event compared to certain anticipation. During the last 2 s before stimulation, control mechanisms are initiated to deal with the increased salience of uncertainty. Furthermore, stimulus-specific preparatory mechanisms during certain anticipation also shaped the response to stimulation, underlining the adaptive value of stimulus-targeted preparatory activity which cannot take place when facing an uncertain event. Understanding the neural basis of pain anticipation and cue-based modulation of pain processing in normally functioning individuals is of particular importance when trying to understand mental states where anticipatory or pain-related processing is disrupted.

Acknowledgements: This study was supported by the research cluster MMI-CNS, funded by the University of Vienna and Medical University of Vienna, Austria, and the Viennese Science and Technology Fund (projects CS11-005 and CS11-016).

A1.44

Monocytes, but not lymphocytes, are severely affected in X-linked adrenoleukodystrophy

Franziska Weber¹, Christoph Wiesinger¹, Sonja Forss-Petter¹, Günther Regelsberger², Hannes Stockinger³ and Johannes Berger^{1,*}

¹Center for Brain Research, Medical University of Vienna, Austria;

²Institute of Neurology, Medical University of Vienna, Austria;

³Center for Pathophysiology, Infectiology and Immunology, Medical University of Vienna, Austria

*E-mail: johannes.berger@meduniwien.ac.at

Intrinsic Activity, 2013; 1(Suppl. 1):A1.44

Background: X-linked adrenoleukodystrophy (X-ALD) is a fatal neurodegenerative disorder with inflammatory demyelination of the brain caused by a deficiency of the ABCD1 protein, encoded by the *ABCD1* gene. The ABCD1 protein, a member of the ATP-binding cassette (ABC) transporter subfamily D, is located in the peroxisomal membrane and transports very-long-chain fatty acids (VLCFA) as CoA esters for degradation by β -oxidation into the peroxisome. Currently, the only curative therapies are allogeneic hematopoietic cell transplantation (HCT) or genetically corrected autologous hematopoietic CD34⁺ stem cell therapy (HSCT). Therefore, we explored the phenotypes of the major immune cell types derived from the CD34⁺ stem cell.

Methods: Immune cells from peripheral blood of controls and X-ALD patients were isolated by magnetic-activated cell sorting (MACS). Purity of cell isolations was verified by flow cytometry. In purified cells, qRT-PCR analysis was used to determine mRNA levels of the ABCD transporters and GC-MS was used for the quantification of VLCFA levels, a diagnostic marker. Additionally, we also measured the peroxisomal β -oxidation capacity in each cell type.

Results: The three peroxisomal ABC transporters were differentially expressed in CD34⁺-derived cell types of healthy controls: ABCD1 and ABCD2 mRNA were inversely expressed in all cell types, whereas ABCD3 was equally distributed. ABCD2, the closest homolog of ABCD1 could be expected to compensate for the loss of ABCD1 function. However, the expression pattern of ABCD2 was unchanged in X-ALD patients; accordingly, cell types lacking ABCD2 mRNA (e.g. monocytes) displayed the most severe biochemical phenotype concerning VLCFA catabolism, whereas cells with substantial ABCD2 expression (e.g. T lymphocytes) were barely affected. Thus, not all investigated immune cells present an intrinsic metabolic defect.

Discussion: Based on these results, we propose that the beneficial effect of HCT and HSCT may rely on the replacement of those cells lacking sufficient ABCD2 expression in ABCD1 deficiency. In addition, these findings support the concept that ABCD2 is a target gene for pharmacological induction, as an alternative treatment strategy, to rescue VLCFA metabolism and possibly halt the inflammation in X-ALD patients.

Acknowledgements: This work was supported by the Austrian Science Fund FWF (project P26112-B19).

A1.45

Subunit composition and distribution of potassium channels of the Slo gene family

Sandra Rizzi¹, Christoph Schwarzer² and Hans-Günther Knaus^{1,*}

¹Division of Molecular and Cellular Pharmacology, Innsbruck Medical University, Austria; ²Institute of Pharmacology, Innsbruck Medical University, Austria

*E-mail: hans.g.knaus@i-med.ac.at

Intrinsic Activity, 2013; 1(Suppl. 1):A1.45

Background: Members of the Slo gene family are structurally highly related potassium channels which markedly differ in their pharmacological and gating properties. Slo1 (BK, big conductance potassium channel) represents the best studied member of the Slo gene family. BK, Slo2.1 and its paralogue Slo2.2 are expressed in the brain. While no accessory subunits have been described for Slo2.1 and Slo2.2, so far BK has been shown to associate with different accessory subunits whose distribution is tissue-specific. In

neurons, two phenotypes of BK channels have been described. Type I BK channels are homotetrameres composed of BK α subunits. Association of BK α subunit with accessory β 4 subunit is conferring characteristics of the type II BK channel. The presence of β 4 subunit strongly influences the functional and pharmacological properties of the BK channel complex, e.g. resistance to specific block by iberiotoxin.

Methods: Little is known regarding the distribution pattern of Slo gene family members in mouse brain. In order to address this issue we are performing *in situ* hybridisation to detect BK α and β 4, Slo2.1 and Slo2.2 mRNA as well as immunohistochemical experiments and western blots. In addition, we are performing iberiotoxin binding studies to specifically detect functional BK type I channels. Comparison of these data will allow us to draw a conclusion of the distribution of type I and type II BK channels in mouse brain.

Results: So far our investigations revealed that the distribution pattern of α and β 4 mRNA overlaps in most brain regions, e.g. the neocortex and principal neurons of the hippocampus do express both, α and β 4 mRNA. However, there are few brain regions, e.g. the amygdala and some thalamic nuclei, which solely express BK channel α , but not β 4 subunit mRNA. Interestingly, there are some brain regions in which β 4 mRNA is expressed in the absence of BK α mRNA, e.g. diagonal band of Broca, paraventricular nucleus, supraoptical nucleus, nucleus facialis and granular cell layer of cerebellar cortex.

Discussion: BK β 4 subunit is not known to have a biological function in the absence of BK α . However, it might well be that it is a promiscuous subunit capable of interacting with other ion channels, e.g. other members of the Slo gene family. To address this issue, we were performing *in situ* hybridisation to detect Slo2.2 mRNA. By comparing Slo2.2 and BK β 4 mRNA distribution patterns we found coexpression in granular cell layer of the cerebellar cortex. To identify novel interaction partners of BK β 4 (possibly including Slo2.2) we presently conduct (co-)immunoprecipitation and mass spectrometry.

Acknowledgements: This project is supported by the Austrian Science Fund FWF (W1206-B05).

A1.46

Y₄ receptors and pancreatic polypeptide are crucial components for fear extinction and permanent suppression of fear

Dilip Verma¹, James Wood¹, Birgit Hörner¹, Sven Hofmann², Annette Beck-Sickinger², Herbert Herzog³, Günther Sperk¹ and Ramon O. Tasan^{1,*}

¹Institute of Pharmacology, Innsbruck Medical University, Austria;

²Institute of Biochemistry, University of Leipzig, Germany;

³Neuroscience Research Program, Garvan Institute of Medical Research, Darlinghurst, Sydney, NSW, Australia

*E-mail: ramon.tasan@i-med.ac.at

Intrinsic Activity, 2013; 1(Suppl. 1):A1.46

Background: Avoiding harmful, dangerous situations and finding food are two closely related behaviours that are essential for surviving in a natural environment. Growing evidence supports an important role of gut-brain peptides, such as pancreatic polypeptide (PP) in modulating not only energy homeostasis but also emotional-affective behaviour. Postprandially released PP reduces food intake by specifically activating Y₄ receptors in brain-stem and hypothalamic nuclei. On the other hand, deletion of Y₄ receptors results in increased stress-induced motor activity, improved stress coping and anxiolytic behaviour. The role of Y₄ receptors in models of conditioned fear and fear extinction, however, has not been addressed so far.

Methods: To investigate the role of Y_4 receptors in conditioned fear we tested Y_4 receptor knockout mice and wild-type mice that were peripherally injected with pancreatic polypeptide.

Results: Here, we demonstrate that in Pavlovian fear conditioning deletion of Y_4 receptors specifically impairs fear extinction in mice while not affecting fear acquisition and recall. Conversely, peripheral injection of a long-acting Y_4 receptor agonist before fear extinction significantly facilitated extinction of cued fear. The effect of PP on extinction of fear was lasting and generalized, suppressing fear in spontaneous recovery, renewal and reinstatement tests. Furthermore, peripherally applied PP during fear conditioning inhibits activation of orexin-expressing neurons in the lateral hypothalamus in wild-type but not in Y_4 knockout mice, suggesting suppression of an overly active arousal as a central mechanism of Y_4 receptor activation.

Discussion: Taken together, our data demonstrate that peripherally released PP facilitates the extinction of conditioned fear by activating central Y_4 receptors, independent of genetic background, age and gender. As central Y_4 receptors are predominantly expressed in brain stem and hypothalamus, our findings provide strong evidence that fear extinction requires the integration of autonomic stimuli, a mechanism that may crucially depend on Y_4 receptors. PP may serve not only as a satiety signal, but may also be useful in promoting fear extinction.

Acknowledgements: Supported by FWF (P25851, P22830) and MUI Start (ST20130420001).

A1.47

Calcium channel $\alpha_2\delta$ subunits: sub-synaptic localization in cultured hippocampal neurons and phenotypic characterization of $\alpha_2\delta$ -1/-3 knockout mice

Clemens L. Schöpf¹, Stefanie Geisler¹, Marta Campiglio¹, Nasreen Sultana¹, Christoph Schwarzer², Ruslan I. Stanika¹, Michaela Kress¹, Bernhard E. Flucher¹ and Gerald J. Obermair^{1,*}

¹Division of Physiology, Innsbruck Medical University, Austria;

²Department of Pharmacology and Toxicology, Innsbruck Medical University, Austria

*E-mail: gerald.obermair@i-med.ac.at

Intrinsic Activity, 2013; **1**(Suppl. 1):A1.47

Background: The $\alpha_2\delta$ subunits of voltage-gated calcium channels are critical factors for the localization, trafficking, and stabilization of the channel complex. Recent developments implicated $\alpha_2\delta$ subunits in specific neuronal functions such as synaptic transmission and synapse formation. In the CNS three $\alpha_2\delta$ isoforms ($\alpha_2\delta$ -1, $\alpha_2\delta$ -2, $\alpha_2\delta$ -3) are stably expressed, however, how the individual $\alpha_2\delta$ isoforms contribute to neuronal functions is largely elusive. The aim of the present study was to characterize the sub-cellular distribution pattern of the three distinct neuronal $\alpha_2\delta$ isoforms and the preliminary characterization of $\alpha_2\delta$ -1/-3 double knockout mice.

Methods: In order to analyze the targeting properties of $\alpha_2\delta$ -1, $\alpha_2\delta$ -2 and $\alpha_2\delta$ -3 in cultured hippocampal neurons each isoform was external epitope-tagged and subsequently transfected into DIV6 hippocampal neurons together with soluble eGFP. Immunofluorescent stainings using an anti-HA antibody together with presynaptic markers were performed at DIV19–25. Double knockout mice for $\alpha_2\delta$ -1 and $\alpha_2\delta$ -3 were established by crossbreeding of $\alpha_2\delta$ -1 and $\alpha_2\delta$ -3 single knockout mice. Phenotypic characterization included homecage activity (general behavior, locomotion), the wirehang test (muscle strength), the catwalk test (gait analysis) as well as the von Frey test (mechanical sensitivity).

Results: Live-cell staining of the HA-tagged $\alpha_2\delta$ isoforms revealed somato-dendritic and axonal surface expression of all three isoforms, whereby $\alpha_2\delta$ -2 showed the strongest surface expression and $\alpha_2\delta$ -3 preferentially accumulated in the axon. All three $\alpha_2\delta$

isoforms were located in presynaptic terminals; however, they displayed a strikingly different sub-synaptic localization pattern. While $\alpha_2\delta$ -1 and $\alpha_2\delta$ -3 formed clusters closely associated with or juxtaposed to synapsin, $\alpha_2\delta$ -2 accumulated in the perisynaptic membrane around the synapsin stain. The $\alpha_2\delta$ -1/-3 double knockout mice display an ~30% reduction in body weight when compared to littermate controls. Reduced homecage activity and muscle strength, as well as altered gait suggest a deficit in motor control. Indeed, α -bungarotoxin staining of diaphragm neuromuscular junctions revealed a higher density of neuromuscular junctions in $\alpha_2\delta$ -1/-3 double knockout mice. Moreover the von Frey assay indicates a highly reduced mechanical sensitivity.

Discussion: The strong dendritic surface expression of $\alpha_2\delta$ -2 and the preferential accumulation of $\alpha_2\delta$ -3 in the axon indicate isoform-specific functions in hippocampal neurons. Differential synaptic localization, especially the perisynaptic expression of $\alpha_2\delta$ -2, indicates unique functional properties of $\alpha_2\delta$ subunits in synapses. The strong phenotype of $\alpha_2\delta$ -1/-3 double knockout mice highlights the importance of $\alpha_2\delta$ -1 and $\alpha_2\delta$ -3 for normal motor control and the peripheral nervous system. In addition, it also reveals a partial functional redundancy of these two $\alpha_2\delta$ isoforms.

Acknowledgements: Austrian Science Fund P24079, P23479, SFB F4406, W01101.

A1.48

Neuropeptide Y Y_2 receptors modulate fear conditioning in distinct nuclei of the amygdala

Dilip Verma¹, Mario Mietzsch², Stefan Weger², Regine Heilbronn², Herbert Herzog³, Günther Sperk¹ and Ramon O. Tasan^{1,*}

¹Department of Pharmacology, Innsbruck Medical University, Austria; ²Institute of Virology, Charité, Campus Benjamin Franklin, Free University of Berlin, Germany; ³Garvan Institute of Medical Research, Darlinghurst, Sydney, NSW, Australia

*E-mail: ramon.tasan@i-med.ac.at

Intrinsic Activity, 2013; **1**(Suppl. 1):A1.48

Background: Neuropeptide Y (NPY) is a 36-amino-acid peptide that is abundantly expressed in the central nervous system. Consistent findings have demonstrated an anxiolytic effect of NPY. The presence of different NPY receptors in the amygdala and the effects of NPY on anxiety raise the question, whether NPY and its receptors may influence acquisition and extinction of conditioned fear. Therefore, we investigated the role of NPY and Y_2 receptors in Pavlovian fear conditioning.

Methods: Pavlovian fear conditioning is a simple form of associative learning that is achieved by repetitive pairing of an initially neutral stimulus, such as a tone with an electric food shock. Testing of the fear memory and extinction of fear is performed the following day by repetitive exposure to the tone in the absence of a foot shock. Here, we combined viral-vector-mediated site-specific deletion of Y_2 receptors and locally restricted over-expression of Y_2 receptor subtype-selective ligands with Pavlovian fear conditioning to elucidate the contribution of Y_2 receptors in different amygdala nuclei in the modulation of learned fear.

Results: Local deletion of Y_2 receptors in the central amygdala (CEA) and in the bed nucleus of the stria terminalis (BNST) resulted in increased freezing during cued fear testing and delayed extinction of conditioned fear, while there was no change in fear acquisition. Deletion of Y_2 receptors in the BLA, however, resulted only in moderately delayed extinction of conditioned fear. On the other hand, rAAV-mediated local over-expression of the Y_2 -specific ligand NPY_{3–36} resulted in facilitated extinction when injected into the BLA, while NPY_{3–36} over-expression in the CEA did not only facilitate fear extinction but also delayed fear acquisition and reduced freezing during cued fear testing.

Discussion: Taken together, our data demonstrate that Y_2 receptor stimulation in the BLA facilitates extinction of fear, while Y_2 receptors in the CEA delay acquisition, reduce fear expression during cued fear testing and promote the extinction of conditioned fear.

Acknowledgements: Supported by the Austrian Science Fund FWF (P22830-B18).

A1.49

Loose coupling between Ca^{2+} channels and sensors enables endogenous buffer control of release probability and short-term dynamics at a cortical synapse

Nicholas P. Vyleta and Peter Jonas*

Institute of Science and Technology (IST), Klosterneuburg, Austria

*E-mail: peter.jonas@ist.ac.at

Intrinsic Activity, 2013; 1(Suppl. 1):A1.49

Background: The distance between Ca^{2+} channels and Ca^{2+} sensors of exocytosis is a key factor determining the speed and efficacy of synaptic transmission. Recent results suggested that transmitter release from presynaptic terminals in the mature mammalian CNS is triggered by Ca^{2+} nanodomains. In contrast, the prevalence of microdomain coupling in the mature CNS is unclear, and its functional significance remains elusive.

Methods: To address these questions, we performed paired recordings between hippocampal mossy fiber terminals and postsynaptic CA3 pyramidal neurons.

Results: Surprisingly, millimolar concentrations of both the fast Ca^{2+} chelator BAPTA and the slow Ca^{2+} chelator EGTA efficiently suppressed transmitter release at mossy fiber synapses. These results suggest loose coupling between Ca^{2+} source and release sensor, with a mean coupling distance of ~ 75 nm. Comparison of release properties of intact and chelator-loaded presynaptic terminals indicated that endogenous Ca^{2+} buffers equivalent to ~ 0.2 – 0.3 mM BAPTA control both release probability and synaptic facilitation. Quantitative modeling demonstrated that endogenous buffer actions were critically dependent on loose channel–sensor coupling.

Discussion: In conclusion, a highly specific coupling configuration explains the unique functional properties of mossy fiber synaptic transmission.

Acknowledgements: This study was supported by the Austrian Science Fund FWF (P24909-824) and the European Union (European Research Council Advanced Grant to P.J.).

A1.50

Phenotypic characterization and brain structure of calcium $\alpha_2\delta$ subunit double knockout mouse models

Stefanie Geisler¹, Clemens L. Schöpf¹, Christoph Schwarzer² and Gerald J. Obermair^{1,*}

¹*Division of Physiology, Innsbruck Medical University, Austria;*

²*Department of Pharmacology and Toxicology, Innsbruck Medical University, Austria*

*E-mail: gerald.obermair@i-med.ac.at

Intrinsic Activity, 2013; 1(Suppl. 1):A1.50

Background: In the central nervous system (CNS) voltage-gated calcium channels (VGCC) regulate neurotransmitter release, gene regulation, and synaptic plasticity. Malfunctions of VGCCs have been linked to neurological diseases, including epilepsy, migraine, and ataxia. Auxiliary $\alpha_2\delta$ subunits regulate trafficking and current properties of VGCCs and may thus modulate specific neuronal functions. Three $\alpha_2\delta$ isoforms ($\alpha_2\delta$ -1, $\alpha_2\delta$ -2, $\alpha_2\delta$ -3) are stably expressed in the CNS; however, their exact roles in normal and diseased nerve cells are largely unknown. Therefore, in order to

elucidate potential specific and redundant functions of $\alpha_2\delta$ isoforms, we generated three distinct $\alpha_2\delta$ double knockout mouse models. Here, we provide the first phenotypic characterization and a preliminary analysis of brain development.

Methods: $\alpha_2\delta$ -1/-2, $\alpha_2\delta$ -1/-3, and $\alpha_2\delta$ -2/-3 double knockout mice were generated by cross-breeding single $\alpha_2\delta$ knockout ($\alpha_2\delta$ -1, $\alpha_2\delta$ -3) or mutant ducky ($\alpha_2\delta$ -2) mice. Phenotypic evaluation included gross behavioral examination and life span analysis. Overall brain structure and development was analyzed in Nissl-stained 20 μ m sagittal cryosections.

Results: $\alpha_2\delta$ -1/-2 and $\alpha_2\delta$ -2/-3 double knockout mice display epileptic seizures and the typical ducky mouse gait. However, unlike ducky ($\alpha_2\delta$ -2 mutant) mice, they show a severely impaired development indicated by an increased mortality during the first month after birth. In contrast, $\alpha_2\delta$ -1/-3 double knockout mice are viable and show muscle weakness, altered gait, and reduced mechanosensitivity (see abstract A1.45 by Schöpf *et al.*). In Nissl-stained histological brain sections, $\alpha_2\delta$ -1/-3 knockout mice show normal brain structure when compared to littermate controls. In contrast, $\alpha_2\delta$ -1/-2 knockout mice display an overall reduction in brain size similar to ducky mice. In addition, specific brain regions, including cortex and cerebellum, are atrophic suggesting impaired development.

Discussion: By generating distinct $\alpha_2\delta$ isoform double knockout mouse models we provide novel insights into isoform-specific functions. While $\alpha_2\delta$ -1/-3 knockout mice are viable with defects in motor control and the peripheral nervous system (see abstract A1.45 by Schöpf *et al.*), $\alpha_2\delta$ -1/-2 and $\alpha_2\delta$ -2/-3 double knockout mice display severe neurological disease, impaired development and reduced life spans. Altogether, these results suggest unique and specific roles for $\alpha_2\delta$ -2, while $\alpha_2\delta$ -1 and $\alpha_2\delta$ -3 isoforms may mediate partially redundant functions.

Acknowledgements: Austrian Science Fund P24079 and SFB F4406.

A1.51

Distribution of $Ca_v1.2$ L-type voltage-gated calcium channels and β -adrenergic receptors signaling complexes in cultured hippocampal neurons

Claudia Ramprecht, Angela Steinberger and Valentina Di Biase*

Institute of Biophysics, Medical University of Graz, Austria

*E-mail: valentina.di-biase@medunigraz.at

Intrinsic Activity, 2013; 1(Suppl. 1):A1.51

Background: In the central nervous system $Ca_v1.2$ L-type voltage gated calcium channels contribute to synaptic plasticity, learning, and memory. Calcium influx via $Ca_v1.2$ channels couples membrane excitation to nuclear transcription by activating specific signaling pathways. The selective activation of individual pathways strictly depends on the specificity of the channel interaction with the associated signaling proteins. $Ca_v1.2$ channels form signaling complexes with β_2 adrenergic receptors (β_2AR) in excitatory neurons. Interestingly, β_2AR regulate synaptic plasticity and share signaling pathways to the nucleus with $Ca_v1.2$ channels.

Methods: Here, by fluorescence immunolabeling techniques and live fluorescence microscopy, we analyze the $Ca_v1.2$ – β_2AR complex at the membrane in subcellular compartments of cultured hippocampal neurons.

Results: Live surface staining of HA in neurons transfected with extracellularly HA-tagged $Ca_v1.2$ channels ($Ca_v1.2$ -HA) shows the distribution of $Ca_v1.2$ channels in clusters along the dendritic shaft and spines. Similarly, immunolabeling experiments of the extracellular FLAG tag in FLAG- β_2AR -transfected neurons shows the distribution of β_2AR in clusters along the shaft and on dendritic spines resembling the discrete clustered distribution of $Ca_v1.2$

channels. Double immunolabeling of HA and FLAG in neurons co-transfected with Ca_v1.2-HA and FLAG-β2AR revealed that Ca_v1.2 channels and β2AR often, but not always, co-localize. A 30-min treatment with the adrenergic agonist isoproterenol decreases the density of Ca_v1.2 clusters along the shaft whereas the density of Ca_v1.2 clusters tends to increase on the spines in the same experimental conditions. Previously, by FRAP experiments on neurons transfected with extracellularly tagged super-ecliptic-phluorin-conjugated Ca_v1.2 channels (Ca_v1.2-SEP), we demonstrated that a population of Ca_v1.2 channels is capable of lateral diffusion [1]. Isoproterenol treatment of Ca_v1.2-SEP-transfected neurons revealed that adrenergic stimulation increases the recovery rate of Ca_v1.2-SEP channels in FRAP experiments.

Discussion: Our data suggest that the adrenergic stimulation may modulate surface traffic of Ca_v1.2 channels. Furthermore, we propose that the formation of the Ca_v1.2–β2AR complex occurs at different subcellular compartments and is subject to activity-driven regulation.

Acknowledgements: Supported by the Austrian Science Fund FWF (grant P25085 to V.D.B.).

Reference

1. Di Biase V, Tuluc P, Campiglio M, Obermair GJ, Heine M, Flucher BE: **Surface traffic of dendritic Ca_v1.2 calcium channels in hippocampal neurons.** *J Neurosci*, 2011; 31(38):13682–13694.

A1.52

Acetylcholine release by nicotinic receptors in CNS

Farahnaz Beiranvand, Sigismund Huck and Petra Scholze*
Department of Pathobiology of the Nervous System, Center for Brain Research, Medical University of Vienna, Austria

*E-mail: petra.scholze@meduniwien.ac.at
Intrinsic Activity, 2013; **1**(Suppl. 1):A1.52

Background: Neuronal nicotinic acetylcholine receptors (nAChR) are ligand-gated ion channels and are composed of a diverse array of nine α (α2–10) and three β (β2–4) subunits. nAChRs in the central nervous system have prominent presynaptic effects by controlling the release of both acetylcholine (ACh) (by autoreceptors) and other neurotransmitters (by heteroreceptors). Although we have made substantial progress in understanding the function of presynaptic nAChRs in enhancing e.g. dopamine and noradrenaline release we know little about their role as autoreceptors. This lack of knowledge is a serious shortcoming considering that nAChRs may be involved in diseases like M. Alzheimer or schizophrenia.

Methods: Brain slices from hippocampus, the parietal cortex, as well as entire interpeduncular nuclei (IPN) and habenulae of both mice and rats were loaded with the ACh precursor [³H]choline and were transferred to superfusion chambers. The release of neurotransmitter was induced by electrical stimulation or by short (30 s) exposure to nicotine. The outflow of radioactivity was determined by scintillation counting.

Results: Nicotine induced the release of [³H]choline from the IPN in a concentration-dependent manner in both rats and mice. The nicotine-induced release was Ca²⁺-dependent but TTX-insensitive. However, the two species differed significantly both in terms of potency and intrinsic activity of nicotine. Nicotine did not trigger any [³H]choline release in mice lacking the β4 subunit, whereas the nicotine-induced release in β2 knockout mice was unaffected. Compared with electrical stimulation, the nicotine-induced [³H]choline release was low in the hippocampus of both rats and mice. Likewise, the nicotine-induced [³H]choline release was low in the habenula of both species despite a high density of nAChRs in this brain region.

Discussion: Taken together, our findings show that nACh autoreceptors play a major role in the IPN but not in the hippocampus, the cortex, and the habenula.

Acknowledgements: Grant support: Austrian Science Fund FWF (project P19325-B09).

Special Session SFB and DK

A2.1

The L-type voltage-gated calcium channel Ca_v1.2 α₁ subunit in activated reactive astrocytes around β-amyloid plaques in an Alzheimer mouse model

Nina Daschil¹, Gerald J. Obermair², Bernhard E. Flucher², Birgit Hutter-Paier³, Manfred Windisch³, Nadia Stefanova⁴, Josef Marksteiner⁵ and Christian Humpel^{1,*}

¹*Department of Psychiatry, Laboratory of Psychiatry and Experimental Alzheimer's Research, Innsbruck Medical University, Austria;* ²*Departments of Physiology and Medical Physics, Innsbruck Medical University, Austria;* ³*JSW-CNS Lifesciences, Grambach, Austria;* ⁴*Departments of Neurology and Neurosurgery, Innsbruck Medical University, Austria;* ⁵*Department of Psychiatry and Psychotherapy, LKH Hall, Hall in Tirol, Austria*

*E-mail: christian.humpel@i-med.ac.at
Intrinsic Activity, 2013; **1**(Suppl. 1):A2.1

Background: Alzheimer's disease (AD) is the most common progressive neurodegenerative disorder in elderly people and leads to a severe cognitive decline. We have recently shown, that the L-type voltage-gated calcium channel (LTCC) Ca_v1.2 α₁ subunit is expressed in reactive astrocytes surrounding β-amyloid (Aβ) plaques in a transgenic (tg) amyloid precursor protein (APP)-overexpressing mouse model. The aim of the present study was (1) to observe, whether the auxiliary β4 subunit colocalizes with the Ca_v1.2 α₁ subunit in these Alzheimer mice and (2) to investigate the mRNA expression of all subunits by *in situ* hybridization. (3) In addition, we wanted to determine the expression levels of all LTCC subunits in wild-type (wt) primary astrocytes and whether exogenous stimuli may modulate their expression.

Methods: Brain sections of wt and tg mice (11 months) were immunohistochemically stained to investigate the cellular expression of Aβ, GFAP, and Ca_v1.2 α₁ and β4 subunits. Furthermore, we performed *in situ* hybridization on brain sections using [³⁵S]-labelled oligonucleotides. Primary astrocytes were isolated from postnatal mice and incubated with various treatments (PKC-ε agonist, cAMP agonist, human and murine Aβ₄₂ peptides, Aβ_{25–35} peptide) to induce cell activation. Following this, the mRNA expression levels were examined by quantitative real-time PCR utilizing subunit-specific Taqman assays.

Results: In 11-month-old tg mice, exhibiting a high number of Aβ plaques, the number of Ca_v1.2 α₁-immunoreactive cells, colocalizing with GFAP-positive astrocytes, increased significantly. A colocalization of Ca_v1.2 α₁-positive cells with the β4 subunit could not be observed. Silver-grain density, which represents radioactive staining of various LTCC subunit oligonucleotides, was significantly enhanced with Ca_v1.2, β2, β4 and α_{2δ}-1 subunits on Aβ plaque cores (60 μm diameter). Interestingly, within the halo area (180 μm diameter) an increase of grain density could only be detected for α_{2δ}-1 and α_{2δ}-2 subunits. Stimulation of primary astrocytes for three days with either a PKC-ε agonist (DCP-LA) or murine Aβ₄₂ peptides (10 μg/ml) showed a significant upregulation of the Ca_v1.2 α₁ subunit.

Discussion: In summary, Ca_v1.2 α₁-subunit-like immunoreactivity, but not mRNA, is strongly expressed in reactive astrocytes close to Aβ plaques in an AD mouse model. Our findings show that activated

astrocytes express almost all auxiliary subunits; however, a colocalization could not be shown so far. It remains unclear whether $Ca_v1.2$ is functionally active in reactive astrocytes and contributes to Ca^{2+} dysregulation and whether it can serve as a target for future therapeutic strategies.

Acknowledgements: This study was supported by the Sonderforschungsbereich SFB F4405-B19 and F4406-B19.

A2.2

Excitation of rat sympathetic neurons via M_1 muscarinic receptors involves protein kinase C and chloride channels

Isabella Salzer, Viola Gindl, Peter Mahlknecht, Hend Gafar, Helmut Drobný and Stefan Boehm*

Department of Neurophysiology and Neuropharmacology, Centre of Physiology and Pharmacology, Medical University of Vienna, Austria

*E-mail: stefan.boehm@meduniwien.ac.at

Intrinsic Activity, 2013; 1(Suppl. 1):A2.2

Background: Acetylcholine is the prime transmitter in all autonomic ganglia and causes excitation of postganglionic neurons via both, nicotinic and muscarinic receptors. The excitation via muscarinic M_1 receptors is believed to rely on an inhibition of K_v7 channels. Here, we searched for alternative signaling mechanisms.

Methods: Patch clamp recordings and [3H]noradrenaline release experiments were performed in primary cultures of superior cervical ganglion (SCG) neurons from neonatal rats.

Results: The muscarinic agonist oxotremorine M (OxoM, 10 μM) depolarized SCG neurons, as did the K_v7 channel blocker XE991. In the presence of XE991, OxoM still caused depolarization which was reduced in the presence of the Cl^- channel blockers niflumic acid and 4-acetamido-4'-isothiocyanostilbene-2,2'-disulphonic acid (SITS). OxoM triggered release of previously incorporated [3H]noradrenaline, and this effect was also diminished by niflumic acid and SITS; reduction of extracellular Cl^- enhanced OxoM-induced release. Thus, the excitatory action was mediated by Cl^- channels. To elucidate the signaling cascade between M_1 receptors and the Cl^- channels, OxoM-triggered [3H]noradrenaline release was tested in the presence of the protein kinase C (PKC) inhibitors staurosporine, GF 109203X, GÖ 6976, and GÖ 6983, all of which led to an inhibition. For comparison, noradrenaline release evoked by electrical field stimulation was not affected, neither by the PKC inhibitors nor by the Cl^- channel blockers.

Discussion: These results suggest that activation of M_1 muscarinic receptors on rat SCG neurons leads to an opening of Cl^- channels via Ca^{2+} -dependent PKC isoforms. This novel signaling mechanism contributes to the ganglionic transmission by acetylcholine via muscarinic receptors.

Acknowledgements: Supported by the doctoral program CCHD which is co-funded by the Austrian Science Fund and the Medical University of Vienna.

A2.3

Lanthanide-resonance-energy-transfer-based distance measurements in the mammalian glutamate transporter (excitatory amino-acid transporter) 3

Kusumika Saha¹, SanthoshKannan Venkatesan¹, Azmat Sohail¹, Thomas Stockner¹, Simon Bulling¹, Walter Sandtner¹, Gerhard F. Ecker² and Harald H. Sitte^{1,*}

¹Institute of Pharmacology, Center for Physiology and Pharmacology, Medical University Vienna, Austria; ²Department of Medicinal Chemistry, Pharmacoinformatics Research Group, University of Vienna, Austria

*E-mail: harald.sitte@meduniwien.ac.at

Intrinsic Activity, 2013; 1(Suppl. 1):A2.3

Background: EAAT3 (excitatory amino-acid transporter 3) mediates the regulation of synaptic transmission by reuptake of glutamate in the synaptic cleft. EAAT3 belongs to the family of soluble carrier family 1 member 1 (SLC1A1) and is selectively enriched in the neurons of the hippocampus, cerebellum and the basal ganglia. The motivation of the study is to gain insight into the structure–function relation of EAAT3. The project utilizes the high-resolution crystal structure of GltPh, the bacterial orthologue of *Pyrococcus horykoshi* to mammalian glutamate transporters. GltPh provides a structural framework for the determination of the helical movement in EAAT3. The structural rearrangement of the protein is caused by the helical movements which will be assessed by distance measurements using the technique of lanthanide resonance energy transfer (LRET).

Methods: LRET relies on Förster's theory of resonance energy transfer where there is distance-dependent transfer of energy between the donor fluorochrome to an acceptor fluorochrome. The protein is expressed in *Xenopus laevis* oocytes. Lanthanide-binding tags (LBT) have been inserted into the protein to chelate the lanthanide terbium which serves as the donor element. Existing amino-acid residues in the protein are mutated to cysteine which then react to an acceptor dye (bodipy FL) serving as acceptor. The energy transferred from the acceptor to the donor can be converted into a specific distance estimate.

Results: The measured distances will allow us to obtain new insights into the structure–function relationship of the glutamate transporters and can be further investigated using different substrates and inhibitors.

Discussion: The results obtained in this project will allow us to better understand pathophysiological conditions associated with loss of function in EAAT3, for instance in ischemia or mutations associated with obsessive compulsive disorder.

Acknowledgements: The study is supported by F3506 and W1232 MolTag.

A2.4

Investigating nucleus accumbens neuronal network activity by multi-electrode array recordings

Kai K. Kummer^{1,*}, Michaela Kress², Alois Saria¹ and Gerald Zernig¹

¹Experimental Psychiatry Unit, Innsbruck Medical University,

Austria; ²Division of Physiology, Innsbruck Medical University,

Austria

*E-mail: kai.kummer@i-med.ac.at

Intrinsic Activity, 2013; 1(Suppl. 1):A2.4

Background: A main challenge in the therapy of drug-dependent individuals is to help them reactivate interest in non-drug-associated activities. Among these activities, social interaction is doubly important because treatment adherence itself depends on it. We recently developed an experimental rat model based on the conditioned place preference (CPP) paradigm, in which only four 15-min episodes of dyadic social interaction with a sex- and weight-matched male conspecific, (i) reverse CPP from cocaine to social interaction and (ii) inhibit the reacquisition / reexpression of cocaine CPP [1]. In concurrently trained animals for CPP, pairing cocaine with one compartment and social interaction with the other (i.e. mutually exclusive stimulus presentation during CPP training), excitotoxic lesioning of the nucleus accumbens core (AcbC) or the basolateral amygdala shifted CPP toward social interaction, whereas nucleus accumbens shell (AcbSh) inactivation shifted CPP toward cocaine [2].

Methods: Network activity was recorded using *in vitro* multi-electrode array recordings (MEA; MultiChannelSystems, Reutlingen) of acute coronal Acb slices (thickness 400 μm) obtained

from (1) cocaine CPP-conditioned (coc-CPP), (2) cocaine control (coc-ctrl), (3) saline control (sal-ctrl), and (4) naive C57BL/6 mice.

Results: Ongoing discharge activity was present in acute brain slices in all treatment groups (i.e. coc-CPP, coc-ctrl, sal-ctrl, naive) in the following regions: AcbC, AcbSh, dorsal striatum, islands of Calleja, ventral pallidum, medial and lateral septum. We found a significant increase in number of spike-recording electrodes in cocaine-administered animals (coc-CPP and coc-ctrl: 506 of 4800) as compared to cocaine-naive animals (sal-ctrl and naive: 337 of 5100; $\chi^2 = 48.62$, $p < 0.0001$), and median spike frequencies (coc-CPP: 0.18 Hz, coc-ctrl: 0.16 Hz, sal-ctrl: 0.12 Hz, naive: 0.12 Hz; $H = 15.24$, $p = 0.0016$) in cocaine-administered animals compared to cocaine-naive animals.

Discussion: In C57BL/6 mice the administration of cocaine led to a significant increase in action potential firing sites and firing frequencies compared to naive and saline control animals. The underlying causes of this change in network activity seen in a variety of subcortical regions are currently under investigation.

Acknowledgements: Supported by the Austrian Science Fund FWF (grant W1206-B18: SPIN graduate program).

References

1. Fritz M, El Rawas R, Salti A, Klement S, Bardo MT, Kemmler G, Dechant G, Saria A, Zernig G: **Reversal of cocaine-conditioned place preference and mesocorticolimbic Zif268 expression by social interaction in rats.** *Addict Biol*, 2011; 16(2):273–284.
2. Fritz M, El Rawas R, Klement S, Kummer K, Mayr MJ, Eggart V, Salti A, Bardo MT, Saria A, Zernig G: **Differential effects of accumbens core vs. shell lesions in a rat concurrent conditioned place preference paradigm for cocaine vs. social interaction.** *PLoS One*, 2011; 6(10):e26761.

A2.5

Stable incorporation versus dynamic exchange of β subunits in a native calcium channel complex

Marta Campiglio¹, Valentina Di Biase^{1,2}, Petronel Tuluc^{1,3} and Bernhard E. Flucher^{1,*}

¹Department of Physiology and Medical Physics, Innsbruck Medical University, Austria; ²current address: Institute of Biophysics, Medical University of Graz, Austria; ³current address: Department of Pharmacology and Toxicology, University of Innsbruck, Austria

*E-mail: bernhard.e.flucher@i-med.ac.at

Intrinsic Activity, 2013; 1(Suppl. 1):A2.5

Background: Voltage-gated calcium channels are multi-subunit membrane proteins which transduce depolarization into cellular functions like excitation–contraction coupling in muscle or neurotransmitter release in neurons. The auxiliary β subunits function in membrane targeting of the channel and modulation of its gating properties. However, whether β subunits can reversibly interact with, and thus differentially modulate, channels in the membrane is still unresolved.

Methods: Here, we applied fluorescence recovery after photobleaching (FRAP) of GFP-tagged α_1 and β subunits expressed in dysgenic myotubes to study the relative dynamics of these calcium channel subunits for the first time in a native functional signaling complex.

Results: Identical fluorescence recovery rates of both subunits indicate stable interactions, distinct rates dynamic interactions. Whereas the skeletal muscle β_{1a} isoform formed stable complexes with α_{1S} and α_{1C} , the non-skeletal muscle β_{2a} and β_{4b} isoforms dynamically interacted with both α_1 subunits. Neither replacing the I–II loop of α_{1S} with that of α_{1A} , nor deletions in the proximal I–II loop, known to change the orientation of β , altered the specific dynamic properties of the β subunits. In contrast, a single residue

substitution in the α interaction pocket of $\beta_{1aM293A}$ increased the FRAP rate threefold.

Discussion: Together these findings indicate that in skeletal muscle triads the homologous β_{1a} subunit forms a stable complex, whereas the heterologous β_{2a} and β_{4b} subunits form dynamic complexes with the calcium channel. The distinct binding properties are not determined by differences in the I–II loop sequences of the α_1 subunits but are intrinsic properties of the β subunit isoforms. New strategies to interfere with this modulatory protein–protein interaction *in vivo* are currently being tested.

Acknowledgements: Funding: FWF P20059, W1101, T443-B18.

A2.6

Transmembrane transporters of *Fasciola hepatica*: new targets of anthelmintic therapy

Sandra Pichler¹, Yaprak Dönmez Çakıl², Florian Koban¹, Peter Chiba², Thomas Stockner¹, Michael Freissmuth¹ and Oliver Kudlacek^{1,*}

¹Institute of Pharmacology, Medical University of Vienna, Austria;

²Institute of Medical Chemistry, Medical University of Vienna, Austria

*E-mail: oliver.kudlacek@meduniwien.ac.at

Intrinsic Activity, 2013; 1(Suppl. 1):A2.6

Background: The liver fluke *Fasciola hepatica* is a parasite infecting farm animals and humans world-wide, causing liver fluke disease (fascioliasis). The drug of choice to treat fascioliasis is the anthelmintic drug triclabendazole (TBZ). After excessive use over the last decades, reports of fluke populations resistant to TBZ are becoming more frequent. Inhibitors of mammalian ABC transporters were shown to revert strains resistant to TBZ into susceptible ones. Therefore, it is thought that ABC transporters of *Fasciola hepatica* are involved in the development of these resistances. Here, we have cloned transporters of the liver fluke and analyzed them for their transport specificities.

Methods: Flukes were isolated at a local slaughterhouse in Lower Austria from bovine liver. RNA was prepared and full length cDNAs for transmembrane transporters were heterologously expressed. Transport of substrates was analyzed using fluorescent or radioactive substrates, respectively. Antibodies recognizing the transporters were generated by immunizing rabbits with short peptides.

Results: We could isolate a transporter from *Fasciola hepatica* showing high homologies to ABC transporters of the B-type family. After expression in HEK 293 fibroblasts we could show that this transporter was able to transport rhodamine 123 and that this transport could be blunted by typical blockers of P-glycoprotein (ABCB1). In addition, the transport via the fluke transporter could be inhibited by TBZ while cells expressing human ABCB1 were not affected by this drug. Using antibodies we could detect the fluke ABC transporter in the tegumental layer of *Fasciola hepatica*.

Discussion: The involvement of ABC transporters in drug resistance of parasites was reported before. Here, we identified an ABC transporter from *Fasciola hepatica* that could be involved in the export of anthelmintic drugs. Efforts in developing ABC transporter blockers to circumvent drug resistance in cancer therapy were not very successful up to now, due to severe side effects of these substances. Proteins of the nematode *Fasciola hepatica* could be different enough from mammalian proteins to be targeted by drugs reverting resistance to anthelmintic drugs without adverse effects on patients. Further analysis of ABC transporters from *Fasciola hepatica* could therefore serve as a starting point in the development of new drugs.

Acknowledgements: This work was supported by the Austrian Science Fund (FWF).

A2.7

Functional and physical interactions between P2Y receptors and ion channels

Hend Gafar¹, Giri K. Chandaka¹, Johannes A. Schmid² and Stefan Boehm^{1,*}

¹Department of Neurophysiology and Neuropharmacology, Center for Physiology and Pharmacology, Medical University of Vienna, Austria; ²Department of Vascular Biology and Thrombosis Research, Center for Physiology and Pharmacology, Medical University of Vienna, Austria

*E-mail: stefan.boehm@meduniwien.ac.at

Intrinsic Activity, 2013; 1(Suppl. 1):A2.7

Background: Neuronal P2Y receptors, i.e. nucleotide-sensitive G protein-coupled receptors (GPCRs), are known to control various voltage-gated ion channels, particularly K_v7 K^+ and $Ca_v2.2$ Ca^{2+} channels. The differential modulation of these ion channels via GPCRs was shown to rely on the presence or absence of scaffold proteins that are believed to bring receptors and channels in close proximity to guarantee efficient G protein-mediated modulation. This project evaluates whether a tight contact between P2Y receptors and ion channels is a prerequisite for their functional interaction.

Methods: P2Y receptors were coexpressed with K^+ or Ca^{2+} channels (labeled with fluorescent CFP or YFP tags) in tsA201 cells. The channel modulation by nucleotides was determined by patch clamp recordings. To evaluate the behavior of the receptors and channels in the membrane, fluorescence recovery after photobleaching (FRAP) was determined by confocal laser microscopy.

Results: Activation of P2Y₁, but not of P2Y₁₂, receptors by ADP inhibited the K^+ currents in a concentration-dependent manner by up to $20.5 \pm 1.9\%$. Conversely, activation of both, P2Y₁ and P2Y₁₂ receptors, reduced the Ca^{2+} currents by up to $60.1 \pm 7.4\%$ and $76.3 \pm 4.2\%$, respectively. In FRAP, the mobility of P2Y receptors alone was compared to their mobility when coexpressed with $K_v7.2/7.3$ or $Ca_v2.2$ channels, respectively. The mobility of P2Y₁ was significantly reduced by 38.6% when coexpressed with $K_v7.2/7.3$ channels, whereas that of P2Y₁₂ was only reduced by 6.5%. Contrarily, coexpression with $Ca_v2.2$ channels reduced the mobility of both receptors significantly (P2Y₁ by 16.0% and P2Y₁₂ by 30.5%) which goes in line with the electrophysiological data. To examine the specificity of the interaction between $Ca_v2.2$ and both P2Y receptors, $Ca_v1.2$ was also investigated. There was no inhibition of $Ca_v1.2$ currents and the mobility of P2Y₁ and P2Y₁₂ was not affected when coexpressed with $Ca_v1.2$. Thus, the modulation of ion channels by P2Y receptors is paralleled by an interaction in FRAP experiments.

Discussion: These results suggest that the functional control of K_v7 and $Ca_v2.2$ channels by P2Y receptors relies on a physical interaction between receptors and channels.

Acknowledgements: This study is supported by the FWF-funded doctoral program CCHD (W1205).

A2.8

Molecular gating mechanism of $Ca_v1.3$ low-voltage-gated L-type calcium channels

Andreas Lieb, Nadine Ortner and Jörg Striessnig^{*}
Pharmacology and Toxicology, Institute of Pharmacy, and Center for Molecular Biosciences, University of Innsbruck, Austria

*E-mail: joerg.striessnig@uibk.ac.at

Intrinsic Activity, 2013; 1(Suppl. 1):A2.8

Background: Within the high-voltage-gated Ca^{2+} channel (VGCC) family, $Ca_v1.3$ has unique negative threshold gating properties, which is further fine-tuned by $Ca_v1.3$ splicing. Shorter variants,

missing a C-terminal regulatory domain (CTM), activate at even more negative potentials. These unique negative gating characteristics allow $Ca_v1.3$ to control hearing, cardiac pacemaking and neuronal excitability. It is unknown if the negative activation threshold is determined by a negative activation range of voltage-sensor movement (measured as ON gating charge, Q_{on}) and/or very efficient coupling of voltage-sensor movements to pore opening.

Methods: We systematically compared VGCC by expression in tsA201 cells and analysis of their functional properties using the whole-cell patch clamp technique.

Results: In this study we show that the low threshold gating properties of $Ca_v1.3$ are determined by their negative Q_{on} -V relationship, which is even more negative than Q_{on} of $Ca_v3.1$, a member of the low-VGCC family. $Ca_v1.3$ showed the lowest coupling efficiency, because in $Ca_v1.3$ 70% charge has to be moved, to achieve half-maximal Ca^{2+} conductance. In contrast, 50% Q_{on} in $Ca_v1.2$ and 25% Q_{on} in $Ca_v3.1$ are sufficient to induce half-maximal activation of I_{Ca} . Furthermore, we demonstrate that the more negative I -V relationship of I_{Ca} through the short $Ca_v1.3$ splice variant $Ca_v1.3_{42A}$ is due to a more efficient coupling of Q_{on} to pore opening without change in the Q_{on} -V relationship. In $Ca_v1.3_{42A}$ only 60% charge has to be moved for half-maximal Ca^{2+} conductance. These findings revealed that the CTM, absent in $Ca_v1.3_{42A}$, has no effect on the voltage sensors, but impairs the coupling efficiency of Q_{on} to the channel activation gate. Additionally, we found that intracellular *N*-methyl-D-glucosamine and tetraethylammonium, frequently used as impermeant cations in patch clamp experiments, significantly shifted the $Ca_v1.3$ gating to even more negative voltages by about 10 mV. A similar shift was found for $Ca_v1.2$ and $Ca_v3.1$ suggesting the presence of a cytoplasmic organic cation binding site facilitating channel gating. These findings imply that organic cations used in standard intracellular solutions represent efficient sensitizers of VGCC gating.

Discussion: In conclusion, we show that the unique negative gating properties of $Ca_v1.3$ are enabled by high voltage sensitivity of Q_{on} , despite low coupling efficiency to pore opening. Enhancement of coupling efficiency is achieved by splicing-induced CTM removal and explains the more negative activation voltage range of I_{Ca} through short $Ca_v1.3$ splice variants.

Acknowledgements: This work was supported by the Austrian Science Fund (F44020 and W11).

A2.9

PDZ-domain scaffold proteins differentially modulate neuronal membrane expression of C-terminal splice variants of the human L-type calcium channel $Ca_v1.3$

Ruslan I. Stanika^{1,*}, Marta Campiglio¹, Amy Lee², Bernhard E. Flucher¹ and Gerald J. Obermair¹

¹Division of Physiology, Innsbruck Medical University, Austria;

²Department of Molecular Physiology and Biophysics, University of Iowa, Iowa City, IA, USA

*E-mail: ruslan.stanika@i-med.ac.at

Intrinsic Activity, 2013; 1(Suppl. 1):A2.9

Background: The multiple isoforms of voltage-gated Ca^{2+} channels (VGCC) achieve signaling specificity by distinct gating and current properties, differential targeting to neuronal compartments, and the formation of macromolecular complexes with specific up- and downstream signaling proteins. The L-type $Ca_v1.3$ Ca^{2+} channels critically contribute to neuronal excitability, pacemaking and the formation of dendritic spines, and have been implicated in the etiology of Parkinson's disease. Alternative splicing gives rise to a long ($Ca_v1.3_L$) and two short ($Ca_v1.3_{42A}$, $Ca_v1.3_{43S}$) C-terminal variants, which differ in their voltage dependence of activation and Ca^{2+} conductance. Here, we analyzed the role of the C-terminus

and its interaction with PDZ-domain scaffold proteins in Ca_v1.3 membrane expression and stability of dendritic spines in cultured hippocampal neurons.

Methods: Primary cultures of hippocampal neurons were transfected with HA-tagged Ca_v1.3 splice variants. Surface (live) staining of Ca_v1.3 was performed 15 days after transfection and image analysis was done using ImageJ and MetaMorph software.

Results: Short and long C-terminal Ca_v1.3 splice variants show a similar overall distribution in cultured hippocampal neurons. However, surface expression levels of the short splice variants Ca_v1.3_{42A} and Ca_v1.3_{43S} reach only ~50% of full-length Ca_v1.3_L. Surface expression is modulated by auxiliary β subunits. Long Ca_v1.3_L splice variants contain a class 1 PDZ-domain-binding C-terminal motif ITTL, which interacts with scaffold proteins such as densin-180, shank and erbin. This interaction plays an important role for channel targeting and neuronal morphology. Deletion of the C-terminal ITTL sequence reduced Ca_v1.3_L membrane expression to the levels of the short splice variants (45% of full-length). Overexpression of either densin or shank (but not erbin) leads to reduced surface expression of Ca_v1.3_L splice variant. These effects are reduced in the short splice variant Ca_v1.3_{42A} and in the mutated long splice variant Ca_v1.3_{ITTL} lacking the ITTL motif. Densin and shank reduced neuronal branching in the long splice variant, but not in the short splice variants or the ITTL mutant. Moreover, reduced branching was accompanied by elongation of dendritic spines.

Discussion: The distal C-terminus of Ca_v1.3 is not essential for the targeting of Ca²⁺ channels into cell surface clusters, as all Ca_v1.3 C-terminus splice variants revealed a clustered distribution on the soma, dendrites, and dendritic spines. The integrity of the C-terminus and particularly the interaction of ITTL domain with PDZ scaffold proteins play a key role in the development of dendrites and the stabilization of spines.

Acknowledgements: This study has been supported by: Austrian Science Fund P23479-B19, P24079-B21, F4406.

A2.10

Differential targeting properties of a new, and two previously known, calcium channel β4 splice variants in primary cultured neurons

Solmaz Etemad¹, Gerald J. Obermaier¹, Ariane Benedetti¹, Verena Burtscher², Alexandra Koschak², Daniel Bindreither³, Reinhard Kofler³ and Bernhard E. Flucher^{1,*}

¹Department of Physiology and Medical Physics, Innsbruck Medical University, Austria; ²Center of Physiology and Pharmacology, Department of Neurophysiology and Neuropharmacology, Medical University of Vienna, Austria; ³Division of Molecular Pathophysiology, Biocenter, Innsbruck Medical University, Austria

*E-mail: bernhard.e.flucher@i-med.ac.at

Intrinsic Activity, 2013; 1(Suppl. 1):A2.10

Background: Voltage-gated calcium channels (VGCC) mediate calcium influx in response to membrane depolarization and regulate numerous cellular functions. Auxiliary β subunits are critical determinants of membrane expression and gating properties of VGCCs. Four distinct β subunit isoforms have been identified, all are expressed in brain. Here, we report the expression and properties of a novel β4 splice variant, β4x, which lacks the variable N-terminus.

Methods: Following methods were used for this study: qRT-PCR, molecular biology, cell culture, transfection, lentiviral infections, immunocytochemistry, electrophysiology and Affymetrix GeneChip analysis.

Results: RT-PCR with exon-specific primers revealed the expression of the novel β4 splice variant, β4x in addition to β4a and β4b in cultured cerebellar granule neurons (CGN) and adult

cerebellum. qRT-PCR in adult cerebellum demonstrated that β4x is the second most abundant splice variant (33%) after β4a (66%), whereas β4b is hardly detectable (1%). Immunofluorescence staining of heterologously expressed β4 splice variants in cultured hippocampal neurons, resulted in similar overall distribution patterns of all β4 splice variants in the somatodendritic compartments. However in the distal axon (> 1 mm from the soma) expression of β4x was 5 times higher than that of β4a and 3 times higher than that of β4b. Overexpression of β4x in neurons increased the average cluster intensity of Ca_v2.1 staining, and its coexpression with Ca_v2.1 in tsA modulated I_{Ca} similar to other β subunits, demonstrating that it functionally interacts with Ca_v2.1. Here we found that β4a, β4b or β4x heterologously expressed in cultured CGNs from lethargic (β4 null) mice differed significantly in the extent of nuclear targeting (β4a: < 20%, β4b: > 65%, β4x: < 13%). Interestingly microarray analysis of cultured CGNs from lethargic mice reconstituted with either one of the β4 splice variants revealed that β4b affected the regulation of 46 genes, β4a that of 3 genes, whereas β4x had no significant effect in gene regulation (using a cut-off of multiple-hypothesis-adjusted *p*-value of < 0.05 and an absolute log-2 fold change of > 0.7).

Discussion: Taken together, these results reveal splice-variant-specific differences in axonal and nuclear targeting properties and the regulation of gene expression. This suggests a functional diversity of calcium channel β4 splice variants that may be achieved by different N-terminal protein-protein interaction partners. The subcellular distribution of β4x suggests a preferential axonal function and no role in the regulation of gene expression in the nucleus.

Acknowledgements: Supported by the Austrian Science Fund: P23479-B19, P24079-B21, W1101-B12, F4406-B19/02 (SBF 044).

A2.11

Direct inhibition of the norepinephrine transporter by the cocaine adulterant levamisole

Tina Hofmaier¹, Anton Luf², Amir Seddik³, Thomas Stockner¹, Marion Holy¹, Michael Freissmuth¹, Gerhard F. Ecker³, Rainer Schmid², Harald H. Sitte^{1,*} and Oliver Kudlacek¹

¹Institute of Pharmacology, Center for Physiology and Pharmacology, Medical University of Vienna, Austria; ²Clinical Department of Laboratory Medicine, Medical University of Vienna, Austria; ³Department of Medicinal Chemistry, University of Vienna, Austria

*E-mail: harald.sitte@meduniwien.ac.at

Intrinsic Activity, 2013; 1(Suppl. 1):A2.11

Background: The anthelmintic drug levamisole is one of the most common cocaine adulterants.

Methods: Uptake and Release Assays: HEK 293 cell lines stably expressing the human isoforms of the serotonin transporter (SERT), the norepinephrine transporter (NET) and the dopamine transporter (DAT) were used for both assays. For inhibition experiments, the specific activity of the tritiated substrate was kept constant: 0.1 μM [³H]DA, 0.015 μM [³H]MPP⁺, 0.1 μM [³H]5-HT. For release studies, cells were preloaded with 0.4 μM [³H]DA, 0.1 μM [³H]MPP⁺, or 0.4 μM [³H]5-HT for 20 min at 37 °C. Tritium was determined by liquid scintillation counting. IC₅₀ values were calculated using non-linear regression fits performed with Prism (GraphPad 5.0).

Homology modelling and docking: Both the neutral and protonated levamisole structures were built and minimized with QSite (version 5.8, Schrödinger) using the B3LYP method applying the 6-31G* basis set. Homology models of human SERT and NET were generated with Modeller 9.12 using the validated human DAT model in the outward-facing conformation as template. The induced fit docking protocol of the Schrödinger package was used for ligand

docking into the central binding site (Glide version 5.8) using standard parameter setting.

Results: Uptake-inhibition experiments were performed with increasing concentrations of levamisole or cocaine. The observed IC_{50} values for cocaine were $1.8 \pm 1.12 \mu\text{M}$ (SERT), $1.0 \pm 1.07 \mu\text{M}$ (NET) and $0.56 \pm 1.12 \mu\text{M}$ (DAT) respectively $849 \pm 14.65 \mu\text{M}$ (SERT), $74.5 \pm 1.12 \mu\text{M}$ (NET), $209.9 \pm 1.31 \mu\text{M}$ (DAT) for levamisole. Uptake-inhibition experiments by increasing cocaine concentrations at a fixed levamisole concentration or vice versa indicated no allosteric effect. Furthermore, we tested the releasing properties of levamisole and observed a slightly increased efflux in NET but not in SERT or DAT. In addition, we found that the levamisole metabolite aminorex preferentially blocked substrate uptake by NET (IC_{50} : $0.33 \pm 1.07 \mu\text{M}$) and DAT (IC_{50} : $0.85 \pm 1.20 \mu\text{M}$), while SERT was inhibited only at 20-fold higher concentrations (IC_{50} : $18.39 \pm 1.12 \mu\text{M}$). The pattern of inhibition (NET > DAT >>> SERT) was reminiscent of the parent compound levamisole, but the inhibitory potency of aminorex was comparable to that of cocaine. We observed significant efflux in SERT, slight efflux in NET but no efflux in DAT for aminorex. Using a ligand docking approach, levamisole was predicted to have the highest affinity for NET (charged: -830 kcal/mol ; neutral: -820 kcal/mol), followed by DAT (charged: -798 kcal/mol ; neutral: -792 kcal/mol) and SERT (charged: -697 kcal/mol ; neutral: -683 kcal/mol). The binding site differs by five residues between DAT and SERT (residues Y95, G100, I172, Y175 and T497 in SERT) and by four residues between NET and SERT (residue Y95, G100, I172 and T497 in SERT). Levamisole was found to be in direct contact with four of these residues.

Discussion: We tested the effects of levamisole on the serotonin transporter (SERT), the norepinephrine transporter (NET) and the dopamine transporter (DAT). Levamisole was 100- and 300-fold less potent than cocaine in blocking norepinephrine and dopamine uptake, respectively, and had only very low affinity for the serotonin transporter. In addition, levamisole did not trigger any appreciable substrate efflux. Furthermore, levamisole did not enhance the inhibitory action of cocaine. Since levamisole is metabolized to aminorex, a formerly marketed anorectic drug, which is classified as an amphetamine-like substance, we examined the uptake-inhibitory and efflux-eliciting properties of aminorex and found it to exert strong effects on all three neurotransmitter transporters in a manner similar to amphetamine. We therefore conclude that while the adulterant levamisole itself has only moderate effects on neurotransmitter transporters, its metabolite aminorex may exert distinct psychostimulant effects by itself. Given that the half-time of levamisole and aminorex exceeds the one of cocaine it may be safe to conclude that after the cocaine effect "fades out" the levamisole/aminorex effect "kicks in".

Acknowledgements: The work was financially supported by the Austrian Science Fund FWF (grant F35).

Austrian Pharmacological Society (APHAR)

A3.1

Opioid activities and antinociceptive properties of differently N-substituted morphinans

Tanila Ben Haddou¹, Szabolcs Béni², Sándor Hosztafi², Davide Malfacini³, Girolamo Calò³, Helmut Schmidhammer¹ and Mariana Spetea^{1,*}

¹Department of Pharmaceutical Chemistry, Institute of Pharmacy and Center for Molecular Biosciences, University of Innsbruck, Austria; ²Department of Pharmaceutical Chemistry, Semmelweis University, Budapest, Hungary; ³Section of Pharmacology, Department of Medical Sciences, University of Ferrara, Italy

*E-mail: mariana.spetea@uibk.ac.at

Intrinsic Activity, 2013; 1(Suppl. 1): A3.1

Background: Morphine and oxycodone, the cornerstone drugs for the treatment of moderate to severe pain, activate the μ opioid (MOP) receptor, the main type targeted for pharmacotherapy of pain. These drugs also share the same pharmacological profile including side effects such as respiratory depression, constipation, tolerance and physical dependence. Chemical approaches towards the identification of novel MOP analgesics with reduced side effects and powerful analgesia include structural modifications of morphinans in key positions that are important for binding, selectivity, potency and efficacy at opioid receptors. The focus of this work is on structure-activity relationship (SAR) studies and *in vitro* and *in vivo* pharmacological investigations on a series of opioid ligands differently substituted in positions 6, 14 and 17 of the morphinan skeleton.

Methods: Radioligand binding assays were performed using rodent brain membranes to evaluate opioid receptor binding and selectivity. [³⁵S]GTPγS functional assays with Chinese hamster ovary (CHO) cells expressing human opioid receptors and calcium mobilization assays in CHO co-expressing human opioid receptors and chimeric G proteins were performed to assess potency and opioid agonism. Antinociceptive activities were established using hot-plate and tail-flick tests in mice after subcutaneous administration.

Results: Binding studies showed that the various N-substituted morphinans display high affinities at the MOP receptor. In both functional assays, the investigated opioid ligands showed high potency. They produced marked antinociceptive effects, being severalfold more potent than the parent compounds.

Discussion: Based on these SAR studies, certain modifications in the substitution pattern, e.g. introduction of an N-beta-phenylethyl group in position 17, a hydroxyl group in position 14 and a keto group in position 6 results in interesting alterations in opioid activity by influencing the pharmacological properties of ligands interacting with opioid receptors. Analysis of the *in vitro* and *in vivo* opioid profile for this series of N-substituted morphinans leads to a better understanding of the relationship between affinity and/or selectivity, agonist activity, antinociceptive potency and the nature of substituents in morphinans. These results represent a useful and valuable outcome for the design and optimization of existing structural templates increasing the chance of identifying clinically useful analgesics for superior pain management.

Acknowledgements: Supported by the Austrian Science Fund (FWF): TRP19-B18.

A3.2

Signaling mechanisms related to regulation of intracellular calcium concentration involved in vascular actions of serotonin and bradykinin on rat peripheral arteries

Marko Stojanović, Miroslav Radenković* and Milica Prostran
Department of Pharmacology, Clinical Pharmacology and Toxicology, Faculty of Medicine, University of Belgrade, Serbia

*E-mail: mradenkovic@med.bg.ac.rs

Intrinsic Activity, 2013; 1(Suppl. 1): A3.2

Background: The most important step in vascular smooth muscle contractions is an increase in intracellular calcium concentration via opening of voltage-gated calcium channels or/and activation of Na^+/K^+ -ATPase. The aim of this study was to determine if voltage-gated Ca^{2+} channels and Na^+/K^+ -ATPase are involved in the transduction mechanisms related to serotonin- and bradykinin-induced contractile vascular effects on isolated carotid and femoral arteries, respectively.

Methods: Experiments were conducted on isolated common carotid and femoral arteries of male Wistar rats. Circular vascular segments were placed in an organ bath with Krebs-Ringer's solution. Concentration–response curves for serotonin and bradykinin were obtained in a cumulative fashion on artery rings previously equilibrated at basal tone. Isometric tension alterations induced by investigated vasoactive substances were continuously recorded.

Results: Serotonin (1–10 μM) produced concentration-dependent contractions of carotid arteries, which were nearly completely reduced by nifedipine (an L-type voltage-gated Ca^{2+} channel blocker; 0.1 μM). In accordance, bradykinin (0.001–0.3 μM) also produced concentration-dependent contractions of femoral arteries. The obtained contractions were significantly, yet only in the first three concentrations fully, inhibited in the presence of nifedipine. Taking into account that nifedipine more effectively inhibited serotonin actions, if compared to the bradykinin-induced effects, the bradykinin-induced vascular contraction was additionally challenged with ouabain (a Na^+/K^+ -ATPase inhibitor; 1 μM). The addition of ouabain resulted in the reduction of the contractile effects of bradykinin; however, without any alteration of maximal obtained contractions in the corresponding blood vessel.

Discussion: Serotonin and bradykinin are endogenous substances involved in regulation and control of many physiological functions, including vascular resistance of different blood vessels. Taking into account previous studies considering mechanisms involved in action of serotonin or bradykinin on various vascular beds, the present experiments were undertaken in order to examine some of the signaling pathways involved in the effect of serotonin and bradykinin in the isolated rat common carotid and femoral arteries, respectively. The results of our experiments showed that the transduction mechanisms involved in the process of serotonin-induced carotid artery contractions include predominant activation of L-type voltage-gated Ca^{2+} channels, whereas bradykinin-induced contractions of femoral arteries were most probably mediated via concomitant opening of L-type Ca^{2+} channels and activation of Na^+/K^+ -ATPase.

Acknowledgements: This investigation was supported by the Ministry of Education and Science, Republic of Serbia, with grant 175023.

A3.3

Niclosamide regulates the cell membrane properties in an intestinal barrier model

Christine Schäfer^{1,2}, Jasmina Weidinger^{1,2}, Klaus R. Schröder^{1,2} and Mohammad R. Lornejad-Schäfer^{1,2,*}

¹BioMed-zet Life Science GmbH, zet-LSL, Linz, Austria; ²zet-Centre for Alternative and Complementary Methods to Animal Testing, Linz, Austria

*E-mail: lornejad@zet.or.at

Intrinsic Activity, 2013; 1(Suppl. 1):A3.3

Background: Niclosamide has been used for a long time as a drug against tapeworm. Currently, niclosamide is also investigated as a potential drug against colon cancer metastasis. The aim of this study was to investigate the effects of niclosamide on cell membrane properties in an intestinal barrier model.

Methods: To establish an intestinal barrier model, Caco-2 cells seeded onto inserts were differentiated for 21 days. After that, the cells were treated apically with various niclosamide concentrations for 24 h. The cell surface was investigated using scanning electron microscopy (SEM) analysis. The rate of cell cytotoxicity of niclosamide was determined using the LDH assay. The cell transepithelial electrical resistance (TER) was measured using impedance (Z) measurement. The membrane permeability was tested by selective transport of small fluorescein thiocarbonyl

(FITC)-dextran (3–5 kDa). The expression and localization of ZO-1 were confirmed by western blot and immunofluorescence analysis.

Results: Niclosamide at a concentration of about 10 μM , which is equivalent to 200 mg per patient [1], significantly changed cell morphology, cell surface topography and number of microvilli. In addition, niclosamide dose-dependently decreased the TER value (membrane integrity), which correlated with increased permeability of small molecules, i.e. FITC-dextran (3–5 kDa). Furthermore, niclosamide affected ZO-1 and occludin protein expression.

Discussion: SEM analysis leads us to assume that niclosamide regulates the absorption process due to reduction of the absorptive cell surface area. Furthermore, we suppose that niclosamide regulates the paracellular transport pathway due to regulation of the tight junction proteins ZO-1 and occludin because both tight junction proteins play an important role in maintaining membrane integrity and regulation of paracellular transport activity. The understanding of niclosamide effects on the absorption process and transporter pathway in an intestinal model can be very helpful to use niclosamide as a safe drug for clinical applications.

Acknowledgements: This work has been supported by the state of Upper Austria.

Reference

1. Varma TK, Shinghal TN, Saxena M, Ahluwalia SS: **Studies on the comparative efficacy of mebendazole, flubendazole and niclosamide against human tapeworm infections.** *Indian J Public Health*, 1990; 34(3):163–168.

A3.4

CDK8-mediated STAT1-S727 phosphorylation restrains NK cell cytotoxicity and tumor surveillance

Eva M. Putz¹, Dagmar Gotthardt¹, Thomas Decker² and Veronika Sexl^{1,*}

¹Institute of Pharmacology and Toxicology, University of Veterinary Medicine Vienna, Austria; ²Max F. Perutz Laboratories, University of Vienna, Austria

*E-mail: veronika.sexl@vetmeduni.ac.at

Intrinsic Activity, 2013; 1(Suppl. 1):A3.4

Background: Natural killer (NK) cells provide immediate defense against tumor and virally infected cells. Signal Transducer and Activator of Transcription (STAT)1 is of major importance in NK cells as *Stat1*^{-/-} NK cells are immature and highly dysfunctional [1,2]. STAT1 activity is regulated post-transcriptionally by phosphorylation of tyrosine and serine residues. Previous studies revealed that knock-in mice with point-mutated STAT1-S727 (*Stat1*-S727A) display reduced anti-microbial activity, suggesting that the S727A mutation generates a hypomorphic *Stat1* allele [3,4].

Methods: NK cells were isolated from spleens of *Stat1*^{-/-}, *Stat1*-S727A and wild-type mice and used to perform *in vitro* cytotoxicity assays (⁵¹Cr release and flow-cytometry-based assays), mRNA (qPCR) and protein expression (immunoblotting and flow cytometry) analysis. The employed *in vivo* tumor models included *v-abl*^f leukemia, B16 melanoma and 4T1 breast cancer. To determine the upstream kinase of STAT1-S727 phosphorylation, *in vitro* kinase inhibitor assays were performed followed by immunoblotting and validation by shRNA-mediated knockdown.

Results: Murine NK cells display constitutive basal phosphorylation of STAT1-S727, which is mediated by the cyclin-dependent kinase (CDK)8. The genetic abrogation of this phosphorylation site (*Stat1*-S727A) significantly enhances NK cell cytotoxicity against a range of tumor cells. The enhanced effector function is accompanied by increased expression of perforin and granzyme B. Accordingly, *Stat1*-S727A mice display significantly delayed disease onset in NK-cell-surveilled tumor models including melanoma, leukemia and metastasizing breast cancer [5].

Discussion: Our study reveals a novel inhibitory role of STAT1-S727 phosphorylation for NK cell cytotoxicity. Inhibition of CDK8-mediated STAT1-S727 phosphorylation may thus represent a novel therapeutic strategy to stimulate NK-cell-mediated tumor surveillance.

Acknowledgements: This work was supported by the Austrian Academy of Science DOC-fORTE fellowship (for E.M.P.) and the Austrian Science Fund FWF grant SFB F28 (all authors).

References

1. Robbins SH, Tessmer MS, Van Kaer L, Brossay L: **Direct effects of T-bet and MHC class I expression, but not STAT1, on peripheral NK cell maturation.** *Eur J Immunol*, 2005; 35(3):757–765.
2. Lee CK, Rao DT, Gertner R, Gimeno R, Frey AB, Levy DE: **Distinct requirements for IFNs and STAT1 in NK cell function.** *J Immunol*, 2000; 165(7):3571–3577.
3. Varinou L, Ramsauer K, Karaghiosoff M, Kolbe T, Pfeffer K, Müller M, Decker T: **Phosphorylation of the Stat1 transactivation domain is required for full-fledged IFN- γ -dependent innate immunity.** *Immunity*, 2003; 19(6):793–802.
4. Pilz A, Kratky W, Stockinger S, Simma O, Kalinke U, Lingnau K, von Gabain A, Stoiber D, Sexl V, Kolbe T, Rüllicke T, Müller M, Decker T: **Dendritic cells require STAT-1 phosphorylated at its transactivating domain for the induction of peptide-specific CTL.** *J Immunol*, 2009; 183(4):2286–2293.
5. Putz EM, Gotthardt D, Hoermann G, Csiszar A, Wirth S, Berger A, Straka E, Rigler D, Wallner B, Jamieson AM, Pickl WF, Zebedin-Brandl E, Müller M, Decker T, Sexl V: **CDK8-mediated STAT1-S727 phosphorylation restrains NK cell cytotoxicity and tumor surveillance.** *Cell Rep*, 2013; 4(3):437–444.

A3.5

Functional properties of L-type calcium channels in ventricular cardiomyocytes from muscular dystrophy mouse models

Lena Rubi¹, Xaver Koenig¹, René Cervenka¹, Vaibhavkumar S. Gawali¹, Péter Lukács¹, Reginald E. Bittner², Hannes Todt¹ and Karlheinz Hilber^{1,*}

¹Center for Physiology and Pharmacology, Medical University of Vienna, Austria; ²Center for Anatomy and Cell Biology, Medical University of Vienna, Austria

*E-mail: karlheinz.hilber@meduniwien.ac.at

Intrinsic Activity, 2013; 1(Suppl. 1):A3.5

Background: Muscular dystrophies are hereditary diseases characterized by progressive muscle weakness and degeneration. Besides the well-described skeletal muscle degenerative processes, several dystrophy types are also associated with severe cardiovascular complications including cardiomyopathy development and cardiac arrhythmias. The current understanding of the cardiac pathomechanisms is very limited but recent research points to a role of dysfunctional ion channels in dystrophic cardiomyocytes.

Methods: Currents through L-type calcium channels were recorded in ventricular cardiomyocytes isolated from the hearts of adult wild-type and dystrophic mice using the whole-cell patch clamp technique. Besides two Duchenne muscular dystrophy (DMD) mouse models (mdx and mdx-utr), we also investigated dysferlin-deficient mice (C57BL/10^{dysf}), which are used as a model for limb-girdle muscular dystrophy 2B (LGMD2B).

Results: The currents through L-type calcium channels were significantly increased in dystrophic mdx and mdx-utr cardiomyocytes when compared with wild-type cells. Moreover, calcium channel inactivation in dystrophic cardiomyocytes was slowed. Both effects increase the calcium entry into the cells during the action potential. *In vivo*, dystrophin-deficient animals showed enhanced atrioventricular conduction, consistent with increased calcium influx. In contrast to mdx and mdx-utr, currents through L-type calcium

channels in dysferlin-deficient C57BL/10^{dysf} cardiomyocytes were normal when compared with wild-type cells.

Discussion: L-type calcium channel abnormalities in dystrophic cardiomyocytes cannot be considered a common feature of the muscular dystrophies.

Acknowledgements: Supported by the Austrian Science Fund FWF (P23060).

A3.6

Investigating the molecular mechanisms underlying the differential subcellular targeting of the metabotropic glutamate receptor 1 (mGlu₁) in the cerebellar cortex

Mahnaz Mansouri¹, Yu Kasugai¹, Federica Bertaso², Fabrice Raynaud², Julie Perroy², Laurent Fagni², Walter A. Kaufmann¹, Herbert Lindner³, Yugo Fukazawa⁴, Masahiko Watanabe⁵, Ryuichi Shigemoto⁴ and Francesco Ferraguti^{1,*}

¹Department of Pharmacology, Innsbruck Medical University, Austria; ²Institut de Génomique Fonctionnelle, Montpellier, France; ³Division of Clinical Biochemistry, Innsbruck Medical University, Austria; ⁴Division of Cerebral Structure, National Institute for Physiological Sciences, Okazaki, Japan; ⁵Department of Anatomy, Hokkaido University School of Medicine, Hokkaido, Japan

*E-mail: francesco.ferraguti@i-med.ac.at

Intrinsic Activity, 2013; 1(Suppl. 1):A3.6

Background: Type 1 metabotropic glutamate (mGlu₁) receptors activate a multitude of signalling pathways important for modulation of excitability and plasticity in the cerebellar cortex. The mGlu₁ receptor is involved in long-term depression at excitatory inputs to Purkinje cells (PC), whereas it is implicated in rebound potentiation of inhibitory post-synaptic potentials at GABAergic synapses. These various forms of plasticity might depend on subsynaptic arrangement of the receptor that can be regulated by protein-protein interactions.

Methods: In the present study we have taken advantage from the SDS-digested freeze-fracture replica labelling (SDS-FRL) technique and have studied the distribution pattern of mGlu₁ receptors in the rat and mouse cerebellar cortex.

Results: The results we have obtained following both N-terminus and C-terminus immunogold labelling confirm the perisynaptic enrichment of mGlu₁ receptors, in particular of the longest splice variant mGlu_{1(a)}, in excitatory synapses between parallel fibres and PCs. Our double immunogold labelling for the mGlu_{1(a)} receptor and the GABA_A $\alpha 1$ subunit shows that besides excitatory synapses the mGlu_{1(a)} receptor is located also in the main body of GABAergic synapses in the cerebellar cortex. A well-described functional regulation of the mGlu_{1(a)} receptor occurs via its direct interaction with Homer proteins that are abundantly present at PC excitatory inputs. We studied the possible role of long Homer proteins on mGlu_{1(a)} receptor localization by using TAT-Homer1a as a dominant-negative peptide to disrupt Homer-associated protein complexes. Our SDS-FRL analysis showed no significant difference in the perisynaptic distribution pattern of the receptor, suggesting that other scaffolding proteins are involved in the subcellular targeting of mGlu₁ receptors. In order to identify other interaction partners that may regulate the targeting of the receptor in GABAergic synapses, we are currently using a proteomic approach, namely co-immunoprecipitation (Co-IP) followed by liquid chromatography-tandem mass spectrometry (LC-MS/MS).

Discussion: Our findings suggest that long Homer proteins may not be the only scaffolding proteins that contribute to mGlu₁ receptor perisynaptic localization in excitatory synapses. Identification of proteins that modulate mGlu₁ receptor differential subsynaptic localization can open new insight into the physiological role of the receptor.

Acknowledgements: This work is supported by the Austrian Science Fund FWF (grant W012060-10 to F.F.).

A3.7

Effect of statins on NF- κ B in human metastatic melanoma cells

Stephan Salzmann, Christine Wasinger and Martin Hohenegger*
Institute of Pharmacology, Medical University of Vienna, Austria
*E-mail: martin.hohenegger@meduniwien.ac.at
Intrinsic Activity, 2013; **1**(Suppl. 1):A3.7

Background: The incidence of melanoma still increases in the western world more than any other type of cancers. Full recovery can be achieved in early stages, while response rates in late stages remain frustrating. Due to its bad prognosis and its resistance to conventional chemotherapeutic schemes new therapeutic approaches have to be established. Statins, competitive inhibitors of the 3-hydroxy-3-methylglutaryl-coenzyme A (HMG-CoA) reductase, inhibit the rate-limiting step of cholesterol biosynthesis and are successfully used in hypercholesterolemia. Besides, statins show pleiotropic effects, such as immunosuppressive, anti-inflammatory and anti-proliferative actions. On the molecular level the anti-inflammatory and anti-proliferative effects are still poorly understood, in particular in metastatic melanoma cells. The nuclear factor kappa B (NF- κ B) is a transcription factor and central regulator of inflammatory processes. Moreover, it may have impact on tumor growth and is frequently deregulated in melanoma. The human metastatic melanoma cell lines A375 and 518A2 are sensitive to simvastatin exposure and undergo apoptosis in a time- and concentration-dependent manner. Previous work has shown that IL-6 secretion of these melanoma cells is suppressed by simvastatin. It was therefore the aim of this work to investigate the downstream effects of simvastatin on NF- κ B activity.

Methods: NF- κ B activity was monitored by the luciferase reporter gene assay in A375 and 518A2 melanoma cells, complemented by western blot analyses.

Results: Within exposure times of 24 hours simvastatin triggered a concentration-dependent activation of NF- κ B activity, which reached values in the range of the positive control TNF- α . Interestingly, longer exposure times led to a reduction of NF- κ B activity in 518A2 melanoma cells, whereas in A375 cells it was further enhanced. Western blot analyses further corroborated these findings.

Discussion: Our findings indicate that statins influence the transcriptional activity of NF- κ B and may thereby influence the formation of an inflammatory microenvironment during malignant progression.

Acknowledgements: This work was supported by Herzfeldersche Familienstiftung and the Austrian Science Fund FWF (P22385).

A3.8

Anti-psoriatic therapy recovers high-density lipoprotein composition and function

Michael Holzer¹, Peter Wolf², Martin Inzinger², Markus Trieb¹, Sanja Čurčić¹, Lisa Pasterk¹, Wolfgang Weger², Ákos Heinemann² and Gunther Marsche^{1,*}

¹*Institute of Experimental and Clinical Pharmacology, Medical University of Graz, Austria;* ²*Department of Dermatology, Medical University of Graz, Austria*

*E-mail: gunther.marsche@medunigraz.at
Intrinsic Activity, 2013; **1**(Suppl. 1):A3.8

Background: Psoriasis is a chronic inflammatory disorder associated with increased cardiovascular mortality. Psoriasis affects high-density lipoprotein (HDL) composition, generating dysfunctional HDL particles. However, data regarding the impact of

anti-psoriatic therapy on HDL composition and function are not available.

Results: HDL was isolated from psoriatic patients at baseline and after effective topical and/or systemic anti-psoriatic therapy, and from age- and sex-matched healthy controls by gradient ultracentrifugation. Assays of HDL-induced cholesterol efflux, antioxidant activity, Lp-PLA₂ and paraoxonase activity were performed, and activities of plasma enzymes involved in HDL metabolism were assessed.

Methods: HDL from psoriatic patients showed a significantly impaired capability to mobilize cholesterol from macrophages (6.4 vs. 8.0% [³H]cholesterol efflux, $p < 0.001$), low paraoxonase (350 vs. 217 μ M/min/mg protein, $p = 0.011$) and increased Lp-PLA₂ activities (19.9 vs. 12.1 nM/min/mg protein, $p = 0.028$). Of particular interest, the anti-psoriatic therapy significantly improved (i) serum lecithin-cholesterol acyltransferase activity and decreased total serum lipolytic activity but did not affect serum levels of HDL-cholesterol. Most importantly, these changes were associated with a significantly improved HDL-cholesterol efflux capability.

Discussion: Our results provide evidence that effective anti-psoriatic therapy recovers HDL composition and function, independent of serum HDL-cholesterol levels and provide support to the emerging concept that HDL function may be a better marker of cardiovascular risk than HDL-cholesterol levels.

Acknowledgements: This work was supported by the Austrian Science Fund FWF (grants P21004-B02 and P22976-B18 to G.M., P22521-B18 to A.H., and W1241 to G.M., P.W. and A.H.) and by the Oesterreichische Nationalbank, Jubiläumsfond (grant 14853).

A3.9

In vitro characterization of human epithelial tissue utilizing a microelectronic impedance sensor with microfluidic medium supply

Heinz D. Wanzenböck^{1,*}, Andreas Exler¹, Alexander Brezina¹, Johann K. Mika¹, Emmerich Bertagnolli¹, Elisabeth Engleder², Franz Gabor² and Michael Wirth²

¹*Institute for Solid State Electronics, Vienna University of Technology, Austria;* ²*Department of Pharmaceutical Technology and Biopharmaceutics, University of Vienna, Austria*

*E-mail: heinz.wanzenboeck@tuwien.ac.at
Intrinsic Activity, 2013; **1**(Suppl. 1):A3.9

Background: Besides classical optical methods, such as fluorescence microscopy, and conventional biochemical analysis of cell cultures, electrical spectroscopy offers another possibility for tissue analysis, which stands out as a continuous, destruction-free measurement method.

Methods: In this work, planar interdigitated electrodes were fabricated on a biocompatible glass substrate using microstructuring techniques. The microelectronic sensors were fabricated by lithography and thin-film deposition methods. CaCo-2 cells in suspension were dispersed simultaneously on four sensor areas and the adhesion and growth of a cell layer was measured by bioimpedance spectroscopy in a frequency range from 50 Hz to 100 kHz. An analysis of the cell culture status was made by interpreting the time-dependent development of the impedance and of the phase angle of the electrical impedance.

Results: In this work we address cell growth on different microelectronic surfaces and in different environmental conditions. The actual condition of a tissue is essential for many pharmaceutical studies of a substance's effect on the integrity of the cell layer. This also affects the capacity of the cell membrane for transcellular and paracellular transport routes. The bioimpedance approach did not only allow to follow the formation of a confluent cell layer but we could also identify the pharmacological effects of

permeation enhancers and study the wound healing of physically inflicted dissection of a confluent cell layer.

Discussion: The purpose of this study to develop an impedance analysis system for analysis of live cell cultures was achieved. Bioimpedance spectroscopy has been shown to be a non-invasive and label-free analysis method for adherent cell cultures. This method has the rare advantage that a controllable cell growth, without influence of markers potentially affecting the cell culture, can be watched. With the additional rapid development of the micro- and nano-technology sector, the impedance spectroscopy can be an important tool for standard analyses in the future.

A3.10

The indole alkaloid ibogaine and its mechanism of $K_{V11.1}$ channel block

Patrick Thurner¹, Hend Gafar², Vaibhavkumar S. Gawali², Oliver Kudlacek¹, Jürgen Zezula¹, Karlheinz Hilber², Stefan Boehm², Walter Sandtner¹ and Xaver Koenig^{2,*}

¹Institute of Pharmacology, Center for Physiology and Pharmacology, Medical University of Vienna, Austria; ²Department of Neurophysiology and Neuropharmacology, Center for Physiology and Pharmacology, Medical University of Vienna, Austria

*E-mail: xaver.koenig@meduniwien.ac.at

Intrinsic Activity, 2013; **1**(Suppl. 1):A3.10

Background: Ibogaine is a psychoactive indole alkaloid with promising anti-addictive properties. Therapeutic administration of this drug, however, was accompanied by QT-interval prolongation and cardiac arrhythmias. This is most likely caused by inhibition of $K_{V11.1}$ potassium channels (hERG, *KCNH2*).

Methods: Here, we studied in detail the interaction of ibogaine with $K_{V11.1}$ channels heterologously expressed in tsA201 cells with the whole-cell patch clamp technique.

Results: Currents through $K_{V11.1}$ channels were blocked by external and internal application of ibogaine and the extent of inhibition was dependent on the relative pH values. Block was observed only after activation of the channels but did not occur for resting channels. This state dependence was reflected in significant changes of $K_{V11.1}$ channel gating including activation, inactivation and deactivation. The potency of ibogaine was reduced by mutations in the putative canonical binding pocket (Y652A and F656A) but was unaltered in the inactivation-deficient double mutant (G628C/S631C). Details of state preference as well as dynamic transitions in state populations were further elucidated by a kinetic model fitting our experimental data. This showed that, although ibogaine binds channels in the open/inactivated conformation, inhibition of $K_{V11.1}$ is dominated by the kinetically favoured association of the alkaloid to the inactive state.

Discussion: $K_{V11.1}$ channels are blocked from the cytosolic side both by the neutral and charged form of ibogaine, and respective currents are altered by relative changes in channel state occupancies over time.

Acknowledgements: This work was supported by the Austrian Science Fund FWF (P19352, P23060 to K.H., W1205 to S.B. and P21002 to J.Z.); P.T. is supported by SFB35-10, H.G. is supported by the doctoral program CCHD of the Medical University of Vienna.

A3.11

A biased non- G_{α} OXE receptor antagonist, Gue1654, inhibits leukocyte activation

Viktória Kónya¹, Stefanie Blättermann², Katharina Jandl¹, Wolfgang Platzer¹, Philipp A. Ottersbach³, Gunther Marsche¹, Michael Gütschow³, Evi Kostenis² and Ákos Heinemann^{1,*}

¹Institute of Experimental and Clinical Pharmacology, Medical University of Graz, Austria; ²Molecular, Cellular and

Pharmacobiology Section, Institute of Pharmaceutical Biology, University of Bonn, Germany; ³Pharmaceutical Institute, Pharmaceutical Chemistry I, University of Bonn, Germany

*E-mail: akos.heinemann@medunigraz.at

Intrinsic Activity, 2013; **1**(Suppl. 1):A3.11

Background: G_{α} -coupled chemoattractant receptors such as the 5-oxo-ETE (OXE) receptor are able to switch on $G_{\alpha}\beta\gamma$ protein-dependent and β -arrestin-related signaling traits. But which of these signaling pathways are truly important for the chemoattractant functions in leukocytes is not clarified yet. As we recently reported, Gue1654 is a unique $G\beta\gamma$ -biased OXE receptor antagonist having no inhibitory activity on G_{α} -related signaling, which makes Gue1654 an unprecedented tool for assessing the involvement of G protein subunits in chemoattractant receptor function.

Methods: β -Arrestin-2 recruitment was studied in OXE-receptor-overexpressing HEK cells using BRET assays. Activation of leukocytes was assessed by flow cytometry assays and by immunofluorescence microscopy. Leukocyte capture to endothelial cells was addressed under physiological flow conditions.

Results: In this study we found that Gue1654 additionally blocks β -arrestin-2 recruitment in HEK cells overexpressing OXE receptors and PTX-insensitive ERK1/2 phosphorylation in human eosinophils and neutrophils. Furthermore, Gue1654 is able to prevent several 5-oxo-ETE-triggered functional events in eosinophils and neutrophils, such as activation of CD11b/CD18 integrins, oxidative burst, actin polymerization and interaction with endothelial cells. In addition, Gue1654 completely prevented 5-oxo-ETE-induced Ca^{2+} influx and chemotaxis of human primary monocytes.

Discussion: Our observations favor the notion that chemoattractant receptors traditionally classified as G_{α} -coupled receptors do not require G_{α} protein to elicit functional responses in leukocytes. Furthermore, Gue1654 as a non- G_{α} -biased antagonist of OXE receptors provides a new basis for therapeutic intervention to treat inflammatory diseases involving activation of eosinophils, neutrophils and monocytes.

Acknowledgements: Austrian Science Fund FWF (grant P25531-B23 to V.K.).

A3.12

F557L – a novel determinant of hERG channel inhibition: allosteric modulation or drug binding?

Priyanka Saxena, Tobias Linder, Igor Barburin, Andreas Windisch, Kirsten Knappe, Eugen Timin, Steffen Hering and Anna Stary-Weinzinger*

Department of Pharmacology and Toxicology, University of Vienna, Austria

*E-mail: anna.stary@univie.ac.at

Intrinsic Activity, 2013; **1**(Suppl. 1):A3.12

Background: The human ether-a-go-go-related gene (hERG, $K_{V11.1}$) plays a pivotal role in repolarization of the ventricles. Understanding the molecular basis of the arrhythmogenicity of hERG inhibition is, therefore, essential for drug development. We have previously shown that π - π stacking interactions between the two cavities facing the aromatic amino acids Y652 and F656 on helix S6 can shape the hERG drug-binding pocket. Loss of π - π stacking interactions caused by Y652A may induce conformational changes in the F656 side chain and affect the binding orientation of blockers [1].

Methods: Molecular dynamics simulations and docking studies revealed that an aromatic amino acid (F557) located in close proximity on helix S5 may also influence the conformation of the drug-binding residues (Y652/F656) and thereby allosterically modulate channel inhibition.

Results: To test this hypothesis, we investigated the effect of mutation F557L on hERG inhibition by seven different hERG blockers. hERG channels were heterologously expressed in *Xenopus laevis* oocytes and channel inhibition was studied by means of the two-microelectrode voltage clamp technique. Comparable IC₅₀ shifts towards higher drug concentrations were induced by F557L and Y652A for all seven compounds (e.g. haloperidol: Δ IC₅₀ [F557L / Y652A] = 43.6 / 49.3 μ M). Remarkably, F557L completely prevented channel block by dofetilide.

Discussion: Our data may be interpreted in two ways: First, the IC₅₀ shifts in F557L are caused by the loss of π - π stacking interactions and resulting changes in the orientation of the drug-binding determinants Y652 and F656. Second, drugs may interact with F557 directly. Docking studies revealed a binding mode orthogonal to the channel between two adjacent subunits supporting the second hypothesis.

Acknowledgements: This work was supported by the Austrian Science Fund FWF (grant P22395); T.L. was supported by a research fellowship 2013 from the University of Vienna, P.S. and T.L. are fellows of the graduate school program MolTag (FWF W1232).

Reference

1. Nape K, Linder T, Wolschann P, Beyer A, Sary-Weinzinger A: **In silico analysis of conformational changes induced by mutation of aromatic binding residues: consequences for drug binding in the hERG K⁺ channel.** *PLoS One*, 2011; 6(12):e28778.

A3.13

Protein acetylation in human rhabdomyosarcoma and neuroblastoma cells induced by simvastatin

Murtaza Kulaksiz and Martin Hohenegger*

Institute for Pharmacology, Medical University of Vienna, Austria

*E-mail: martin.hohenegger@meduniwien.ac.at

Intrinsic Activity, 2013; 1(Suppl. 1):A3.13

Background: Statins inhibit 3-hydroxy-3-methylglutaryl-CoA (HMG-CoA) reductase. Based on this feature, they are widely and successfully used against hypercholesterolemia and in the treatment of cardiovascular diseases. Epigenetic modifications play a crucial role in diverse post-translational modifications including acetylation, methylation, phosphorylation and ubiquitinylation, which are important in many cellular processes like proliferation, survival, differentiation and motility. To our knowledge, we here present for the first time that simvastatin, which possesses structural homology with some histone deacetylase (HDAC) inhibitors, is able to acetylate proteins in human rhabdomyosarcoma (RD) and neuroblastoma (SH-SY5Y) cells.

Methods: Western blot analyses were performed for detection of acetylated proteins in RD cells and SH-SY5Y cells. The activity of HDAC I, II and III (sirtuins) was quantified in cytoplasmic and nuclear fractions of simvastatin-treated cells based on fluorometric assays with specific substrates and was compared with extracts from untreated cells.

Results: Simvastatin enhanced acetylation of proteins in the nuclear fractions in comparison to cytoplasmic fractions. The observed effects were concentration-dependent in both cell lines. Moreover, simvastatin inhibited all HDACs; however, this inhibition was only significant for sirtuin activity. The expression on protein level of HDACs was not affected by simvastatin.

Discussion: Simvastatin is able to enhance acetylation of histones as well as non-histone proteins by inhibiting HDACs. Interestingly, HDACs on protein level were not affected by simvastatin treatment in both cell lines.

Acknowledgements: This work was supported by Herzfeldersche Familienstiftung and Austrian Science Fund FWF (P22385).

A3.14

Role of ATP and electrical stimulation on the expression of muscle-specific genes

Martin Plaikner and Lukas G. Weigl*

Department of Special Anaesthesia and Pain Therapy, Medical University of Vienna, Austria

*E-mail: lukas.weigl@meduniwien.ac.at

Intrinsic Activity, 2013; 1(Suppl. 1):A3.14

Background: The mechanisms of muscle hypertrophy due to mechanical stimulation are not well understood. ATP is a co-transmitter of acetylcholine in the neuromuscular junction. Its release and the activation of the P2Y₁ purinergic receptor in muscle cells due to increased neuromuscular activity might be a modulating mechanism leading to alterations in gene transcription and protein expression [1]. To mimic the effect of mechanical load on cultured muscle cells, one group of the cells was electrically stimulated and the effect of ATP on the transcription of several muscle-specific genes was assessed.

Methods: C2C12 cells were cultivated and differentiated into myotubes. One group was electrically stimulated and treated with the non-degradable agonist of the P2Y₁ receptor, MeSATP. As a control, stimulated cells were also treated with an antagonist of the receptor (MRS2179) or a combination of both. These treatments were also performed with non-stimulated cells. The effects on gene expression were measured with qPCR on cDNA transcripts from whole cellular RNA.

Results: The data retrieved so far indicate an increase in transcription of muscle-specific genes in the electrically stimulated group treated with the P2Y₁ receptor agonist compared to the electrically stimulated group with no further treatment.

Discussion: Although the receptor ligands were selected as specific for the P2Y₁ receptor, interactions with other subtypes of purinoceptors, e.g. the P2X ligand-gated channel, cannot be excluded. The P2Y₁ receptor might be a pharmacological target for the treatment of dystrophic muscle diseases by helping to sustain the muscle mass although further research on this topic is necessary for a better understanding of the receptor's effects.

Acknowledgements: C2C12 cells were a generous gift of K. Hilber. This work was supported by the Austrian Science Fund FWF (P24922-B13) and the Verein zur Förderung von Wissenschaft und Forschung in der Anästhesie und Schmerztherapie.

Reference

1. May C, Weigl L, Karel A, Hohenegger M: **Extracellular ATP activates ERK1/ERK2 via a metabotropic P2Y₁ receptor in a Ca²⁺ independent manner in differentiated human skeletal muscle cells.** *Biochem Pharmacol*, 2006; 71(10):1497–1509.

A3.15

Characterization of drug interaction of pore-exposed tyrosine residues

Yaprak Dönmez Çakıl¹, Narakorn Khunweeraphong², Zahida Parveen², Diethart Schmid³, Matthias Artaker⁴, Gerhard F. Ecker⁵, Harald H. Sitte¹, Oliver Pusch⁶, Peter Chiba² and Thomas Stockner^{1,*}

¹*Institute of Pharmacology, Medical University of Vienna, Austria;*

²*Institute of Medical Chemistry, Medical University of Vienna,*

Austria; ³*Institute of Physiology, Medical University of Vienna,*

Austria; ⁴*Department of Medical Biochemistry, Max F. Perutz*

Laboratories, Medical University of Vienna, Austria; ⁵*Emerging Field*

Pharmacoinformatics, Department of Medicinal Chemistry,

University of Vienna, Austria; ⁶*Department of Cell and*

Developmental Biology, Medical University of Vienna, Austria

*E-mail: thomas.stockner@meduniwien.ac.at

Intrinsic Activity, 2013; 1(Suppl. 1):A3.15

Background: Many of the ABC transporters are essential for human health. P-glycoprotein (ABCB1), a multispecific efflux transporter, plays an important role in drug disposition and resistance. No transporter has been characterized in sufficient detail to fully understand transporter–drug interaction at the molecular level. Composite solute translocation paths, which allow movement of structurally diverse compounds across the plasma membrane, are formed at the interface of the transmembrane domains. The rotational C2 symmetry of ABC transporters implies the existence of two symmetry-related sets of substrate-interacting amino acids.

Methods: P-glycoprotein mutants were transiently expressed in HEK 293 cells. Efflux of rhodamine 123 and inhibition of rhodamine 123 efflux by propafenones were determined by FACS analysis.

Results: We explored the role of pore-exposed tyrosine hydroxyl groups for hydrogen bonding interactions with propafenone-type ligands in their preferred binding site 2. Either or both of the two site-2 tyrosines (residue 950 and 953) were found to form hydrogen bonds with propafenone analogs, but also with the preferred site-1 substrate rhodamine 123.

Discussion: The present study serves as a proof of concept that contribution of single residues can be studied individually.

Acknowledgements: This study was supported by SFB 35 project part 3509 and FWF P23319.

A3.16

The puzzling C-tail and the part it plays in the folding and ER export trajectory of the serotonin transporter

Sonja Sucic, Ali El-Kasaby, Harald H. Sitte and Michael Freissmuth*
Institute of Pharmacology, Centre of Physiology and Pharmacology, Medical University of Vienna, Austria

*E-mail: michael.freissmuth@meduniwien.ac.at
Intrinsic Activity, 2013; 1(Suppl. 1):A3.16

Background: The serotonin transporter (SERT) mediates the reuptake of its eponymous substrate serotonin from the synaptic cleft into presynaptic specialisations. Like other membrane proteins, SERT is co-translationally inserted into the ER membrane. After adopting its folded state, it must reach the ER exit sites to recruit components of the COPII coat, i.e. the SEC23/SEC24 dimer to allow for their export from the ER. COPII-dependent ER export is absolutely required for correct targeting to the synaptic specialization of neurotransmitter transporters, e.g. GAT1 and SERT [1,2]. Interestingly, SERT recruits SEC24C, although its close relatives (DAT, NET, GAT1) all require SEC24D [2]. Amino acid residues flanking the ER export motif on SERT (R⁶⁰⁷I⁶⁰⁸) must specify/direct SERT exit from the ER compartments.

Methods: Mutations of interest were generated by site-directed mutagenesis using the QuikChange™ kit (Stratagene) and wild-type human SERT as template. HEK 293 cells were transfected with plasmids encoding the wild-type and mutant SERTs by lipofection (Invitrogen). All constructs had yellow fluorescent protein tags on their N-termini to allow visualization by confocal laser scanning microscopy. Functional activity was assessed by radiolabeled serotonin uptake assays. Radiolabeled imipramine binding was used to examine protein folding. To address SEC24 dependence, we used siRNAs to knock-down SEC24 isoforms A–D, as described previously [2,3].

Results: The replacement of an aromatic Phe 604, and of nonpolar aliphatic Ile residues 608 and 612, by polar uncharged Gln residues (i.e. mutants F604Q, I608Q and I612Q, respectively) lead to marked reductions in [³H]5-HT uptake levels, compared to wild-type SERT. Confocal microscopy experiments revealed that the impaired functional activity resulted from intracellular retention of the SERT protein. The mutants could become targeted to the plasma

membrane upon an introduction of a second site suppressor E136A mutation. E136A locks the transporter in an inward-facing conformational state; albeit perfectly expressed at the cell surface, it lacks any appreciable uptake due to the defective transport cycle.

Discussion: Non-conservative mutations of F604, I608 and I612 cause ER retention of SERT by inducing folding defects, but not due to the loss of interaction with the COPII component SEC24C. Residue 604 must be hydrophobic for SERT to fold correctly, and although the F604Q mutant is retained in the ER, it can be rescued by various chemical and pharmacological chaperones. Current experiments begin to shed new light onto the folding trajectory and ER export of monoamine transporters.

Acknowledgements: This work was supported by SFB 35.

References

- Reiterer V, Maier S, Sitte HH, Kriz A, Rüegg MA, Hauri HP, Freissmuth M, Farhan H: **Sec24- and ARFGAP1-dependent trafficking of GABA transporter-1 is a prerequisite for correct axonal targeting.** *J Neurosci*, 2008; 28(47):12453–12464.
- Sucic S, El-Kasaby A, Kudlacek O, Sarker S, Sitte HH, Marin P, Freissmuth M: **The serotonin transporter is an exclusive client of the coat protein complex II (COPII) component SEC24C.** *J Biol Chem*, 2011; 286(18):16482–16490.
- Sucic S, Koban F, El-Kasaby A, Kudlacek O, Stockner T, Sitte HH, Freissmuth M: **Switching the clientele: a lysine residing in the C terminus of the serotonin transporter specifies its preference for the coat protein complex II component SEC24C.** *J Biol Chem*, 2013; 288(8):5330–5341.

A3.17

The role of heat shock proteins in ER export mechanisms of the human serotonin transporter

Ali El-Kasaby, Sonja Sucic, Harald H. Sitte and Michael Freissmuth*
Institute of Pharmacology, Centre of Physiology and Pharmacology, Medical University of Vienna, Austria

*E-mail: michael.freissmuth@meduniwien.ac.at
Intrinsic Activity, 2013; 1(Suppl. 1):A3.17

Background: ER export of members of solute carrier family 6 (SLC6) relies on the recruitment of the COPII (coat protein complex II) coat to the transporter. The COPII component SEC24 binds to an ER export motif (RL/RI/KL) located on the C-terminus of the cargo proteins. The serotonin transporter (SERT) is exported from the ER compartments by recruiting the SEC24 isoform C to its C-terminus [1,2]. The same region also provides a docking site for proteinaceous chaperones (heat shock protein (HSP) isoforms), which assist in protein folding [3]. Based on these observations, we postulate sequential exchange of the chaperone(s) for the COPII coat, as a mechanism to prevent premature ER export of partially folded SERTs.

Methods: In order to examine the exact functional role of HSPs in regulating the folding of SERT proteins and in the formation of COPII vesicles, we treated HEK 293 cells expressing wild-type SERT or several C-terminal mutants (including the RI-607,608-AA mutant, which is located at the putative ER export motif site of SERT) with different HSP inhibitors (e.g. 17-DMGA and geldanamycin), as well as with an ERAD inhibitor (kifunensine) or chemical (such as 4-PBA and DMSO) and pharmacochaperones (e.g. noribogaine).

Results: We determined the effects of these compounds on transporter surface expression levels by: (i) measuring specific [³H]5-HT uptake, (ii) immunoblotting and (iii) confocal laser scanning microscopy. We subsequently replicated the same series of experiments in JAR cells, a human choriocarcinoma cell line which endogenously expresses the SERT. Other experiments are underway to optimise the conditions for mass spectrometry studies.

Discussion: Collectively, these data will help us to elucidate the specific HSP isoforms associated with and regulating the ER export of SERT, as well as other SLC6 transporters.

Acknowledgements: This work was supported by SFB 35.

References

1. Susic S, El-Kasaby A, Kudlacek O, Sarker S, Sitte HH, Marin P, Freissmuth M: **The serotonin transporter is an exclusive client of the coat protein complex II (COPII) component SEC24C.** *J Biol Chem*, 2011; 286(18):16482–16490.
2. Susic S, Koban F, El-Kasaby A, Kudlacek O, Stockner T, Sitte HH, Freissmuth M: **Switching the clientele: a lysine residing in the C terminus of the serotonin transporter specifies its preference for the coat protein complex II component SEC24C.** *J Biol Chem*, 2013; 288(8):5330–5341.
3. El-Kasaby A, Just H, Malle E, Stolt-Bergner PC, Sitte HH, Freissmuth M, Kudlacek O: **Mutations in the carboxyl-terminal SEC24 binding motif of the serotonin transporter impair folding of the transporter.** *J Biol Chem*, 2010; 285(50):39201–39210.

A3.18

Unfolding the structure of LeuT_{Aa} employing luminescence resonance energy transfer

Azmat Sohail¹, Peggy Stolt-Bergner², Gerhard F. Ecker³, Michael Freissmuth¹, Walter Sandtner¹ and Harald H. Sitte^{1,*}

¹Institute of Pharmacology, Medical University of Vienna, Austria;

²Research Institute of Molecular Pathology, Campus Vienna

³Biocenter, Vienna, Austria; ³Department of Medicinal Chemistry, University of Vienna, Austria

*E-mail: harald.sitte@meduniwien.ac.at

Intrinsic Activity, 2013; 1(Suppl. 1):A3.18

Background: Neurotransmitter sodium symporters (NSS) are located in the brain and retrieve neurotransmitters from the synaptic cleft to end synaptic transmission. Solute carrier class 6 proteins (SLC6) are of great pharmacological importance in terms of their localization and function. The crystal structures obtained from a bacterial homolog, the leucine transporter LeuT_{Aa}, in open-to-outward, occluded, and open-to-inward conformations are present in frozen state with high resolution [1]. Due to its close kinship with SLC6 proteins, LeuT_{Aa} serves as a paradigm for these transporters.

Methods: In order to address the dynamics of the substrate transport cycle in LeuT_{Aa}, we use the lanthanide-based resonance energy transfer (LRET) technique. This method is a spin-off of the fluorescence resonance energy transfer method according to Förster, employing the introduction of the genetically encoded lanthanide-binding tags (LBT) as donor elements. Exogenous cysteine residues labelled with cysteine-specific fluorophores are used as acceptor elements. This technique is an alternative to address the movement of helices with great resolution and has been employed successfully to examine potassium channels [2].

Results: We screened for the functional LBT mutants using the scintillation proximity assay. The LeuT-A335-LBT-G336 mutant displayed function in terms of its binding activity. Within this background, we generated cysteine mutants. To date, we have successfully measured the intramolecular distances in different LBT-LeuT-Cys mutants. Furthermore, we observed intramolecular distance changes from these purified proteins in detergent micelles.

Discussion: Our LRET measurements will help us to understand the transport cycle and help to complete the missing steps in the substrate transport cycle of LeuT_{Aa}. Currently, we focus on the reconstitution of purified LeuT_{Aa} into liposomes and use our LRET measurements in a reconstituted system that allows using more physiological ionic gradients.

Acknowledgements: Supported by the Austrian Science Fund FWF (SFB 3506) to H.H.S. and partially funded by HEC to A.S.

References

1. Krishnamurthy H, Gouaux E: **X-ray structures of LeuT in substrate-free outward-open and apo inward-open states.** *Nature*, 2012; 481(7382):469–474.
2. Sandtner W, Bezanilla F, Correa AM: **In vivo measurement of intramolecular distances using genetically encoded reporters.** *Biophys J*, 2007; 93(9):L45–L47.

A3.19

FGFR3 and FGFR4 contribute to resistance in the therapy of colorectal cancer *in vitro*

Zeynep N. Erdem, Christine Heinzle, Gudrun Sonvilla, Bettina Grasl-Kraupp, Klaus Holzmann, Michael Grusch, Walter Berger and Brigitte Marian*

Institute for Cancer Research, Department of Internal Medicine I, Medical University of Vienna, Austria

*E-mail: brigitte.marian@meduniwien.ac.at

Intrinsic Activity, 2013; 1(Suppl. 1):A3.19

Background: Colorectal cancer is one of the leading causes of death worldwide. Although therapy has been improved, survival rates for late-stage tumours have not significantly changed. Response to classical chemotherapy drugs as well as to drugs targeting EGFR signalling failed to achieve the desired effect as resistance develops after some time. Mechanisms described in the literature suggest an important role of FGF signalling, be it by the positive regulation of anti-apoptotic signals or by triggering G₁ arrest.

Methods: Using the colorectal cancer cell line SW480 and appropriate vectors, we created cells overexpressing FGFR3-IIIb, FGFR3-IIIc and FGFR4^{arg} as well as FGFR4^{gly}, and established dose–response relationships for the chemotherapy drugs oxaliplatin and irinotecan and the EGFR/HER2 dual inhibitor lapatinib as well as the FGFR3 inhibitor PD173074.

Results: Here, we report a significantly decreased sensitivity to (i) oxaliplatin in cells overexpressing FGFR3-IIIb (IC₅₀ = 3.7 μM) as well as FGFR3-IIIc (4 μM) when compared to the control cell line (3 μM). Significantly higher IC₅₀ values were also observed when (ii) irinotecan was added to cells transfected with FGFR4^{arg} (18.4 μM), FGFR3-IIIb (41.5 μM) and FGFR3-IIIc (36.7 μM) when compared to control (11.3 μM). Treating the cells with the FGFR3 inhibitor PD173074 revealed a significantly higher sensitivity of FGFR4^{gly}-overexpressing cells (14.8 μM) than control cells (18.9 μM) while FGFR3-IIIb-overexpressing cells were more resistant (22.8 μM).

Discussion: The presence of FGFR3 splice variants as well as the FGFR4 G388R polymorphism may lead to less cell damage and may negatively affect responses to chemotherapy drugs and EGFR-targeting compounds. Based on these results, combination treatment with oxaliplatin/irinotecan and PD173074 as well as with lapatinib and PD173074 is currently being tested.

A3.20

Contribution of alveolar epithelial cells to the protective function of PGE₂ in acute lung injury

Thomas Bärnthaler, Ilse Lanz, Wolfgang Platzer, Ákos Heinemann and Viktória Kónya*

Institute of Experimental and Clinical Pharmacology, Medical University of Graz, Austria

*E-mail: viktoria.konya@medunigraz.at

Intrinsic Activity, 2013; 1(Suppl. 1):A3.20

Background: We have recently observed that PGE₂ exerted anti-inflammatory effects in the LPS-induced acute lung injury mouse model. In particular, PGE₂ markedly reduced infiltration of neutrophils into the mouse lung after LPS inhalation. However, the

exact mechanism is not elucidated yet. We aim here to investigate the contribution of alveolar epithelial cells to the PGE₂-induced anti-inflammatory function.

Methods: We isolate and cultivate mouse alveolar epithelial cells. The epithelial barrier function will be measured using electric cell substrate impedance sensing (ECIS). ECIS enables highly reproducible and precise determination of the barrier function of different cell layers.

Results: After optimizing the isolation and cultivation of mouse alveolar epithelial cells we assess the possible barrier-promoting effect of PGE₂. PGE₂ has got four receptors and the EP₄ receptor was found to mediate the anti-inflammatory function of PGE₂ in pulmonary inflammation. Hence, we investigate the impact of selective EP₄ receptor agonists and antagonists on the alveolar epithelial barrier function.

Discussion: Our results will indicate the role of the alveolar epithelial barrier in the anti-inflammatory function of PGE₂ in acute lung injury.

Acknowledgements: Austrian Science Fund FWF (grant P25531-B23 to V.K.).

A3.21

Pharmacological stimulation of hematopoietic stem cells

Zahra Kazemi¹, Christian Bergmayr¹, Andreas Kerschbaumer¹, Wolfgang Strohmaier², Michael Freissmuth¹ and Eva Zebedin-Brandl^{1,*}

¹Institute of Pharmacology, Center for Physiology and Pharmacology, Medical University of Vienna, Austria;

²SciPharm SàRL, Junglinster, Luxembourg

*E-mail: eva-maria.zebedin@meduniwien.ac.at

Intrinsic Activity, 2013; 1(Suppl. 1):A3.21

Background: The transplantation of hematopoietic stem cells (HSC) is a standard procedure in the treatment of hematological disorders and applicable to support chemotherapy in cancer. In practice, the clinical outcome is often hampered by severe infections. Hence there is a need for new pharmacological tools which facilitate functional bone marrow reconstitution. In recent years it has been shown that the G_{α_s} signaling pathway and stimulation of G_{α_s}-coupled EP₂ and EP₄ prostanoid receptors play an important role in migration and homing of transplanted HSC to the bone marrow niche [1,2]. Here we test the hypothesis that pretreatment of HSC with treprostnil, a stable analogue of prostacyclin (PGI₂), might be a promising therapeutic strategy to shorten the time period until the onset of the transplant.

Methods: Generation of murine HSC: Undifferentiated HSC (Lin⁻ SCA1⁺ c-Kit⁺) were isolated from murine bone marrow (BM), separated by MACS (magnetic-activated cell sorting) and characterized by fluorescence-activated cell sorting (FACS) [3].

Migration Assay: HSC were pretreated *in vitro* in the absence or presence of 10 μM treprostnil in combination with 30 μM forskolin (FSK). After incubation for either 1 h or 24 h at 37 °C in StemSpan™ SFEM containing growth factors, 100 μl cells were placed on the top of 2-chamber transwells followed by 4 h incubation at 37 °C with or without 100 ng/ml SDF-1 (R&D Systems) in bottom chambers. Completely migrated cells through 5-μm filter are counted by a cell counter. **Real-time PCR:** Total RNA was isolated and reversely transcribed from pretreated and untreated cells according to standard protocol. CXCR4 expression is quantified semi-quantitatively, as adjusted to expression of GAPDH or by RT-PCR.

Results: Pretreatment of murine HSC with treprostnil and forskolin was able to enhance HSC chemotaxis to SDF-1. This functional effect is also reflected at the mRNA level. In addition, preliminary data obtained in classical homing assays indicate an *in vivo* relevance of our findings.

Discussion: To date no pharmacological strategies are approved for direct stimulation of engraftment and/or homing of HCS. The therapeutic potential and clinical relevance rests in the unmet medical need of patients with either limited HCS cell number availability and/or high risk of infections.

References

1. Adams GB, Alley IR, Chung UI, Chabner KT, Jeanson NT, Lo Celso C, Marsters ES, Chen M, Weinstein LS, Lin CP, Kronenberg HM, Scadden DT: **Haematopoietic stem cells depend on G_{α_s}-mediated signalling to engraft bone marrow.** *Nature*, 2009; 459(7243):103–107.
2. Hoggatt J, Singh P, Sampath J, Pelus LM: **Prostaglandin E₂ enhances hematopoietic stem cell homing, survival, and proliferation.** *Blood*, 2009; 113(22):5444–5455.
3. Bergmayr C, Balasz C, Kazemi Z, Hussain F, Bauer T, Strobl H, Selzer P, Strohmaier W, Freissmuth M, Zebedin-Brandl E: **Pharmacological stimulation of murine and human hematopoietic stem cells.** *BMC Pharmacol Toxicol*, 2012; 13(Suppl. 1):A67.

A3.22

The relevance of the CDK4/6–p16INK4A axis for the development of lymphoid leukemia

Florian Bellutti, Michaela Prchal-Murphy, Karoline Kollmann and Veronika Sexl*

Institute of Pharmacology and Toxicology, University of Veterinary Medicine Vienna, Austria

*E-mail: veronika.sexl@vetmeduni.ac.at

Intrinsic Activity, 2013; 1(Suppl. 1):A3.22

Background: Cyclin-dependent kinase (CDK) 4 and 6 are key players mediating G₁ progression of the cell cycle. Hyperactivity of CDK6, as it is frequently observed in human leukemia and lymphoma [1], is often achieved by a functional loss of its predominant negative regulator p16INK4A. Moreover, recent studies have underlined the importance of the CDK6–p16INK4A axis for the development and maintenance of certain cancers in mouse models [2,3]. Nevertheless, the debate whether CDK6 represents a *bona fide* cancer target is still ongoing. Efforts were made to design small-molecule inhibitors perturbing signaling mediated by various CDKs, which are currently in clinical trials [4]. This study aims to combine knowledge obtained from previous work [5] with novel insights into the role of CDK6 for the pathogenesis of BCR-ABL⁺ lymphoid leukemia. Thus, it is expected to provide a rational basis for the selection of patients for whom a treatment with CDK4/CDK6 inhibitors might represent a beneficial therapeutic option.

Methods: Bone marrow cells were isolated from wild-type, INK4A/ARF^{-/-} as well as mice that harbor INK4-insensitive CDK6 (R31C) and CDK4 (R24C), respectively. Leukemic cell lines were generated by infecting the cells with a retrovirus encoding p185BCR-ABL. Pro-B-cell characteristics of all cell lines were verified using flow cytometry. The clonogenic potential of the different cell lines was compared in colony-forming cell assays. The proliferation kinetics was evaluated by counting cumulative cell numbers.

Results: We observed a slightly reduced level of CDK6-R31C protein in most cell lines tested compared to wild-type. In contrast, we failed to detect any significant alterations in mRNA levels. This reduction in CDK6-R31C protein was not compensated by an up-regulation of the close homologue CDK4. This observation was paralleled by a reduced level of retinoblastoma phosphorylated at threonine 821/826, two of the phosphorylation sites of CDK6 and CDK4 in cell lines harboring INK4-insensitive CDK6 and CDK4, respectively. Leukemic cells lacking INK4A/ARF displayed enhanced proliferative capacity as well as a higher clonogenic

potential *in vitro* compared to wild-type. This was not observed for cells harboring the INK4-insensitive CDKs.

Discussion: Loss of INK4A/ARF confers a proliferative advantage and a higher clonogenic potential to leukemic cells *in vitro*. Interestingly, this is not true for cells harboring INK4-insensitive CDK6/4, indicating a reduced catalytic activity upon ablation of INK4 binding. To understand the importance of these genetic alterations for the onset and progression of lymphoid leukemia we will extend our analysis by additional *in vitro* and *in vivo* experiments.

Acknowledgements: This work was supported by the Austrian Science Fund FWF (grant P24297 "Uncoupling CDK6 from p16INK4A – effects for hematopoiesis and lymphomagenesis").

References

1. Chilosi M, Doglioni C, Yan Z, Lestani M, Menestrina F, Sorio C, Benedetti A, Vinante F, Pizzolo G, Inghirami G: **Differential expression of cyclin-dependent kinase 6 in cortical thymocytes and T-cell lymphoblastic lymphoma/leukemia.** *Am J Pathol*, 1998; 152(1):209–217.
2. Hu MG, Deshpande A, Enos M, Mao D, Hinds EA, Hu GF, Chang R, Guo Z, Dose M, Mao C, Tschlis PN, Gounari F, Hinds PW: **A requirement for cyclin-dependent kinase 6 in thymocyte development and tumorigenesis.** *Cancer Res*, 2009; 69(3):810–818.
3. Kollmann K, Heller G, Schneckenleithner C, Warsch W, Scheicher R, Ott RG, Schäfer M, Fajmann S, Schleder M, Schiefer AI, Reichart U, Mayerhofer M, Hoeller C, Zöchbauer-Mueller S, Kerjaschki D, Bock C, Kenner L, Hoefler G, Freissmuth M, Green AR, Moriggl R, Buslinger M, Malumbres M, Sexl V: **A kinase-independent function of CDK6 links the cell cycle to tumour angiogenesis.** *Cancer Cell*, 2013; 24(2):167–181.
4. Diaz-Moralli S, Tarrado-Castellarnau M, Miranda A, Cascante M: **Targeting cell cycle regulation in cancer therapy.** *Pharmacol Ther*, 2013; 138(2):255–271.
5. Kollmann K, Heller G, Ott RG, Scheicher R, Zebelin-Brandl E, Schneckenleithner C, Simma O, Warsch W, Eckelhart E, Hoelbl A, Bilban M, Zöchbauer-Müller S, Malumbres M, Sexl V: **c-JUN promotes BCR-ABL-induced lymphoid leukemia by inhibiting methylation of the 5' region of *Cdk6*.** *Blood*, 2011; 117(15):4065–4075.

A3.23

In vivo effects of statins on SH-SY5Y and RD cells

Bihter Atil* and Martin Hohenegger

Institute of Pharmacology, Medical University of Vienna, Austria

*E-mail: bihter.atil@meduniwien.ac.at

Intrinsic Activity, 2013; 1(Suppl. 1):A3.23

Background: Statins are HMG-CoA reductase inhibitors derived from fungi metabolites and are successfully used in the treatment of hypercholesterolemia or, in addition, for prevention of cardiovascular diseases. Several studies have shown pleiotropic effects of statins, such as anti-inflammatory, anti-thrombogenic and anti-proliferative actions. Interestingly, they also possess the ability to directly inhibit ATP-binding cassette transporters like ABCB1, which is the most prominent challenge in chemoresistant tumor cells. Previously, we could show inhibition and deglycosylation of ABCB1 due to simvastatin treatment in the neuroblastoma cell line SH-SY5Y and in rhabdomyosarcoma RD cells [1,2]. Here, we confirm these observations by *in vivo* data.

Methods: Human SH-SY5Y and RD cells were inoculated in CD-1 nude mice for a xenograft experiment. Controls were compared with simvastatin-treated (1.1 mg/kg/day) mice with respect to body weight, tumor size and weight, and ABCB1 expression. Immunohistochemistry was supplemented by detection of apoptosis, PARP and caspase 3 cleavage.

Results: Tumor progression was significantly slowed in the simvastatin-exposed group, although body mass of mice was not altered. Total expression of ABCB1 was reduced in neuroblastoma and rhabdomyosarcoma following simvastatin exposure. However, the core glycosylated 140 kDa band of ABCB1 was significantly increased in both tumors. Similarly, apoptosis was enhanced in both tumors of simvastatin-treated animals.

Discussion: Here, we confirm that pharmacologically relevant human doses of simvastatin are capable to downregulate ABCB1 in neuroblastoma and rhabdomyosarcoma, and reduce tumor progression. The concerted action of well-tolerated statins together with conventional chemotherapeutics, which are substrates for ABCB1, may open a new area of adjuvant chemotherapy. Statins like simvastatin may represent a class of lead compounds which overcome ABCB1-mediated multidrug resistance by reducing its topological correct expression.

Acknowledgements: This work was supported by the Austrian Science Fund FWF and Herzfeldersche Familienstiftung.

References

1. Werner M, Atil B, Sieczkowski E, Chiba P, Hohenegger M: **Simvastatin-induced compartmentalisation of doxorubicin sharpens up nuclear topoisomerase II inhibition in human rhabdomyosarcoma cells.** *Naunyn-Schmiedeberg's Arch Pharmacol*, 2013; 386(7):605–617.
2. Sieczkowski E, Lehner C, Ambros PF, Hohenegger M: **Double impact on p-glycoprotein by statins enhances doxorubicin cytotoxicity in human neuroblastoma cells.** *Int J Cancer*, 2010; 126(9):2025–2035.

A3.24

Exploring the druggability of STAT5a in BCR-ABL⁺ leukemia

Angelika Berger¹, Andrea Hoelbl-Kovacic¹, Wolfgang Warsch¹, Jérôme Bourgeois², Ernestine Leitner³, Stefan Kubicek³, Richard Moriggl⁴, Fabrice Gouilleux² and Veronika Sexl^{1,*}

¹*Institute of Pharmacology and Toxicology, University of Veterinary Medicine, Austria;* ²*Génétique, Immunothérapie, Chimie et Cancer, CNRS UMR 7292, Université François Rabelais, Tours, France;* ³*CeMM Research Center for Molecular Medicine, Austrian Academy of Sciences, Vienna, Austria;* ⁴*Ludwig Boltzmann Institute for Cancer Research (LBI-CR), Vienna, Austria*

*E-mail: veronika.sexl@vetmeduni.ac.at

Intrinsic Activity, 2013; 1(Suppl. 1):A3.24

Background: The STAT proteins are often deregulated in cancers —STAT3 and STAT5 in particular. A constitutively active form of STAT5a (cSTAT5a) is capable of triggering a multi-lineage leukemia in mice. In human hematological malignancies such as chronic myeloid leukemia (CML) an oncogenic tyrosine kinase (BCR-ABL) activates STAT5 directly and causes leukemia. Here, STAT5 is crucial for leukemic development. STAT5a was shown to be highly phosphorylated on serine sites S725 and S779 in human samples. In cSTAT5a-driven leukemia, phosphorylation of these sites is critical for transformation. We investigated the role of STAT5a serine phosphorylation in BCR-ABL⁺ leukemia and identified the upstream kinases phosphorylating STAT5a on S725 and S779.

Methods: We established a chemical compound screen using viability as a read-out system. BCR-ABL^{p185+} cells expressing wild-type or mutant STAT5 variants were seeded in 384-well plates. Kinase inhibitors were added at a screening concentration of 10 μ M. Cells were incubated with positive hit compounds, lysed and subjected to immunoblotting with antisera specific for pSTAT5^{S725} and pSTAT5^{S779}. We used over-expression of pMSCV-IRES-GFP-based constructs encoding an individual serine kinase and *in vitro* kinase assays to verify our data.

Results: STAT5a harbors two conserved serine sites at position 725 and 779 in the C-terminal transactivation domain. Expression of

a Stat5a mutant that could not be phosphorylated on S725 and S779 (STAT5^{SASA}) was sufficient to induce apoptosis in BCR-ABL⁺ cells. Expression of Stat5a mutants that mimicked serine phosphorylation (STAT5^{SDSD}) did not hamper cell proliferation and was used as control for screening. Mitogen-activated kinases (MAPK) and cyclin-dependent kinases (CDK) were consistently identified by screening. Inhibition of MAPKs did not alter STAT5 serine phosphorylation. The CDK inhibitor flavopiridol reduced pSTAT5^{S725} levels whereas roscovitine and olomoucine did not change pSTAT5^{S725} levels. Over-expression of CDK8 resulted in elevated pSTAT5^{S725}. Furthermore, the up-stream kinase of STAT5^{S779} was identified and will be presented.

Discussion: Tyrosine kinase inhibitors (TKI) are well-established agents in the treatment of CML but lifelong treatment and the rise of mutations make an alternative therapeutic strategy inevitable. STAT5 is indispensable for leukemic transformation and maintenance. This dependence on STAT5 is conserved in leukemic cells that are resistant towards TKI therapy. We show that expression of STAT5^{SASA} kills leukemic cells. Further, STAT5 is phosphorylated by two different up-stream serine kinases on S725 and S779. These findings open the field of CML treatment towards serine kinase inhibitors and propose two novel and independent modes to target STAT5 activity in BCR-ABL⁺ leukemia.

APHAR Section of Clinical Pharmacology

A4.1

Effect of liposomal curcumin on red blood cells *in vitro*

Angela Storka¹, Uros Klikovic¹, Brigitta Vcelar², Lawrence Helson³ and Michael Wolzt^{1,*}

¹Department of Clinical Pharmacology, Medical University of Vienna, Austria; ²Polymun Scientific Immunbiologische Forschung GmbH, Klosterneuburg, Austria; ³SignPath Pharma Inc., Quakertown, PA, USA

*E-mail: michael.wolzt@meduniwien.ac.at

Intrinsic Activity, 2013; 1(Suppl. 1):A4.1

Background: Curcumin exerts anti-cancer, anti-inflammatory, antioxidant and antimicrobial properties but has a poor oral bioavailability and solubility in plasma. Accordingly, various drug delivery systems, such as liposomal preparation, have been developed to enhance bioavailability after intravenous administration. Since blood cells are the first point of contact for liposomal curcumin when administered intravenously, we investigated the effect of curcumin on human red blood cell (RBC) morphology *in vitro*.

Methods: Whole blood buffered with EDTA was incubated with different concentrations (1, 10, 100 µg/ml) of free or liposomal formulations of curcumin. RBC morphology and mean cellular volume were examined after 30 minutes, 1 hour, 2 hours and 4 hours of incubation and compared to untreated cells.

Results: After incubation with free and liposomal curcumin, with a threshold concentration of 10 µg/ml, a concentration-dependent echinocyte formation was observed. The peak effect was noted after 30 minutes of incubation. Treatment with empty liposomes also resulted in RBC shape change. Furthermore, a concomitant increase in mean RBC volume from 85.0 fl to a maximum of 87.7 fl was observed.

Discussion: Curcumin caused concentration-dependent changes in RBC morphology, which was also seen with liposomes and liposomal curcumin. These effects were additive and may represent a sign of toxicity following intravenous administration.

A4.2

Pulmonary surfactant inhibits killing of micafungin against *Candida krusei*

Peter Matzneller, Sabine Strommer, Zoe Österreicher and Markus Zeitlinger*

Department of Clinical Pharmacology, Medical University of Vienna, Austria

*E-mail: markus.zeitlinger@meduniwien.ac.at

Intrinsic Activity, 2013; 1(Suppl. 1):A4.2

Background: Pulmonary surfactant is a key component of epithelial lining fluid and reduces surface tension in pulmonary alveoli. Influence of pulmonary surfactant on the antimicrobial activity of selected antimicrobial drugs has been shown previously. In analogy, pulmonary surfactant might impact the anti-infective efficacy of antifungal drugs meant to treat pulmonary mycoses. The present *in vitro* experiments investigated the effect of pulmonary surfactant on antifungal killing of micafungin against *Candida krusei*.

Methods: Minimal inhibitory concentration (MIC) of micafungin (Astellas Pharma, Vienna, Austria) against *C. krusei* ATCC 6258 was determined in RPMI growth medium following EUCAST recommendations. Accordingly, the MIC was defined as a 50% reduction in fungal growth. In time-kill studies against *C. krusei* ATCC 6258, micafungin was tested at concentrations 1-fold, 4-fold and 16-fold the MIC for the test strain (Mica1, Mica4 and Mica16, respectively). Killing of all micafungin concentrations was tested in Sabouraud-dextrose broth (SDB) alone and in the presence of surfactant (Curosurf®) at a concentration of 1 mg/l. In addition, Mica1 was tested in the presence of lower surfactant concentrations (0.1 and 0.01 mg/l, respectively). Experiments were performed in triplicate.

Results: MIC of micafungin against *C. krusei* ATCC 6258 was 0.125 mg/l. In time-kill studies, surfactant had no effect on antifungal activity of Mica16, which achieved complete killing after 4 hours. Addition of surfactant at a concentration of 1 mg/l to Mica4, however, led to a 3 log step reduction in fungal killing (1 log step reduction in fungal growth after 24 hours instead of 4 log steps). For Mica1, addition of surfactant at a concentration of 1 mg/l completely abolished its antifungal activity, producing fungal growth rates identical to growth control. Addition of lower surfactant concentrations (0.1 and 0.01 mg/l) to Mica1 revealed a clear concentration-dependent pattern of micafungin killing impairment by pulmonary surfactant, since 0.1 mg/l showed a less marked inhibition of micafungin killing (1 log step reduction in colony counts with regrowth to initial levels at 24 hours), and 0.01 mg/l had no effect at all. Growth control curves of *C. krusei* ATCC 6258 were not influenced by addition of surfactant.

Discussion: The present data demonstrate that pulmonary surfactant inhibits antifungal activity of micafungin against a *C. krusei* strain in a concentration-dependent manner. This finding, if confirmed with other compounds and more fungal strains, may have important implications for the treatment of invasive mycoses of the lung, and needs to be validated in clinical studies.

A4.3

Blood-brain barrier P-glycoprotein activity in patients with therapy-refractory epilepsy before and after surgical focal resection assessed with (R)-[¹¹C]verapamil and positron emission tomography

Martin Bauer¹, Rudolf Karch², Markus Zeitlinger¹, Wolfgang Wadsak³, Markus Mitterhauser³, Markus Müller¹, Ekaterina Patarai⁴ and Oliver Langer^{1,5,*}

¹Department of Clinical Pharmacology, Medical University of Vienna, Austria; ²Center for Medical Statistics, Informatics and Intelligent Systems, Medical University of Vienna, Austria;

³Department of Biomedical Imaging and Image-guided Therapy, Division of Nuclear Medicine, Medical University of Vienna, Austria;

⁴Department of Neurology, Medical University of Vienna, Austria;

⁵AIT Austrian Institute of Technology, Seibersdorf, Austria

*E-mail: oliver.langer@meduniwien.ac.at

Intrinsic Activity, 2013; 1(Suppl. 1):A4.3

Background: About one-third of epilepsy patients are pharmacoresistant. Epileptic seizures are known to induce up-regulation of P-glycoprotein (P-gp) at the blood–brain barrier (BBB), which is thought to reduce target-site concentrations of antiepileptic drugs [1].

Methods: We assessed P-gp function at the BBB using the radiolabelled P-gp substrate (R)-[¹¹C]verapamil (VPM) and positron emission tomography (PET) in seven patients with temporal lobe epilepsy (TLE) before and after epilepsy surgery. VPM uptake (K_1) in different temporal lobe brain regions was used as a measure of P-gp activity at the BBB with high K_1 indicating low P-gp activity.

Results: After epilepsy surgery the antiepileptic drug load was reduced in all patients. Five patients were completely seizure-free, one patient had recurrent auras and one patient had a maximum of 3 seizure days a year. VPM metabolism did not differ between the pre- and the post-surgery PET scan (paired *t*-test of VPM area under the curve, $p = 0.24$). Following surgery, VPM K_1 in different temporal lobe brain regions was reduced on average by 5% relative to scans before surgery with large variations between patients (–46% to +39%). In the two patients that were medication- and seizure-free after surgery, regional VPM K_1 was increased in all examined temporal lobe regions in the post-surgery scan (+16% to +39%).

Discussion: VPM K_1 increases in post-surgery PET in patients with good outcome point to diminished P-gp activity at the BBB which may be caused by reduced seizure frequency and lower antiepileptic drug load.

Acknowledgements: The study was funded by FWF project “Transmembrane Transporters in Health and Disease” (SFB F35) and EU FP7 programme (EURIPIDES number 201380).

Reference

1. Feldmann M, Asselin MC, Liu J, Wang S, McMahon A, Anton-Rodriguez J, Walker M, Symms M, Brown G, Hinz R, Matthews J, Bauer M, Langer O, Thom M, Jones T, Vollmar C, Duncan JS, Sisodiya SM, Koepp MJ: **P-glycoprotein expression and function in patients with temporal lobe epilepsy: a case-control study.** *Lancet Neurol*, 2013; 12(8):777–785.

A4.4

Ketamine-induced time-dependent modulation of the thalamo-cortical network in healthy volunteers

Anna Höflich¹, Andreas Hahn¹, Georg S. Kranz¹, Thomas Vanicek¹, Christian Windischberger², Siegfried Kasper¹, Dietmar Winkler¹ and Rupert Lanzenberger^{1,*}

¹Department of Psychiatry and Psychotherapy, Medical University of Vienna, Austria; ²MR Center of Excellence and Center of Medical Physics and Biomedical Engineering, Medical University of Vienna, Austria

*E-mail: rupert.lanzenberger@meduniwien.ac.at

Intrinsic Activity, 2013; 1(Suppl. 1):A4.4

Background: A number of studies have described disturbances of thalamic functioning in schizophrenia [1]. In the light of recent evidence suggesting a significant impact of the glutamatergic system on key symptoms of this disorder, we aimed to assess whether changes in thalamic functional connectivity are driven by alterations of the glutamatergic system. Using ketamine, a selective NMDA receptor antagonist, we assessed time-dependent changes

of functional connectivity before, during and after intravenous application of a subanaesthetic dose of esketamine using long-term resting-state functional MRI (fMRI). We specifically aimed to analyse ketamine-induced effects on cortico-thalamic functional connections.

Methods: Thirty healthy volunteers (25 ± 4.6 years, 18 males) underwent two fMRI sessions in a double-blind, placebo-controlled study design. Subjects underwent a resting-state fMRI scan lasting for 55 minutes. During fMRI either esketamine hydrochloride (mean dose 15.5 ± 3.1 mg) or placebo (0.9% saline solution) was applied intravenously over a time period of 20 minutes using a fully automated MRI-compatible infusion system. Resting-state measurements were performed at 3 Tesla (Siemens Trio, Erlangen, Germany) using single-shot gradient-recalled EPI with TR/TE = 1800/38 ms, a matrix size of 128 × 128 voxel and a field-of-view of 190 × 190 mm. Preprocessing was performed as described previously [2] using SPM8 (www.fil.ion.ucl.ac.uk/spm). For the calculation of thalamo-cortical connectivity the cortex was divided in non-overlapping regions of interest (prefrontal cortex, motor cortex/supplementary motor area, somatosensory cortex, temporal lobe, posterior parietal cortex, occipital lobe—based on the automated anatomical labeling atlas (AAL)) and used as seed regions in a seed–voxel correlation analysis.

Results: Analysis revealed significant increase of cortico-thalamic connectivity of the somatosensory and temporal cortex. Immediately after the start of the ketamine infusion a significant increase in functional connectivity of the postcentral gyrus with the ventrolateral region of the thalamus was observed, with significant difference to the placebo condition ($p < 0.05$, FWE-corrected). The analysis of temporo-thalamic connections revealed a ketamine-associated increase of the temporal seed region with the medial dorsal nucleus. Again, differences between the ketamine scan and the placebo scan were present shortly after start of the ketamine application ($p < 0.05$, FWE-corrected). For both seed regions, effects of esketamine on cortico-thalamic connectivity were evident during the entire duration of the ketamine infusion and the following 2.5 minutes.

Discussion: Our results point toward the fact that changes of thalamic functioning as described for schizophrenia can be partly mimicked by NMDA receptor blockage. This adds substantial knowledge about the neurobiological mechanisms underlying the profound changes of perception and behaviour during the application of NMDA receptor antagonists.

Acknowledgements: This research was funded by Austrian National Bank (grant 14193).

References

1. Woodward ND, Karbasforoushan H, Heckers S: **Thalamocortical dysconnectivity in schizophrenia.** *Am J Psychiatry*, 2012; 169(10):1092–1099.
2. Hahn A, Wadsak W, Windischberger C, Baldinger P, Höflich AS, Losak J, Nics L, Philippe C, Kranz GS, Kraus C, Mitterhauser M, Karanikas G, Kasper S, Lanzenberger R: **Differential modulation of the default mode network via serotonin-1A receptors.** *Proc Natl Acad Sci USA*, 2012; 109(7):2619–2624.

A4.5

Missing short-term influence from ketamine on gray matter

Sebastian Ganger¹, Anna Höflich¹, Andreas Hahn¹, Natalia Lipskaia¹, Christian Windischberger² and Rupert Lanzenberger^{1,*}

¹Department of Psychiatry and Psychotherapy, Medical University of Vienna, Austria; ²Center for Medical Physics and Biomedical Engineering, Medical University of Vienna, Austria

*E-mail: rupert.lanzenberger@meduniwien.ac.at

Intrinsic Activity, 2013; 1(Suppl. 1):A4.5

Background: Voxel-based morphometry (VBM) of structural MRI data has become a useful tool to investigate pathological alterations and longitudinal changes of gray matter volume. A recent pharmacological challenge demonstrated reversible short-term effects even within a few hours [1]. In this work, we investigated the effect of ketamine-infusion on VBM estimates of the gray matter.

Methods: In this study 28 subjects (15 female) aged 24.8 ± 4.6 years, underwent MRI in a Siemens Trio 3 Tesla scanner. T1-weighted structural images were acquired using a MPRAGE sequence, with a resolution of $1.1 \text{ mm} \times 1 \text{ mm} \times 1 \text{ mm}$ (matrix = $160 \times 240 \times 256$ voxel). All subjects underwent a placebo-controlled cross-over trial, comprising two measurement sessions (verum and placebo), each consisting of two runs (before and after infusion). The first run of each session was acquired before, and the second run after intravenous administration of either ketamine (esketamine hydrochloride, mean dose 15.0 ± 3.0 mg) or placebo (0.9% saline solution). The delay between the two structural scans was about 95 min, during which additional functional scans were acquired. T1-weighted images were segmented using VBM8's DARTEL algorithm. Statistical inference was made using repeated-measures ANOVA, correcting for multiple comparisons with the family-wise error rate at $p < 0.05$.

Results: There was no significant interaction of drug administration with time, indicating no direct effect before versus after ketamine infusion as compared to placebo, yet there was a significant effect of time (i.e. pre- vs. post-injection) independent of ketamine or placebo administration. Here, decreases in gray matter volume were observed within the superior frontal cortex ($t = 7.62$) and bilaterally in the inferior temporal lobe ($t = 7.11$).

Discussion: It has been shown previously that VBM can reveal gray matter differences after pharmacological challenge with a dopamine D₂ antagonist [1]. However, we were not able to reproduce similar short-term effects of ketamine although this drug has been shown to elicit neuroplasticity effects via the NMDA receptor [2]. The missing validation of previously reported short-term changes in gray matter volume may in part relate to the different study drugs used. However, taking into account that both ketamine and placebo infusion induced gray matter decreases, one needs to consider that such short-term differences in VBM metrics could also be explained by the infusion effect *per se*. Similarly, it remains to be investigated whether the effects observed here are caused by physiological and/or scanner-specific artefacts, as the MRI signal in brain areas close to air cavities is sensitive to signal loss.

References

1. Tost H, Braus DF, Hakimi S, Ruf M, Vollmert C, Hohn F, Meyer-Lindenberg A: **Acute D₂ receptor blockade induces rapid, reversible remodeling in human cortical-striatal circuits.** *Nature Neurosci*, 2010; 13(8):920–922.
2. Coyle JT, Tsai G: **NMDA receptor function, neuroplasticity, and the pathophysiology of schizophrenia.** *Int Rev Neurobiol*, 2004; 59:491–515.

A4.6

SSRI-induced occupancy of the serotonin transporter investigated with positron emission tomography

Georg S. Kranz¹, Rupert Lanzenberger^{1,*}, Daniela Haeusler², Pia Baldinger¹, Markus Savli¹, Marie Spies¹, Gregor Gryglewski¹, Wolfgang Wadsak², Markus Mitterhauser² and Siegfried Kasper¹
¹Department of Psychiatry and Psychotherapy, Medical University of Vienna, Austria; ²Department of Biomedical Imaging and Image-guided Therapy, Division of Nuclear Medicine, Medical University of Vienna, Austria

*E-mail: rupert.lanzenberger@meduniwien.ac.at

Intrinsic Activity, 2013; 1(Suppl. 1):A4.6

Background: According to the law of mass action, and assuming that serotonin transporter (SERT) availability is proportional to its density, SERT occupancy by selective serotonin reuptake inhibitors (SSRIs), defined as percent signal reduction should be similar across regions. However, an earlier positron emission tomography (PET) study found SERT occupancies to vary across regions [1]. We therefore tested the homogeneity of regional SERT occupancy and its dependence on pretreatment SERT availability in depressed subjects.

Methods: Nineteen out-patients suffering from major depression received oral doses of either escitalopram (10 mg/day, 10 subjects) or citalopram (20 mg/day, 9 subjects) (Lundbeck A/S, Denmark) and underwent one [¹¹C]DASB PET scan before treatment (PET1) and one 6 hours following the first SSRI dose (PET2). SERT binding potential (BP_{ND}) was quantified and occupancy was defined as: occupancy (%) = $(1 - \text{BP}_{\text{ND}}\text{PET2}/\text{BP}_{\text{ND}}\text{PET1}) \times 100$. Regional SERT occupancies were compared to mean occupancies across regions. Associations between SERT occupancy and pretreatment availability were tested using two different approaches to avoid statistical artefacts [2]: (i) regression of residual SERT availability on pretreatment availability; (ii) correlation of the mean between pretreatment and residual availability (Oldham's transformation) and absolute SERT reduction.

Results: Occupancies at PET2 ranged between $43.53 \pm 18.09\%$ and $82.16 \pm 7.36\%$. Mean cortical occupancy values were significantly lower than mean subcortical occupancy values ($65.66 \pm 10.60\%$ vs. $72.99 \pm 6.75\%$, $p = 0.001$, paired samples *t*-test). Repeated-measures ANOVA and post-hoc paired samples *t*-tests revealed that middle and inferior temporal cortex had significantly lowered occupancies, whereas subgenual cingulate cortex had significantly greater occupancies compared to mean cortical occupancies. Likewise, subcortical regions such as the putamen and thalamus, exhibited decreased occupancies, whereas amygdala and raphe nuclei had greater occupancies compared to mean subcortical occupancies (all $p < 0.05$ corrected). Regression analysis revealed a strong positive effect of pretreatment SERT binding on residual SERT binding ($R^2 = 0.92$, $\beta = 0.96$, $T = 15.10$, $p < 0.001$). Similarly, high associations were found between Oldham's transformation and absolute change after treatment across brain regions ($r = 0.99$, $p < 0.001$). That is, regions with higher baseline SERT BP_{ND} were significantly more occupied by acute SSRI treatment.

Discussion: Our results indicate regional differences in SERT occupancy associated with acute treatment with SSRIs. Furthermore, our study reveals a strong dependence of regional SERT blockage and residual availability on pretreatment SERT availability. These findings corroborate sustained SERT binding and rebinding of SSRIs in regions with high SERT availability as mechanisms of prolonged antidepressant drug action [3].

References

1. Meyer JH, Wilson AA, Sagrati S, Hussey D, Carella A, Potter WZ, Ginovart N, Spencer EP, Check A, Houle S: **Serotonin transporter occupancy of five selective serotonin reuptake inhibitors at different doses: an [¹¹C]DASB positron emission tomography study.** *Am J Psychiatry*, 2004; 161(5):826–835.
2. Gill JS, Zezulka AV, Beevers DG, Davies P: **Relation between initial blood pressure and its fall with treatment.** *Lancet*, 1985; 325(8428):567–569.
3. Vauquelin G, Charlton SJ: **Long-lasting target binding and rebinding as mechanisms to prolong *in vivo* drug action.** *Br J Pharmacol*, 2010; 161(3):488–508.

A4.7

The influence of cross-sex hormone therapy on stop-signal-task-related brain activation measured with 7T fMRI

Marie Spies¹, Georg S. Kranz¹, Sebastian Ganger¹, Ronald Sladky², Martin Küblböck², Thomas Vanicek¹, Andreas Hahn¹, Christian Windischberger², Siegfried Kasper¹ and Rupert Lanzenberger^{1,*}

¹Department of Psychiatry and Psychotherapy, Medical University of Vienna, Austria; ²Center for Medical Physics and Biomedical Engineering, Medical University of Vienna, Austria

*E-mail: rupert.lanzenberger@meduniwien.ac.at

Intrinsic Activity, 2013; 1(Suppl. 1):A4.7

Background: The stop-signal task (SST) is widely applied as a functional magnetic resonance imaging (fMRI) paradigm as it specifically activates brain regions associated with motor inhibition. A possible sex-hormone effect on motor inhibition is suggested by sex differences in related brain activation patterns [1,2] and is further supported by an association between SST inhibitory control and estrogen levels [3]. This study aims to further investigate the effect of cross-sex hormone therapy in transsexuals on motor-inhibition-related regional brain activation using the SST and ultrahigh-field 7T fMRI.

Methods: Nine female-to-male (FtM) (mean age \pm SD: 26.0 \pm 6.0 years) and eight male-to-female (MtF) (29.5 \pm 7.0 years) transsexual subjects participated in this study. Two 7T fMRI scans during which subjects performed an SST with an event-related design were acquired. The first and second scans took place at baseline and after approximately four weeks (range 23–51 days) of cross-sex hormone therapy, respectively. Transsexual subjects received cross-sex hormone treatment according to protocols routinely implemented at the Unit for Gender Identity Disorder at the Medical University of Vienna. Functional data were acquired using a Siemens Magnetom 7T scanner (EPI sequence, TE/TR = 23/1.4 s, 128 \times 128 voxels, 32 slices). Standard preprocessing was carried out using SPM8. Statistics were calculated using SPM8 including

repeated-measures ANOVA with group (MtF, FtM) as the between-subject and fMRI scan session as the within-subject factor, as well as post-hoc one-sample *t*-tests.

Results: Group and interaction effects were found within regions relevant to motor inhibition. FtM subjects exhibited greater activation than MtF within the precentral cortex ($t = 5.92$) while the supplementary motor area (SMA) showed an interaction effect ($t = -4.17$). Post-hoc one-sample *t*-tests revealed that MtF subjects showed activation within the SMA before cross-sex hormone therapy ($t = 5.19$), while FtM showed activation in this region after four weeks of hormone therapy ($t = 4.89$, all $p < 0.001$ uncorrected).

Discussion: The group effect found within the precentral cortex only allows for limited interpretation on the role cross-sex hormone therapy may play, as an effect of time and fundamental differences between subject groups cannot be excluded. The interaction effect found within the SMA, however, does point towards a possible cross-sex hormone influence. Testosterone modulation of motor-inhibition-related activation within this region is suggested by activation of the SMA in MtF during scan one, and in FtM in scan two. This is supported by evidence of greater motor-inhibition-related activity in the SMA in men than in women [1].

Acknowledgements: This study is financed by a grant awarded to R.L. by the Austrian Science Fund FWF (P23021).

References

- Li CS, Huang C, Constable RT, Sinha R: **Gender differences in the neural correlates of response inhibition during a stop signal task.** *NeuroImage*, 2006; 32(4):1918–1929.
- Li CS, Zhang S, Duann JR, Yan P, Sinha R, Mazure, CM: **Gender differences in cognitive control: an extended investigation of the stop signal task.** *Brain Imaging Behav*, 2009; 3(3):262–276.
- Colzato LS, Hertsig G, van den Wildenberg WP, Hommel B: **Estrogen modulates inhibitory control in healthy human females: evidence from the stop-signal paradigm.** *Neuroscience*, 2010; 167(3):709–715.

Author Index (Numbers refer to abstract no.)

Aigner, L. ... A1.23, A1.28, A1.30	Béni, Sz. ... A3.1	Cervenak, J. ... A1.15	Eigner, S. ... A1.42
Artaker, M. ... A3.15	Berger, A. ... A3.24	Cervenka, R. ... A1.19, A3.5	El-Kasaby, A. ... A3.16, A3.17
Assadpour, E. ... A1.18	Berger, J. ... A1.31, A1.35, A1.44	Chandaka, G.K. ... A2.7	Engleder, E. ... A3.9
Atil, B. ... A3.23	Berger, M. ... A1.21	Chen, W.-Q. ... A1.25	Erdem, F.A. ... A1.25
Baker, S. ... A1.40	Berger, W. ... A3.19	Chiba, P. ... A2.6, A3.15	Erdem, Z.N. ... A3.19
Baldinger, P. ... A1.38, A4.6	Bergmayr, C. ... A3.21	Couillard-Després, S. ... A1.23, A1.28, A1.30	Ernst, M. ... A1.26, A1.34
Balioová, M. ... A1.10, A1.14	Bertagnolli, E. ... A1.17, A3.9	Ćurčić, S. ... A3.8	Etemad, S. ... A2.10
Balla, Gy.Y. ... A1.15	Bertaso, F. ... A3.6	Daschil, N. ... A1.47, A2.1	Exler, A. ... A3.9
Baran, H. ... A1.41, A1.42	Bieler, L. ... A1.23	Decker, T. ... A3.4	Fagni, L. ... A3.6
Barburin, I. ... A3.12	Bindreither, D. ... A2.10	Di Biase, V. ... A1.51, A2.5	Farzi, A. ... A1.4
Barna, L. ... A1.15	Bittner, R.E. ... A3.5	Diao, W. ... A1.37	Feldbauer, R.V. ... A1.26
Bärnthaler, T. ... A3.20	Blättermann, S. ... A3.11	Dimitrova, M. ... A1.2	Fernández, E. ... A1.40
Bauer, A. ... A1.39	Boehm, S. ... A1.18, A1.25, A1.27, A2.2, A2.7, A3.10	Dimitrova, S. ... A1.2	Ferraguti, F. ... A3.6
Bauer, J. ... A1.35	Bongard, M. ... A1.40	Ding, Y.-S. ... A1.39	Flucher, B.E. ... A1.5, A1.9, A1.47, A2.1, A2.5, A2.9, A2.10
Bauer, M. ... A4.3	Bourgeois, J. ... A3.24	Dönmez Çakıl, Y. ... A3.15, A2.6	Forss-Petter, S. ... A1.31, A1.35, A1.44
Beck-Sickingler, A. ... A1.46	Brezina, A. ... A3.9	Drexel, M. ... A1.11	Förste, A. ... A1.12
Beiersdorf, J. ... A1.7, A1.8	Brunner, S. ... A1.4	Drobny, H. ... A2.2	Freissmuth, M. ... A2.6, A2.11, A3.16, A3.17, A3.18, A3.21
Beiranvand, F. ... A1.52	Bulling, S. ... A2.3	Dudok, B. ... A1.15	Fukazawa, Y. ... A3.6
Beisteiner, R. ... A1.21	Calò, G. ... A3.1	Dürnberger, G. ... A1.22	Gabor, F. ... A3.9
Bellutti, F. ... A3.22	Campiglio, M. ... A1.47, A2.5, A2.9	Ebner, S. ... A1.4	
Ben Haddou, T. ... A3.1	Camurdanoglu, B.Z. ... A1.22	Ecker, G.F. ... A2.3, A2.11, A3.15, A3.18	
Benedetti, A. ... A1.5, A2.10			
Benedetti, B. ... A1.9			

- Gafar, H. ... A2.2, A2.7, A3.10
Ganger, S. ... A4.5, A4.7
García Garrido, M. ... A1.40
Gawali, V.S. ... A1.19, A3.5, A3.10
Geier, P. ... A1.27
Geisler, S. ... A1.47, A1.50
Geley, S. ... A1.1
Georgieva, L. ... A1.2
Gindl, V. ... A2.2
Glösmann, M. ... A1.40
Gotthardt, D. ... A3.4
Gouilleux, F. ... A3.24
Grahl, A. ... A1.33, A1.43
Grasl-Kraupp, B. ... A3.19
Grusch, M. ... A3.19
Gryglewski, G. ... A4.6
Gundelfinger, E. ... A1.36
Gupta, K.D. ... A1.27
Gütschow, M. ... A3.11
Haeusler, D. ... A4.6
Hahn, A. ... A1.33, A1.38, A1.43, A4.4, A4.5, A4.7
Hausott, B. ... A1.12
Heilbronn, R. ... A1.48
Heinemann, Á. ... A3.8, A3.11, A3.20
Heinzle, C. ... A3.19
Helson, L. ... A4.1
Henstridge, C.M. ... A1.15
Herbst, R. ... A1.22
Hering, S. ... A3.12
Herrera-Molina, R. ... A1.36
Herrzog, H. ... A1.46, A1.48
Hilber, K. ... A1.19, A3.5, A3.10
Hirtenlehner, S. ... A1.6
Hoelbl-Kovacic, A. ... A3.24
Höflich, A. ... A4.4, A4.5
Hofmaier, T. ... A2.11
Hohenegger, M. ... A3.7, A3.13, A3.23
Hohsfield, L.A. ... A1.1
Holub, B. ... A1.4
Holy, M. ... A2.11
Holzer, M. ... A3.8
Holzer, P. ... A1.4
Holzmann, K. ... A3.19
Hörner, B. ... A1.46
Hosztafi, S. ... A3.1
Hrovat, C. ... A1.22
Hua, H. ... A1.13
Huck, S. ... A1.7, A1.8, A1.52
Hummer, A. ... A1.33, A1.43
Humpel, C. ... A1.1, A1.47, A2.1
Hutter-Paier, B. ... A1.47, A2.1
Ianos, B. ... A1.7
Inzinger, M. ... A3.8
Jagirdar, R. ... A1.11
Jandl, K. ... A3.11
Jonas, P. ... A1.13, A1.21, A1.49
Jurský, F. ... A1.10, A1.14
Just, W.W. ... A1.35
Kacskovits, I. ... A1.15
Kadiysky, D. ... A1.2
Karch, R. ... A4.3
Kasper, S. ... A1.38, A1.39, A4.4, A4.6, A4.7
Kasugai, Y. ... A3.6
Katona, I. ... A1.15
Kaufmann, W.A. ... A3.6
Kazemi, Z. ... A3.21
Kepplinger, B. ... A1.41, A1.42
Kerov, V. ... A1.40
Kerschbaumer, A. ... A3.21
Khunweeraphong, N. ... A3.15
Klein, B. ... A1.28
Kleiter, I. ... A1.23
Klickovic, U. ... A4.1
Klimaschewski, L. ... A1.12
Knape, K. ... A3.12
Knaus, H.-G. ... A1.45
Knoflach, D. ... A1.40
Koban, F. ... A2.6
Koenig, X. ... A1.19, A1.25, A3.5, A3.10
Kofler, B. ... A1.4
Kofler, R. ... A2.10
Kollmann, K. ... A3.22
Kónya, V. ... A3.11, A3.20
Koschak, A. ... A1.40, A2.10
Kostenis, E. ... A3.11
Kovács, G.G. ... A1.29
Kranz, G.S. ... A1.33, A1.43, A4.4, A4.6, A4.7
Kraus, C. ... A1.33, A1.38, A1.43
Kress, M. ... A1.47, A2.4
Kubicek, S. ... A3.24
Kubista, H. ... A1.18, A1.20, A1.27
Küblböck, M. ... A1.33, A1.43, A4.7
Kudlacek, O. ... A2.6, A2.11, A3.10
Kulaksiz, M. ... A3.13
Kummer, K.K. ... A2.4
Lagler, M. ... A1.27
Lamm, C. ... A1.33, A1.43
Lang, A. ... A1.4
Lang, R. ... A1.4
Langer, O. ... A4.3
Lanz, I. ... A3.20
Lanzenberger, R. ... A1.33, A1.38, A1.39, A1.43, A4.4, A4.5, A4.6, A4.7
Lee, A. ... A1.40, A2.9
Lee, S.-H. ... A1.15
Leitner, E. ... A3.24
Lieb, A. ... A2.8
Linder, T. ... A3.12
Lindner, H. ... A3.6
Liou, I. ... A1.35
Lipskaia, N. ... A4.5
Liu, X. ... A1.40
Locker, F. ... A1.4
Lornejad-Schäfer, M.R. ... A3.3
Lubec, G. ... A1.25
Luf, A. ... A2.11
Lukács, P. ... A1.19, A3.5
Madalinski, M. ... A1.22
Mahlknecht, P. ... A2.2
Malfacini, D. ... A3.1
Mangger, S. ... A1.12
Mansouri, M. ... A3.6
Marian, B. ... A3.19
Marksteiner, J. ... A1.47, A2.1
Marschallinger, J. ... A1.23, A1.30
Marsche, G. ... A3.8, A3.11
Matolcsi, M. ... A1.15
Matzner, P. ... A4.2
Mayr, J. ... A1.4
Mechtler, K. ... A1.22
Melis, M. ... A1.15
Mietzsch, M. ... A1.48
Miháliková, A. ... A1.10, A1.14
Mihivilović, M. ... A1.34
Mika, J.K. ... A1.17, A3.9
Mirheydari, P. ... A1.34
Mitterhauser, M. ... A1.38, A1.39, A4.3, A4.6
Montag, D. ... A1.36
Moriggl, R. ... A3.24
Müller, M. ... A4.3
Muneer, Z. ... A1.31
Neumeister, A. ... A1.39
Nyilas, R. ... A1.15
Obermair, G.J. ... A1.5, A1.40, A1.47, A1.50, A2.1, A2.9, A2.10
Ortner, N. ... A2.8
Österreicher, Z. ... A4.2
Ottersbach, P.A. ... A3.11
Parnia, S. ... A1.21
Parveen, Z. ... A3.15
Pasterk, L. ... A3.8
Pataria, E. ... A4.3
Paul, K. ... A1.33, A1.43
Pernia-Andrade, A. ... A1.32
Perroy, J. ... A3.6
Petrova, E. ... A1.2
Pfabigan, D.M. ... A1.33, A1.43
Pichler, S. ... A2.6
Pintér, B. ... A1.15
Pistis, M. ... A1.15
Plaikner, M. ... A3.14
Platzter, W. ... A3.11, A3.20
Pollak, D.D. ... A1.24, A1.37
Prchal-Murphy, M. ... A3.22
Prostran, M. ... A3.2
Pusch, O. ... A3.15
Puthenkalam, R. ... A1.26
Putz, E.M. ... A3.4
Radenković, M. ... A3.2
Ramerstorfer J. ... A1.34
Rami-Mark, C. ... A1.38
Ramprecht, C. ... A1.51
Raynaud, F. ... A3.6
Redl, M. ... A1.35
Regelsberger, G. ... A1.44
Reindl, M. ... A1.1
Reuss, J. ... A1.41
Rizzi, S. ... A1.45
Römer, H. ... A1.6
Ronovski, M. ... A1.24
Rotheneicher, P. ... A1.30
Rubi, L. ... A1.27, A1.19, A3.5
Ruiß, M. ... A1.20
Saha, K. ... A2.3
Salzer, I. ... A2.2
Salzmann, S. ... A3.7
Sandtner, W. ... A2.3, A3.10, A3.18
Saria, A. ... A2.4
Sarto-Jackson, I. ... A1.36
Sartori, S.B. ... A1.40
Savalli, G. ... A1.24, A1.37
Savli, M. ... A1.39
Savli, M. ... A4.6
Saxena, P. ... A3.12
Schäfer, C. ... A3.3
Schandl, U. ... A1.27
Schicker, K.W. ... A1.40
Schmid, D. ... A3.15
Schmid, J.A. ... A2.7
Schmid, R. ... A2.11
Schmidhammer, H. ... A3.1
Schmuckermair, C. ... A1.30, A1.40
Scholze, P. ... A1.7, A1.8, A1.17, A1.52
Schöpf, C.L. ... A1.47, A1.50
Schröder, K.R. ... A3.3
Schulz, S. ... A1.37
Schwarz, K. ... A1.17
Schwarzer, C. ... A1.3, A1.45, A1.47, A1.50
Seddik, A. ... A2.11
Seeliger, M. ... A1.40
Seidel, E.-M. ... A1.33, A1.43
Semler-Sedlnitzky, B. ... A1.41, A1.42
Sexl, V. ... A3.4, A3.22, A3.24
Shigemoto, R. ... A3.6
Sieghart, W. ... A1.34, A1.36
Singewald, N. ... A1.30

- Sitte, H.H. ... A2.3, A2.11, A3.15, A3.16, A3.17, A3.18
Sladky, R. ... A1.33, A1.43, A4.7
Smalla, K.-H. ... A1.36
Sohail, A. ... A2.3, A3.18
Soltesz, I. ... A1.15
Sonvilla, G. ... A3.19
Sothilingam, V. ... A1.40
Sperk, G. ... A1.11, A1.16, A1.46, A1.48
Spetea, M. ... A3.1
Spies, D. ... A1.27
Spies, M. ... A4.6, A4.7
Stanika, R.I. ... A1.47, A2.9
Stary-Weinzinger, A. ... A3.12
Stefanova, N. ... A1.47, A2.1
Steinberger, A. ... A1.51
Sterz, F. ... A1.21
Stockinger, H. ... A1.44
Stockner, T. ... A2.3, A2.6, A2.11, A3.15
Stojanović, M. ... A3.2
Stolt-Bergner, P. ... A3.18
Storka, A. ... A4.1
Striessnig, J. ... A2.8
Strohmaier, W. ... A3.21
Strommer, S. ... A4.2
Sucic, S. ... A3.16, A3.17
Sultana, N. ... A1.5, A1.47
Szabadits, E. ... A1.15
Szabó, Sz. ... A1.15
Tasan, R.O. ... A1.11, A1.16, A1.46, A1.48
Thalhammer, J. ... A1.28
Thrun, A. ... A1.7, A1.8
Thurner, P. ... A3.10
Timin, E. ... A1.19, A3.12
Todt, H. ... A1.19, A3.5
Todtova, K. ... A1.37
Tomschik, M. ... A1.22
Topalović, Z. ... A1.35
Trieb, M. ... A3.8
Tuluc, P. ... A1.5, A2.5
Vanicek, T. ... A4.4, A4.7
Varagić, Z. ... A1.34
Varga, Cs. ... A1.15
Vcelar, B. ... A4.1
Venkatesan, S. ... A2.3
Verma, D. ... A1.16, A1.46, A1.48
Voigtländer, T. ... A1.31
Vyleta, N.P. ... A1.49
Waclawiczek, A. ... A1.30
Wadsak, W. ... A1.38, A1.39, A4.3, A4.6
Wanzenböck, H.D. ... A1.17, A3.9
Warsch, W. ... A3.24
Wasinger, C. ... A3.7
Watanabe, M. ... A1.15, A3.6
Weber, F. ... A1.44
Weger, S. ... A1.48
Weger, W. ... A3.8
Weidinger, J. ... A3.3
Weigl, L.G. ... A3.14
Weiss, R. ... A1.28
Wiesinger, C. ... A1.31, A1.44
Wimmer, L. ... A1.34
Windisch, A. ... A3.12
Windisch, M. ... A1.47, A2.1
Windischberger, C. ... A1.33, A1.43, A4.4, A4.5, A4.7
Winkler, D. ... A4.4
Wirth, M. ... A3.9
Wolf, P. ... A3.8
Wolzt, M. ... A4.1
Wood, J. ... A1.16, A1.46
Woodhams, S.G. ... A1.15
Xanthos, D. ... A1.7, A1.8
Yang, J.-W. ... A1.25
Zangrandi, L. ... A1.3
Zaunmair, I. ... A1.23
Zebedin-Brandl, E. ... A3.21
Zeitlinger, M. ... A4.2, A4.3
Zernig, G. ... A2.4
Zezula, J. ... A3.10

